La mer 45 : 105-116, 2007
Société franco-japonaise d'océanographie, Tokyo

Mesocosm studies on phytoplankton community succession after inputs of the water-soluble fraction of Bunker A oil

Hideaki NOMURA[1]*, Keita TOYODA[2], Mihoko YAMADA[3], Ken OKAMOTO[4], Minoru WADA[1], Masahiko NISHIMURA[1], Akihiro YOSHIDA[1], Akira SHIBATA[1], Hideshige TAKADA[3] and Kouichi OHWADA[5]

Abstract: We monitored the succession of a phytoplankton community for 10 days in an enclosed meso-scale seawater tank (mesocosm) , into which the water-soluble fraction of Bunker A oil was spiked, with or without a chemical dispersant. Diatoms such as *Chaetoceros* spp. and *Skeletonema costatum* contributed more than 50% of the total phytoplankton abundance for the first 3 days in all tanks. In the seawater tank that was devoid of the oil contamination, phytoplankton abundance fluctuated greatly, but diatoms predominated until day 8. However, in the oil-spiked tanks, autotrophic flagellates predominated over diatoms by day 5 after the oil addition. Daily monitoring of sediment trap contents revealed that the oil-spiked seawater resulted in a significantly reduced flux of diatom cells compared with the seawater tank. The decline in the diatom contribution to total phytoplankton abundance in both seawater and trap contents was more pronounced in the presence of the dispersant than in its absence. From these results, the mesocosm experiments clearly demonstrated adverse effects of Bunker A oil components on planktonic diatom assemblages under experimental conditions similar to those found in natural coastal environments. A combination of careful observation of the succession within the phytoplankton population in the water column and analysis of sediment trap samples have provided insights into the possible impacts of low levels of oil contamination on grazing food webs in natural marine environments.

Keywords: *diatoms, flagellates, phytoplankton, succession, oil, dispersants, mesocosms*

Introduction

Accidental oil spillage is one of the severe problems facing marine ecosystems, because the chemical components that diffuse from spilled oil often show acute or chronic eco–toxicity to diverse types of plants and animals (ALBERS, 1995). Evaluation of the environmental damage caused by such spilled oil has been a substantial challenge because of the lack of baseline information about the species present at a site, and their interactions and physiological states prior to the oil contamination. Although laboratory experiments on the effects of oil contamination on particular species of marine organisms are necessary, it is often difficult to apply the results of these studies directly to predict population– or community–level impacts that would affect the structure and function of the natural ecosystem.

Field experiments in a meso–scale, controlled ecosystem (mesocosm) have been conducted to overcome such difficulties in evaluating the impacts of pollutants on biological processes (LEE and TAKAHASHI, 1977; OVIATT *et al.*, 1982; PARSONS *et al.*, 1984; LINDÉN *et al.*, 1987). In

1. Ocean Research Institute, The University of Tokyo
2. Laboratory of Aquatic Science Consultant Co., Ltd.
3. Institute of Symbiotic Science and Technology, Tokyo University of Agriculture and Technology
4. Graduate School of Agricultural and Life Science, The University of Tokyo
5. Faculty of Environmental and Symbiotic Sciences, Prefectural University of Kumamoto

*Corresponding author
Ocean Research Institute, The University of Tokyo, Minami-dai, Nakano, Tokyo 164-8639, Japan
Tel: +81-3-5351-6483, Fax: +81-3-5351-6482
E-mail address: nmr@ori.u-tokyo.ac.jp

contrast to a glass flask in a laboratory, a mesocosm tank is designed to hold a water mass large enough to allow a diverse array of planktonic organisms at different trophic levels to exist under conditions similar to the natural environment in terms of temperature, sunlight, wind, and rainfall (MENZEL, 1977; PARSONS *et al.*, 1984). An enclosed marine mesocosm near the mouth of Lake Hamana (Hamana–ko), a seawater lake in Shizuoka prefecture, Japan, has been used to study the impacts of contamination from the water–soluble fraction (WSF) of Bunker A oil on the microbial food web in seawater (OHWADA *et al.*, 2003; TOYODA *et al.*, 2005; NISHIMURA *et al.*, 2006; YOSHIDA *et al.*, 2006). One of the conclusions from these studies was that even low levels of oil contamination can disturb species composition and trophic interactions in the microbial food web.

In the present paper, we report on the succession of the phytoplankton community in the same mesocosm system, into which the WSF of Bunker A oil was added, with or without a chemical dispersant. We also describe the phytoplankton composition in sediment trap samples retrieved daily from the mesocosm. From these results, we discuss the possible impacts of low concentrations of the oil components on the phytoplankton community and grazing food web in natural marine environments.

Materials and methods

The mesocosm experiments were carried out from 23 May to 2 June 2001 using three experimental tanks. Each cylindrical tank has a 1.5–m diameter, a 3.0–m depth, and a 5000–L capacity (OHWADA *et al.*, 2003). Surface water from Hamana–ko was introduced into the two reservoirs for three tanks by using an electric submersible pump (OMORI and JO, 1989), and then distributed equally into the experimental tanks. On 22 May, nutrients (KNO_3, 100 μg N L^{-1}; KH_2PO_4, 10 μg P L^{-1}; Na_2SiO_3–$9H_2O$, 10 μg Si L^{-1}) were added to each experimental tank to maintain biological activity during the experiment, and the tanks were stirred for 0.5 h using stainless–steel blades (YOSHIDA *et al.*, 2006).

We prepared a mixture of the WSF of Bunker A oil and autoclaved seawater from Hamana–ko (YAMADA *et al.*, 2003). We also prepared a mixture of the WSF and a chemical dispersant (nonionic surfactant; Taiho Self Mixing S–7, Taiho Industries, Tokyo, Japan). Details of the procedure for the preparation and handling of the WSF and the dispersant were described in YAMADA *et al.* (2003) and YOSHIDA *et al.* (2006). After introducing water into the experimental tanks, either the WSF or the mixture of WSF and chemical dispersant was added to the mesocosm tanks, which were designated as the "OIL" tank or the "OD" tank, respectively. The last tank was kept free of contamination from both oil and dispersant as a control and was designated as the "SEA" tank.

Oil concentration just after the addition of the WSF in the OIL tank was estimated to be 224 μg L^{-1}, as measured by fluorometric analysis according to the method of Integrated Global Ocean Services System (IGOSS, 1974; referenced in: the Oceanographic Society of Japan, 1979). This oil concentration is comparable to that found in the inner part of the port of Tokyo Bay and is similar to that of MARL experiments in the early 1980s (OVIATT *et al.*, 1982). Determination of the oil concentration in the OD tank failed due to a poor extraction efficiency caused by the dispersant used (M. YAMADA, personal communication). Concentrations of four representative polyaromatic hydrocarbon (PAH) compounds– naphthalene ($C_{10}H_8$), phenanthrene ($C_{14}H_{10}$), fluoranthene ($C_{16}H_{10}$), and chrysen ($C_{18}H_{12}$) –were determined by gas chromatography–mass spectrometry (YAMADA *et al.*, 2003).

Before pouring the oil–water mixture into the tanks, a sample of tank water was collected and subjected to microscopic observation of phytoplankton. For chemical analysis, another water sample was collected just after the introduction of the oil–water mixture. These are referred to as "day 0" samples. Water samples were siphoned to collect periodically from day 0 through day 10 from a depth of 0.5 m, using teflon tubing attached to the stainless–steel pipe, carefully introduced into glass bottles, and stored at appropriate temperature until analysis. At the same time as water sampling, a portable STD system (model 610–DM; YSI,

Table 1. Changes of water temperature, salinity, and PAHs in the subsurface water during the mesocosm experiments.

Time (days)		0	1	2	3	4	5	10
Temperature (℃)	SEA	19.6	19.7	20.4	22.6	23.6	22.7	22.0
	OIL	20.1	20.0	20.2	21.4	22.4	22.1	23.1
	OD	20.1	20.0	20.2	21.4	22.3	22.0	22.8
Salinity	SEA	31.63	31.54	31.44	31.40	30.92	31.42	31.43
	OIL	31.54	31.21	30.92	31.18	31.13	31.20	31.22
	OD	31.53	31.28	31.23	31.19	31.20	31.09	30.99
PAH s (ngL^{-1})								
Naphthalene	SEA	149.6	168.9			190.2		152.8
	OIL	3777.1	3606.8	276.9	113.5		190.8	205.9
	OD	5059.7	5613.0	349.1	159.6		146.1	158.9
Phenanthrene	SEA	7.3	6.6			7.4		9.7
	OIL	600.8	489.4	6.7	11.1		11.2	13.7
	OD	999.6	1159.0	82.2		11.1	12.1	19.6
Fluoranthene	SEA	3.6	3.4			4.6		3.6
	OIL	14.5	13.2	6.9	6.4		8.0	3.0
	OD	19.6	25.3	24.0	15.1		10.4	6.5
Chrysene	SEA	0.3	0.2			0.3		0.3
	OIL	2.9	2.6	2.7	2.5		2.3	1.5
	OD	4.0	5.0	4.8	4.7		6.3	4.9

SEA:natural seawater without oil and/or chemical dispersant
OIL:seawater with oil alone
OD:seawater with oil plus chemical dispersant

Yellow Springs, OH, USA) was used to make a depth profile of temperature, salinity, and dissolved oxygen. Water temperature and salinity in all the experimental tanks ranged from 19.6 to 23.1 ℃, and from 30.9 to 31.6, respectively, during the 10 days of incubation (Table 1).

Water samples were fixed with formalin (final concentration: 1%, v/v) and observed with an inverted Nomarsky–type microscope (model TE300; Nikon, Tokyo, Japan) to taxonomically identify and enumerate phytoplankton cells. A 25% glutaraldehyde solution (final concentration: 2%, v/v) was used to gently fix autotrophic nanoflagellates (ANFs) in water samples. The ANF cells were stained with FITC and DAPI (SHERR and SHERR, 1983), filtered onto a polycarbonate Nuclepore (Whatman, Springfield Mill, UK) membrane (pore size, 0.8 μm), and counted under an epifluorescence microscope (type E800; Nikon) in a dark room. ANFs were distinguished from heterotrophs by the autofluorescence of photosynthetic pigments observed under blue light excitation. To minimize the masking effect of the protein–binding dye FITC to the autofluorescence of photosynthetic pigments (SHERR *et al.*, 1993), we empirically set the staining time (5 minutes) and the final concentration (3 μg ml^{-1}).

To measure the concentration of chlorophyll *a* (Chl), a 100–ml water sample was filtered through a Whatman GF/F glass–fiber filter (Whatman, Springfield Mill, UK), and the filters were soaked in N,N–dimethylformamide (SUZUKI and ISHIMARU, 1990). Filters were stored in the dark at approximately −20 ℃for fewer than 10 days before Chl content was measured with a fluorometer (type 10R; Turner Designs, Sunnyvale, CA, USA). A calibration curve was obtained using a Chl standard (Sigma, St. Louis, MO, USA). The filtrate collected during Chl sample preparation was used to analyze for nitrogen (NO_2^- + NO_3^-) and phosphate (PO_4^{3-}) concentrations using an auto–analyzer (model AAAC3; BRAN+LUEBBE, Norderstedt, Germany).

Every day, four glass vials (120–mm height, 30–mm inner diameter, and 100–ml volume) were suspended in the tanks using a thread at a depth of 2.5 m to collect sinking particles. Vials were gently retrieved after 1 day and used

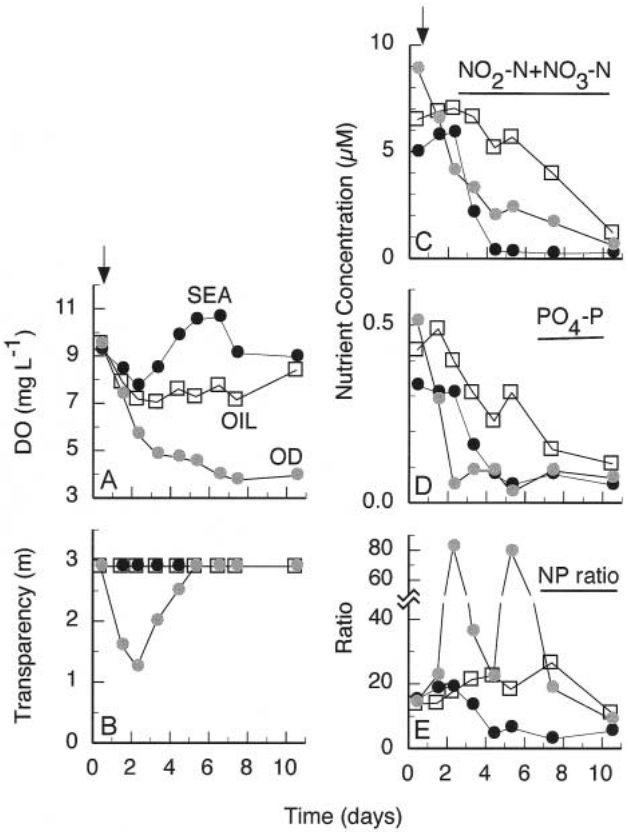

Fig. 1. Temporal variation of concentration of dissolved oxygen (DO) (A), transparency (B), nitrogen (N: NO_2-N + NO_3-N) (C), phosphate (P: PO_4-P) (D), and NP ratio (E) during the mesocosm run from 23rd of May to 2nd of June in 2001. The arrow denotes the time of oil contamination. SEA: natural seawater in the mesocosm tank, OIL: natural seawater with WSF mixture, OD: natural seawater with WSF-chemical dispersant mixture.

for analysis of phytoplankton abundance and Chl content. The phytoplankton trapped in the vials were fixed immediately by formalin (final concentration: 1%, v/v) and stored in the dark at 4 ℃ until microscopic analysis. Identification and enumeration were conducted in the same way as described for the water samples.

We measured water transparency by using a white ceramic disc 80 mm in diameter (smaller than a standard Secchi disc, which is 200 or 300 mm in diameter). According to PREISENDORFER (1986), transparencies measured with the smaller disc and the standard ones are practically the same. The compensation depth (*CD*, m) was calculated using transparency depth (*Ds*, m) with the equation described in ARUGA (1986) : $CD = 2.67Ds$.

Results and discussion

Changes in physico–chemical parameters

The highest concentrations of PAHs were found in the tank to which seawater and the WSF of Bunker A oil and a dispersant (OD) were added (Table 1). Relatively lower molecular weight (LMW) PAHs, naphthalene and phenanthrene, dramatically decreased to less than 10% of the initial concentrations in the first 2 days, whereas higher molecular weight (HMW) PAHs, fluoranthene and chrysene, decreased more slowly. The rapid decrease in the LMW–PAHs can be ascribed to microbial degradation, and the slower removal of the HMW–PAHs (and HMW–alkanes and hopanes; data not shown), from the water column presumably results from settling or sedimentation

(YAMADA *et al.*, 2003).

Dissolved oxygen (DO) concentration in all the tanks was initially 9.5 mg L^{-1}, decreasing by day 7 to 7.2 mg L^{-1} in the OIL tank and to 3.8 mg L^{-1} in the OD tank (Fig. 1A). DO concentrations in the OIL tank became to initial level by day 10, while those in the OD tank continued to decrease. In the control seawater (SEA) tank, DO fluctuated greatly, but it remained above 7.5 mg L^{-1} during the entire incubation period. It is likely that bacterial respiration during the degradation of hydrocarbons in the WSF, the dispersant, or both, substantially contributed to the decline in DO (YOSHIDA *et al.*, 2006).

Initial concentrations of inorganic nitrogen ($NO_2^- + NO_3^-$) and phosphate (PO_4^{3-}) in the tanks ranged from 5 to 9 μM and from 0.3 to 0.5 μM, respectively (Fig. 1C, D). Although both nitrogen and phosphate disappeared almost entirely by day 10, the patterns of disappearance varied between the nutrients and between the tanks. Nitrogen decreased more slowly in both the OIL and the OD tanks compared with that in the SEA tank. Phosphate tended to disappear more rapidly than nitrogen, particularly in the OD tank during the first 2 days. These differences in nutrient removal from the tanks were reflected in the molar ratio of nitrogen to phosphorus (N:P ratio) (Fig. 1E). The N:P ratio was about 14:1 in all of the tanks at day 0 and decreased to less than 10 by day 5 in the SEA tank. In contrast, the N:P ratios in the OIL and OD tanks remained above the initial value through through day 7, with larger fluctuations in the OD tank. Because the N:P ratio of the natural phytoplankton community is 16:1 (REDFIELD *et al.*, 1963), the SEA tank was under N–limited conditions from day 5, whereas the OIL and OD tanks were under P–limited conditions for almost the entire period of the experiment.

Differences in phytoplankton community structure

A total of 62 species of phytoplankton, comprising 47 diatoms, 10 dinoflagellates, and 5 other species, was found in the mesocosm tanks during the experiment (Table 2). While most of them (59 species) were found in the SEA tank, about half were found in the OIL and the OD tanks, suggesting that phytoplankton species richness was higher in the SEA tank.

During the initial phase of the incubation (from day 0 to day 3), planktonic diatoms, including some chain–forming species such as *Chaetoceros seiracanthus, C. debilis, C. dydimus*, and *S. costatum*, contributed more than 50% of the total phytoplankton abundance in all of the tanks (Fig. 2). The rest of the phytoplankton population during this period was mainly composed of autotrophic flagellates, such as *Prorocentrum minimum*, and coccolithophorids.

After day 3, the relative contribution of diatoms to the total phytoplankton population became less pronounced. Although diatoms continued dominating total phytoplankton abundance in the SEA tank until day 8, autotrophic flagellates, namely *P. minimum*, gradually increased after day 5 and finally became dominant (75% of the total phytoplankton population) by day 10. In addition to flagellates, coccolithophorids contributed about 20% of the total phytoplankton population at day 10 in the SEA tank. A succession from diatoms to flagellates in a phytoplankton population is a typical phenomenon in an enclosure system devoid of water turbulence (LEE and TAKAHASHI, 1977; EGGE and AKSNES, 1992). In contrast, autotrophic flagellates, particularly ANFs, rapidly dominated the phytoplankton populations in the OIL and OD tanks after day 5. In the oil–contaminated tanks (with and without dispersant), coccolithophorids disappeared from the water column by day 6.

Beneficial or adverse effects of petroleum substances on phytoplankton should vary depending on the phytoplankton species. Based on previous studies certain autotrophic flagellates appeared to be petroleum–insensitive (PULICH *et al.*, 1974; PARSONS *et al.*, 1976; LEE and TAKAHASHI, 1977; KARYDIS, 1981; MORALES–LOO and GOUTX, 1990; SIRON *et al.*, 1991; OKUMURA *et al.*, 2003), although coccolithophorids suffered severely under oil–contaminated conditions. In another set of mesocosm studies using the same tanks, we confirmed by a vital FDA (fluorescein

Table 2. List of phytoplankton species occurred from the water column of mesocosm tanks during experiments. Water from the surface layer of the mouth part of Hamana-ko was directly brought into tanks via an under-ground tubing water supply pump on May 22, 2001.

Species	Tanks SEA	OIL	OD
Division Dinophyta			
Class Dinophyceae			
Order Prorocentrales			
Prorocentrum compressum	+	−	−
P. dentatum	+	+	−
P. micans	+	−	−
P. minimum	+	+	+
P. triestinum	+	+	+
Order Dinophysiales			
Oxyphysis oxitoxoides	−	−	+
Order Gymnodiniales			
Gymnodinium sp.	+	−	−
Order Gonyaulacales			
Ceratium kofoidii	−	+	−
Order Peridiniales			
Peridinium quinquecorne	+	+	+
Protoperidinium spp.	+	−	+
Division Heterokontophyta			
Class Chrysophyceae			
Order Dictyochales			
Ebria tripartita	+	−	−
Dictyocha fibula	+	−	−
Distephanus speculum	+	+	+
Class Bacillariophyceae			
Order Centrales			
Actinoptychus senarius	+	−	−
Bacteriastrum delicatulum	−	−	+
Chaetoceros atlanticus	+	−	−
C. borealis	+	+	−
C. compressus	+	+	+
C. coronatus	+	−	−
C. curvisetus	+	+	−
C. debilis	+	+	+
C. decipens	+	−	−
C. densus	+	+	+
C. dydimus	+	+	+
C. lorenzianus	+	+	+
C. seiracanthus	+	+	+
C. simplex	+	−	−
Chaetoceros spp.	+	+	+
Coscinodiscus gigas	+	+	−
C. perforatus	+	−	−
Dactyliosolen bravyanus	+	+	+
D. fragilissimus	+	+	−
Detonula pumila	+	−	−
Dytilum brightwellii	+	−	−
Eucampia zodiacus	+	−	+
Guinardia delicatula	+	+	−
G. striata	+	+	+
Hemialus hauckii	+	+	−
Lauderia annulata	+	−	−

+: occurred, −: not occurred

Table 2. continued.

Species	Tanks SEA	OIL	OD
Leptocylindrus minimus	+	+	+
Neostreptotheca subindica ?	+	−	−
Odontella longicruris	+	−	−
Pseudosolenia calcar-avis	+	+	−
Rhizosolenia hebetata f. *hebetata*	+	+	+
R. setigera	+	+	+
R. styliformis	+	−	−
Skeletonema costatum	+	+	+
Thalassiosira anguste-lineata	+	−	−
T. hyalina	+	−	−
T. rotula	+	+	+
T. weissflogii	+	−	−
Thalassiosira spp.	+	+	+
Order Pennales			
Asterionellopsis gracialis	+	+	−
Cylindrotheca closterium	+	+	+
Nitzschia longissima	+	+	+
Nitzschia spp.	+	+	−
Pleurosigma spp. ?	+	−	−
Pseudo-nitzschia spp	+	+	+
Thalassionema frauenfeldii	+	−	+
T. nitzschioides	+	+	+
Division Haptophyta			
Class Coccosphaerales			
unidentified species	+	+	+
Division Euglenophyta			
Class Euglenophyceae			
unidentified species	+	+	+

+: occurred, −: not occurred

diacetate) staining (BENTLEY–MOWAT, 1982) that most autotrophic flagellates were active even at the same levels of WSF of Bunker A oil used in the present study (data not shown).

Phytoplankton in sediment trap samples

Daily monitoring of sediment trap samples from the mesocosm tanks revealed that downward fluxes of Chl in the SEA, OIL, and OD tanks averaged 8.7 (1.0–19.3), 2.8 (0.4–5.6), and 1.7 (0.8–3.7) mg m^{-2} d^{-1}, respectively (Fig. 3). The total phytoplankton and diatom fluxes in the SEA tank averaged 2.3×10^{9} and 2.2×10^{9} cells m^{-2} d^{-1}, respectively, which were one order of magnitude higher than those in the OIL and OD tanks. Although Chaetoceros vegetative cells mainly contributed to the fluxes in the SEA tank during the entire incubation period, their resting spores clearly increased in the latter half of the incubation period, exhibiting a peak of more than 5×10^{7} cells m^{-2} d^{-1} on day 7. In contrast, the number of the resting spore in the trap samples from the OIL and OD tanks was extremely low, fewer than 1×10^{6} cells m^{-2} d^{-1} on average, whereas autotrophic flagellates contributed more to the total phytoplankton fluxes in the oil–contaminated tanks than in the SEA tank.

Species of *Chaetoceros* produce resting spores immediately following blooms (e.g., ODATE and MAITA, 1990), and nitrogen depletion is one of the essential factors inducing spore formation in centric diatoms (FRENCH and HARGRAVES, 1980; KUWATA and TAKAHASHI, 1990; OKU and KAMATANI, 1995, 1997; MCQUOID and HOBSON, 1996). Our results are consistent with these observations; resting spore formation by *Chaetoceros* in the SEA tank became intensive after nitrogen was depleted from the seawater. Besides nitrogen, phosphate depletion can be a factor leading to resting spore formation in diatoms (OKU and KAMATANI, 1995). However,

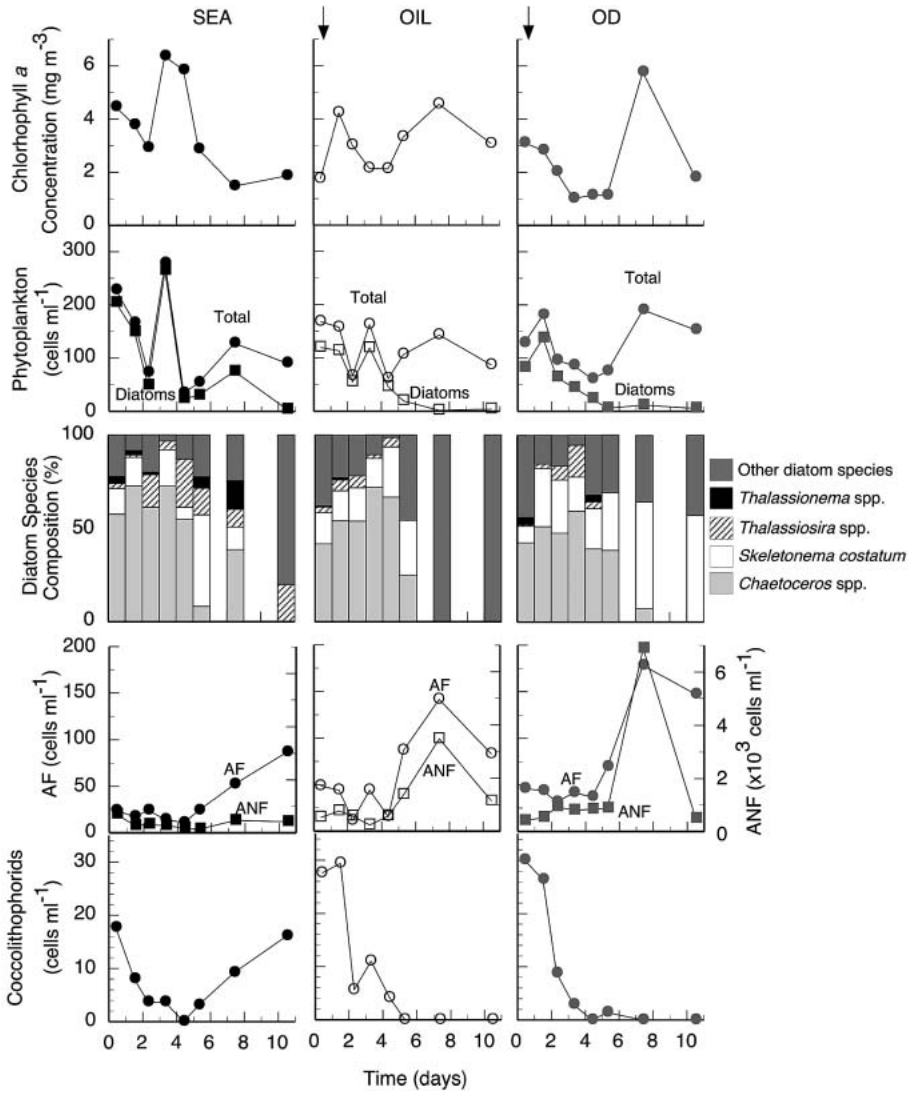

Fig. 2. Temporal variation of concentrations of chlorophyll *a* concentration, phytoplankton cell density, diatom species composition, cell density of autotrophic flagellate (AF) and autotrophic nanoflagellate (ANF) and coccolithophorid during the mesocosm run from 23rd of May to 2nd of June in 2001. The arrows denote the time of oil contamination. SEA: natural seawater in the mesocosm tank, OIL: natural seawater with WSF mixture, OD: natural seawater with WSF–chemical dispersant mixture.

this probably did not occur in our mesocosm tanks, because phosphate was depleted faster in the OD tank than in the SEA tank (see Fig. 1D) and yet the OD tank had fewer spores than the SEA tank (Fig. 3). Although the lower numbers of resting spores in the OIL and OD tanks may be partly explained by the relatively slow depletion of nitrogen compared with the SEA tank, it is more likely that chemical components in the WSF of Bunker A oil were responsible for limiting spore formation.

Because the spore formation by planktonic diatoms in the SEA tank is adequately explained by nitrogen limitation alone, it is unlikely that other elements such as silicon (Si) were limiting for diatom growth and spore formation in the present study. In support of this, we did not observe any Si depletion in the

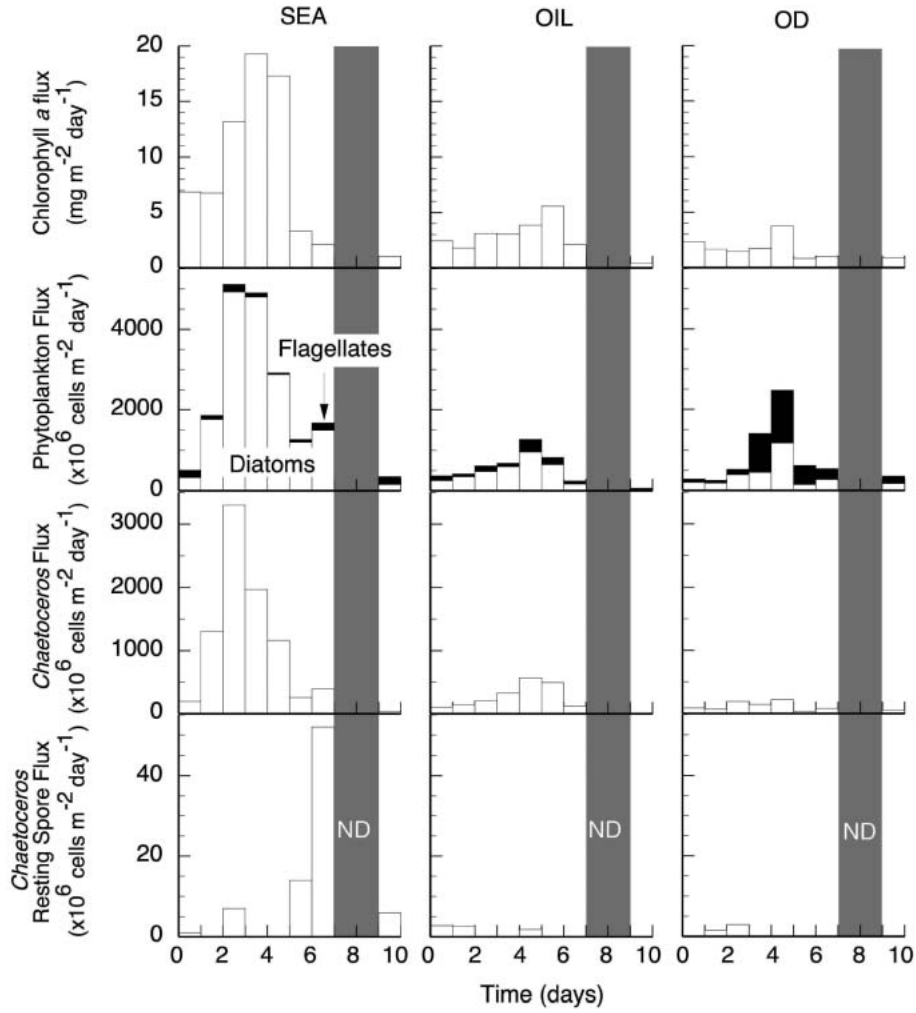

Fig. 3. Temporal variation of downward flux, chlorophyll *a*, total phytoplankton cell, *Chaetoceros* cell, and *Chaetoceros* resting spore, during the mesocosm run from 23rd of May to 2nd of June in 2001. SEA: natural seawater in the mesocosm tank, OIL: natural seawater with WSF mixture, OD: natural seawater with WSF –chemical dispersant mixture. ND: no data.

previous mesocosm study with the same experimental conditions. For instance, the Si:N ratio in the seawater tank in the previous experiment (autumn 2000) ranged from 0.9:1 to 1.2:1 (average = 1.1:1) during the initial 9 days of incubation (data not shown). Actively growing diatom cells have a Si:N composition ratio of 1.2:1 (BRZEZINSKI, 1985), so it is likely that diatoms in the SEA tank did not face serious Si depletion either in the present or in the previous experiments.

MORINAGA and ARAKAWA (2000) reported that an oil slick on the sea surface attenuated the photosynthetically available radiation (PAR) below the sea surface. Such changes in the optical environment can be detrimental to autotrophic plankton, although the optimum PAR may vary depending on the species. PARSONS *et al.* (1984) reported depressed primary production in the mesocosm tank resulting from light attenuation after the input of dispersed oil. In the present study, the transparency of the OD tank immediately decreased from 3 to 1.3 m after the addition of the

mixture of the WSF of Bunker A oil and a dispersant. It took 5 days to return to the original level of transparency, whereas transparency remained constant in the SEA tank and the OIL tank (see Fig. 1B). Based on ARUGA's equation, the compensation depth of the OD tank on day 2 was estimated to be 3.3 m. However, it was more than 7.7 m in the SEA and OIL tanks. Because sunlight attenuates drastically with depth, diatoms that cannot maintain their vertical position at a depth of optimum light conditions are likely to be outcompeted by motile flagellates.

Spilled oil has both inhibitory and stimulatory impacts on phytoplankton, which vary with the type of oil and concentrations of the petroleum components (ALBERS, 1995). Results of the present study suggest that the WSF of Bunker A oil is detrimental to diatoms, whereas it is less inhibitory to the flagellate population. Consequently, flagellates gained better access to the light and nutrients in the water column. Dispersants increase the concentrations of oil components in the water, thereby creating more harsh conditions for the diatom population (PARSONS *et al.*, 1984; YAMANE *et al.*, 1984; SIRON *et al.*, 1996). In the context of grazing food webs, the WSF of Bunker A oil altered not only the community structure but also the functions of the primary producers. The decreased flux of diatom cells from the upper layer implies a reduced transport of organic matter in the water column, which could interrupt the plankton–benthos coupling in natural environments (AMBROSE and RENAUD, 1995).

The physical microturbulence in a water mass is removed or weakened in an enclosed mesocosm (LALLI and PARSONS, 1993), therefore, it might be difficult for planktonic diatoms to remain suspended in the water column in mesocosm tanks such as those used in the present study, which could complicate interpretation of our results. Due to this intrinsic characteristic of these tanks, they may only be suitable for short–term observations of diatom populations in the water column. Nonetheless, the combination of careful observations of the phytoplankton population in the water column and in the sediment trap samples makes it possible to determine with great sensitivity the impacts of low levels of spilled oil on both the phytoplankton community structure and the trophic interactions in the grazing food webs in aquatic environments.

Acknowledgements

We are grateful to professors Dr. Akinori HINO and Dr. Yuzuru SUZUKI of the Fisheries Laboratory, Graduate School of Agricultural and Life Sciences, The University of Tokyo, and to several staff members of the Fisheries Laboratory, for providing experimental space and accommodations. We thank Dr. Osamu OKU of Meikai University for his important information and comments, and Mr. Jay Melton of Prefectural University of Kumamoto for proofreading our English in an earlier draft of this manuscript. We also thank Showa Shell Sekiyu Co. for kindly supplying us with the Bunker A heavy oil. This work was supported by the Research for the Future Program sponsored by the Japan Society for the Promotion of Science (JSPS).

References

ALBERS, P.H. (1995) : Petroleum and individual polycyclic aromatic hydrocarbons. *In* Handbook of Ecotoxicology. Hoffman, D.J., B.A. Rather, G.A. Burton, Jr. and J. Cairns, Jr. (eds.), Lewis Pub., Florida, p. 330–347.

AMBROSE, W.G., Jr. and P.E. RENAUD (1995) : Benthic response to water column productivity patterns: evidence for benthic–pelagic coupling in the Northeast Water Polynya. J. Geophys. Res., Oceans, **100**, 4411–4421.

ARUGA, Y. (1986) : Production ecology of marine phytoplankton. *In* Sohrui–no–seitai (Algal Ecology). Akiyama, M., Y. ARUGA, M. Sakamoto and Y. Yokohama (eds.), Uchida Rokakuho, Tokyo, p. 81–121. (in Japanese)

BENTLEY–MOWAT, J.A. (1982) : Application of fluorescence microscopy to pollution studies on marine phytoplankton. Bot. Mar., **25**, 203–204.

BRZEZINSKI, M.A. (1985) : The Si:C:N ratio of marine diatoms: interspecific variability and the effect of some environmental variables. J. Phycol., **21**, 347–357.

EGGE, J.K. and D.L. AKSNES (1992) : Silicate as regulating nutrient in phytoplankton competition. Mar. Ecol. Prog. Ser., **83**, 281–289.

FRENCH, F.W. and P.E. HARGRAVES (1980) : Physiological characteristics of plankton diatom

resting spores. Mar. Biol. Lett., **1**, 185–195.
KARYDIS, M. (1981) : The toxicity of crude oil for the marine alga *Skeletonema costatum* (Greille) Cleve in relation to nutrient limitation. Hydrobiologia, **85**, 137–143.
KUWATA, A. and M. TAKAHASHI (1990) Life–form population responses of a marine planktonic diatom, *Chaetoceros pseudocurvisetus*, to oligotrophication in regionally upwelled water. Mar. Biol., **107**: 503–512.
LALLI, C.M. and T.R. PARSONS (1993) : Biological oceanography: an introduction. Butterworth–Heinemann, Oxford, 301pp.
LEE, R.F. and M. TAKAHASHI (1977) : The fate and effect of petroleum in controlled ecosystem enclosures. Rapp. P. –v. Rèun. Cons. int. Explor. Mer, **171**, 150–156.
LINDÉN, O., A. ROSEMARIN, A. LINDSKOG, C. HÖGLUND and S. JOHANSSON (1987) : Effects of oil and oil dispersant on an enclosed marine ecosystem. Environ. Sci. Technol., **21**, 374–382.
MCQUOID, M.R. and L.A. HOBSON (1996) : Diatom resting stages. J. Phycol., **32**, 889–902.
MENZEL, D.W. (1977) : Summary of experimental results: controlled ecosystem pollution experiment. Bull. Mar. Sci., **27**, 142–145.
MORALES–LOO, M.R. and M. GOUTX (1990) : Effects of water–soluble fraction of the Mexican crude oil "Isthmus Cactus" on growth, cellular content of chlorophyll a, and lipid composition of planktonic microalgae. Mar. Biol., **104**, 503–509.
MORINAGA, T. and H. ARAKAWA (2000) : Distribution of underwater irradiances and estimated light attenuation by oil slick in the ROPME Sea area. La mer, **37**, 173–181.
NISHIMURA, M., A. YOSHIDA, K. TOYODA, M. YAMADA, H. NOMURA, M. WADA, K. OKAMOTO, A. SHIBATA, H. TAKADA and K. OHWADA (2006) : Mesocosm experiment on the succession of microbial community in response to oil contamination to coastal seawater. La mer, **44**, 59–65.
Oceanographic Society of Japan, The (1979) : Kaiyo–Kankyou–Chosa–Ho (Methods of Marine Environmental Research). Kouseisha–Kouseikaku, Tokyo, 666pp.
ODATE, T. and Y. MAITA (1990) : Seasonal distribution and vertical flux of resting spores of *Chaetoceros* (Bacillariophyceae) species in the nertic water of Funka Bay, Japan. Bull. Fac. Fish. Hokkaido Univ., **41**, 1–7.
OHWADA, K., M. NISHIMURA, M. WADA, H. NOMURA, A. SHIBATA, K. OKAMOTO, K. TOYODA, A. YOSHIDA, H. TAKADA and M. YAMADA, (2003) : Study of the effect of water–soluble fractions of heavy–oil on coastal marine organisms using enclosed ecosystems, mesocosms. Mar. Poll. Bull., **47**, 78–84.
OKU, O. and A. KAMATANI (1995) : Resting spore formation and phosphorus composition of the marine diatom *Chaetoceros pseudocurvisetus* under various nutrient conditions. Mar. Biol., **123**, 393–399.
OKU, O. and A. KAMATANI (1997) : Resting spore formation of the marine planktonic diatom *Chaetoceros anastomosans* induced by high salinity and nitrogen depletion. Mar. Biol., **127**, 515–520.
OKUMURA, Y., J. KOAYAMA and S. UNO (2003) : The relationship between logPow and molecular weight of polycyclic aromatic hydrocarbons and EC50 values of marine microalgae. La mer, **41**, 182–191.
OMORI, M. and S.–G. JO (1989) : Plankton sampling system with a new submersible vortex pump and its use to estimate small–scale vertical distributuion of eggs and larvae of *Sergia lucens*. Bull. Plankton Soc. Japan, **36**, 19–26.
OVIATT, C., J. FRITHSEN, J. GEARING and P. GEARING (1982) : Low chronic additions of No. 2 fuel oil: chemical behavior, biological impact and recovery in a simulated estuarine environment. Mar. Ecol. Prog. Ser., **9**, 121–136.
PARSONS, T. R., W. K. W. LI and R. WATERS (1976) : Some preliminary observations on the enhancement of phytoplankton growth by low levels of mineral hydrocarbons. Hydrobiol., **51**, 85–89.
PARSONS, T. R., P. J. HARRISON, J. C. ACREMAN, H. M. DOVEY, P. A. THOMPSON, C. M. LALLI, K. LEE, G. LI and X. CHEN (1984) : An experimental marine ecosystem response to crude oil and Corexit 9527: part 2 – biological effects. Mar. Environ. Res., **13,** 265–275.
PREISENDORFER, R.W. (1986) : Secchi disk science: visual optics of natural waters. Limnol. Oceanogr., **31**, 909–926.
PULICH, W. M. Jr., K. WINTERS and C. VAN BAALEN (1974) : The effects of a No. 2 fuel oil and two crude oils on the growth and photosynthesis of microalgae. Mar. Biol., **28**, 87–94.
REDFIELD, A.C., B.H. KETCHUM and F.A. RICHARDS (1963) : The influence of organisms on the composition of seawater. *In* The sea, vol. 2. M.N. Hill (ed.), Wiley Interscience, New York, p.26–77.
SHERR, E.B. and B.F. SHERR (1983) : Double–staining epifluorescence technique to assess frequency of dividing cells and bacteriovory in natural populations of heterotrophic microprotozoa. Appl. Environ. Microbiol., **46**, 1388–1393.
SHERR, E.B., D.A. CARON and B.F. SHERR (1993) : Staining of heterotrophic protists for visualization via epifluorescence microscopy. *In* Handbook of methods in aquatic microbial ecology, Kemp, P.F., B.F. SHERR, E.B. SHERR and J.J. Cole, (eds.), CRC Press LLC, Florida, USA, 213–

227.

Siron, R., G. Giusti, B. Berland, R. Morales–Loo and É. Pelletier (1991) : Water–soluble petroleum compounds: chemical aspects and effects on the growth of microalgae. Sci. Total Environ., **104**, 211–227.

Siron, R., É. Pelletier and S. Roy (1996) : Effects of dispersed and adsorbed crude oil on microalgal and bacterial communities of cold water. Ecotoxicol., **5**, 229–251.

Suzuki, R. and T. Ishimaru (1990) : An improved method for determination of phytoplankton chlorophyll using N,N–dimethylformamide. J. Oceanogr. Soc. Japan, **46**, 190–194.

Toyoda, K., A. Shibata, M. Wada, M. Nishimura, H. Nomura, A. Yoshida, K. Okamoto, M. Yamada, H. Takada, K. Kogure and K. Ohwada (2005) : Trophic interactions among marine microbes in oil–contaminated seawater at mesocosmic scale. Microb. Environ., **20**, 104–109.

Yamada, M., H. Takada, K. Toyoda, A. Yoshida, A. Sibata, H. Nomura, M. Wada, M. Nishimura, K. Okamoto and K. Ohwada (2003) : Study on the fate of petroleum–derived polycyclic aromatic hydrocarbons (PAHs) and the effect of chemical dispersant using an enclosed ecosystem, mesocosm. Mar. Poll. Bull. **47**, 105–113.

Yamane, A. N., M. Okada and R. Sudo (1984) : The growth inhibition of planktonic algae due to surfactants used in washing agents. Water Res., **18**, 1101–1105.

Yoshida, A., H. Nomura, K. Toyoda, T. Nishino, Y. Seo,M. Yamada, M. Nishimura, M. Wada, K. Okamoto, A. Shibata, H. Takada, K. Kogure and K. Ohwada (2006) : Microbial responses using the denaturing gradient gel electrophoresis to oil and chemical dispersant inputs in enclosed ecosystems. Mar. Poll. Bull., **52**, 89–95.

Received October 27, 2005
Accepted November 26, 2007

La mer 45 : 117-134, 2007
Société franco-japonaise d'océanographie, Tokyo

Role of tidal flat in material cycling in the coastal sea

Yumiko YARA[1]*, Tetsuo YANAGI[2], Shigeru MONTANI[3] and Kuninao TADA[4]

Abstract: A simple tidal flat model with pelagic and benthic ecosystems was developed in order to analyze the nitrogen cycling in an inter–tidal flat of the Seto Inland Sea, Japan. After the verification of calculation results with the observed results in water quality and benthic biomasses, the role of this tidal flat in nitrogen cycling was evaluated from the viewpoint of water quality purification capability. When there is no suspension feeder in the tidal flat, the water quality purification capability of this tidal flat becomes lower because the outflow of organic nitrogen increases compared to the present case, and the red tides may be generated.

Keywords: *tidal flat, ecosystem model, nitrogen cycling, water quality purification capability*

1. Introduction

A tidal flat is known as the important place for the biological production in the coastal sea. Moreover a tidal flat is paid to attention because the removing function of bio–elements such as nitrogen and phosphorus from the water column is very high. NAKATA and HATA (1994) claims that the material cycling (mineralization or organization of bio–elements) in the tidal flat determines the water purification function there. SASAKI (2001) qualitatively points out that bivalves in the tidal flat play an important role in the water purifying function in the coastal sea. It is necessary to clarify the material cycling and budget quantitatively in order to understand the ecosystem characteristics and the purification function of the tidal flat. A numerical ecosystem model is a very useful tool to clarify them.

For the ecosystem model of the tidal flat, the Ems–Dollard ecosystem model (BARETTA and RUARDIJ, 1988) is very famous. Their model is constructed with pelagic, benthic and epi–benthic sub–models and simulates the seasonal variation in the tidal flat ecosystem, focusing on the carbon cycling. In Japan, HATA *et al.* (1995) produced a tidal flat ecosystem model based on the Ems–Dollard ecosystem model. Their model emphasizes the benthic ecosystem, focusing on the nitrogen cycling. SOHMA *et al.* (2000) produced a new numerical ecosystem model for the tidal flat and simulated the eco–dynamics over a short–time scale (< 24h). However, these models are too complex to interpret well the calculated results.

In this paper, a simple tidal flat ecosystem model with pelagic and benthic ecosystems is developed on the basis of a pelagic ecosystem model of KAWAMIYA *et al.* (1995). We reproduce the seasonal variation of the observed nitrogen values in a tidal flat of the Seto Inland Sea, Japan from January to December 2000 using the developed simple ecosystem model. From this model results, we clarify the nitrogen cycling and budget in the tidal flat. The relation between a decrease of the biomass of

1. Department of Earth System Science and Technology, Interdisciplinary Graduate School of Engineering Science, Kyushu University, 6–1 Kasuga Koen, Kasuga, Fukuoka 816–8580, Japan
*Present address:
Graduate School of Environmental Science Hokkaido University, Kita 10 Nishi 5, Kita-ku, Sapporo 060-0813 Hokkaido, Japan
2. Research Institute for Applied Mechanics, Kyushu University, 6–1 Kasuga Koen, Kasuga, Fukuoka 816–8580, Japan
3. Graduate School of Environmental Science, Hokkaido University, Kita 13 Nishi 8, Kita–ku, Sapporo 060–0813 Hokkaido, Japan
4. Department of Life Sciences, Kagawa University, 2393 Ikenobe, Miki–cho, Kita–gun, Kagawa 761–0795, Japan

bivalve and the red tide occurrence is investigated by using this model. Finally, the role of this tidal flat is evaluated from the viewpoint of water purifying function in the coastal environment.

2. Study area and Observed data

Our study area is a sandy tidal flat located in the central part of the Seto Inland Sea, southwestern Japan (Fig. 1). The tidal flat covers an area of about 148,000 m^2 and has an average depth of 1 m with the average tidal range of about 2 m. Station B4 is an observation point of benthic biomass in the tidal flat. Stations U and K are the observation points of water characteristics above the tidal flat. Stations KA9 and KA10 are the observation points outside the tidal flat. Station M is an observation point of meteorological parameters by the Takamatsu Meteorological Observatory. There are river discharges into this tidal flat from the Shin, Kasuga and Tsumeta Rivers (Fig. 1).

Samplings were conducted every month at low tide from January to December 2000. At Stn. B4, water temperature, Dissolved Inorganic Nitrogen (DIN) and Chlorophyll. *a* (Chl. *a*) concentrations at the surface (0.0–0.5 cm) and sub–surface (0.5–2.0 cm) layers in the pore water of tidal flat were observed. Nitrogen concentration of microphytobenthos was estimated using C:Chl. *a* ratio (C:Chl. *a*=33.7:1; MONTANI *et al.*, 2003) and C:N ratio (C:N=75.7:10.1; MONTANI *et al.*, 2003). The sampling of macrozoobenthos (polychaeta and bivalve) was carried out between 0 and 10 cm depth by a 10 × 10 cm quadrat method at the same time. Nitrogen concentrations of macrozoobenthos were estimated using a linear empirical equation based on the field observations, that is, the nitrogen concentration of polychaeta N_P (gN) $=0.45 \times 0.17 \times (0.2 \times$ total wet weight (g)), and that of bivalave N_B (mgN) $=96.5 \times (0.184 \times (0.167 \times$ total wet weight (g) $+0.025) + 0.0005)$. We assume that the data at Stn. B4 are representative throughout this tidal flat shown in Fig. 1, that is, the observed data of surface and sub–surface layers in the pore water are assumed to be the data of Box 2 and Box 3 shown in Fig. 2, respectively. While, at Stns. U (water depth was 20 cm in winter and 50 cm in summer) and K (water depth was 20 cm in winter and 50 cm in summer), water temperature, salinity, DIN, Particulated Organic Nitrogen (PON) and Chl. *a* concentrations in the surface water were observed. Nitrogen concentration of phytoplankton was estimated using C:Chl. *a* ratio (C:Chl. *a*=30:1; PARSONS *et al.*, 1984) and Redfield ratio (C:N=106:16; REDFIELD *et al.*, 1963). The observations at Stns. U and K were conducted within one hour before or after the

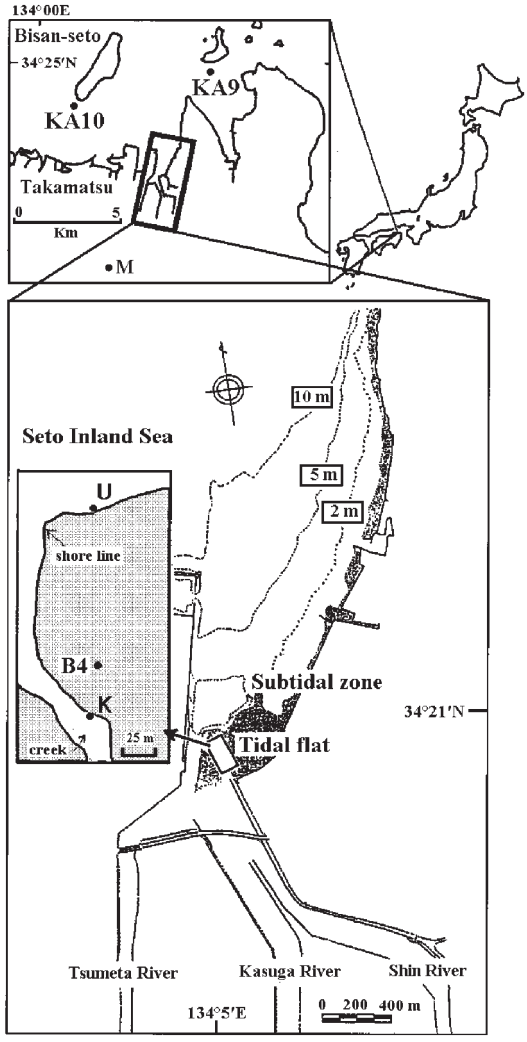

Fig. 1. Study area and location of sampling stations. Stn. B4: station for Box 2 and Box 3 in sediment, Stn. U and Stn. K: stations for Box 1 in water column, Stn. KA9 and Stn. KA10: stations for Box 4 in Bisan-seto, M: Takamatsu Meteorological Observatory.

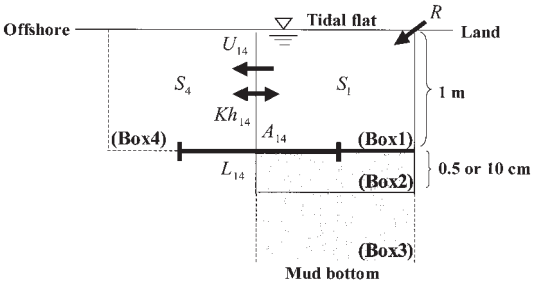

Fig. 2. Horizontal and vertical divisions of the box model. As for symbols, see the text in more detail.

observation at Stn. B4. We can expect that the water at Stn. U covers this tidal flat during the flood tidal current and that at Stn. K during the ebb tidal current, therefore the average data at Stns. U and K represent the sea–water characteristics above this tidal flat, that is, the average observed data at Stns. U and K are the data of Box 1 shown in Fig. 2.

At the same time, the observations of salinity, DIN and Chl. *a* concentrations at Stns. KA9 and KA10 in the Bisan–seto were carried out every month from January to December 2000 by the Kagawa Prefectural Fisheries Experimental Station. We assume that the average data of Stns. KA9 and KA10 are the boundary condition offshore, that is, the observed average data at Stns. KA9 and KA10 are the data of Box 4 shown in Fig. 2.

The load of Total Nitrogen (TN) from three rivers is estimated based on the monthly averaged values of river discharges from three rivers and annually averaged values of TN concentrations in three rivers. The annually averaged river discharge from three rivers and annually averaged TN concentration in three rivers in 2000 are 0.63 $m^3\ s^{-1}$ and 2.4 mg L^{-1}, respectively. The monthly averaged river discharge (R) was estimated from the monthly averaged water levels in three rivers, which were measured by Kagawa Prefecture. We assumed that TN concentrations in three rivers did not change seasonally in 2000 because there was no data on the seasonal variations of TN concentrations in three rivers.

The monthly averaged data of solar radiation and wind speed in 2000 at the Takamatsu Meteorological Observatory were quoted from the Geophysical Review published by the Japan Meteorological Agency.

3. Box model

Fig. 2 shows the box model of this tidal flat. Box 1 is the pelagic ecosystem with 1 m water depth, and Box 2 is the benthic ecosystem for the benthic algae with 0 to 0.5 cm sediment depth and that for the suspension and deposit feeders with 0 to 10 cm sediment depth. We consider the pelagic ecosystem with 1 m depth above the tidal flat because the average tidal range at this tidal flat is about 2 m (MONTANI *et al.*, 2003) and we focus the annually averaged ecosystem there. The boundary condition for Box 2 is given at Box 3, and the boundary condition offshore of Box 1 is given at Box 4 in the Bisan–seto.

The horizontal advection velocity (U_{14}) and the horizontal eddy diffusivity (Kh_{14}) required for the ecosystem model calculation in this study are decided by the physical box model. The equation of water mass conservation is expressed by:

$$R = U_{14} \times A_{14} \tag{1}$$

where R ($m^3\ s^{-1}$) is the river discharge from three rivers (shown in Fig. 3 d), U_{14} ($m\ s^{-1}$) is the horizontal advection velocity between Box 1 and Box 4, A_{14} (m^2) is the cross–sectional area between Box 1 and Box 4 (shown in Table 1).

The equation of salt conservation is expressed by:

$$-U_{14} \times S_1 \times A_{14} + Kh_{14} \times \frac{S_4 - S_1}{L_{14}} \times A_{14} = 0 \tag{2}$$

where S_1 and S_4 are salinity of Box 1 and Box 4, respectively (shown in Fig. 3 c). Kh_{14} ($m^2\ s^{-1}$) is the horizontal eddy diffusivity between Box 1 and Box 4, and L_{14} (m) is the length between Box 1 and Box 4 (shown in Table 1). The temporal variation term in salinity is assumed to be zero because it is much smaller than the spatial variation terms in Eq. (2). The advection and mixing effects by tidal current is expressed by this horizontal eddy diffusivity Kh_{14} in this analysis.

U_{14} and Kh_{14} computed from equations (1) and (2) using the observed data are shown in Fig. 3 (g), (h) respectively.

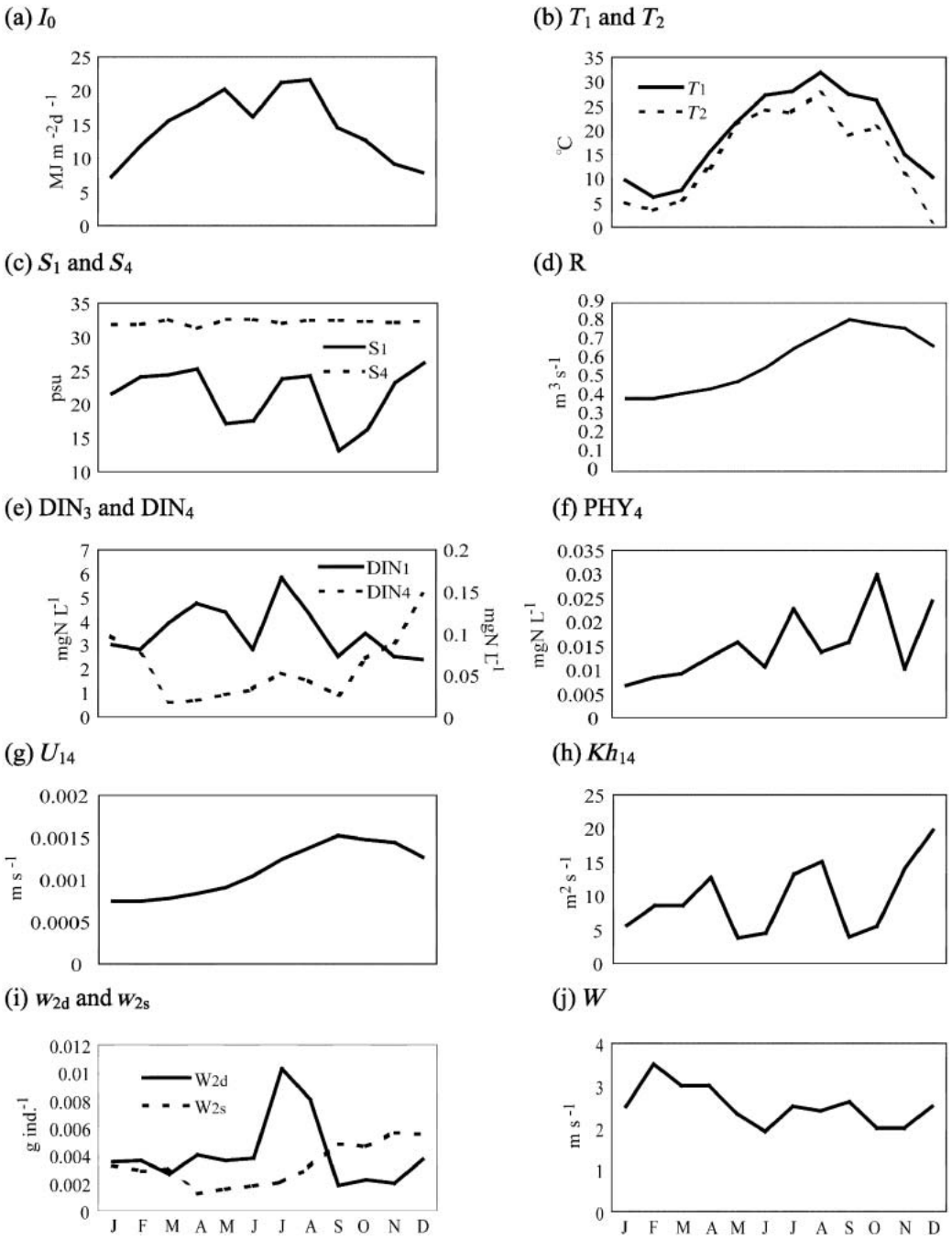

Fig. 3. Seasonal variations in monthly mean input data and boundary conditions for the model calculation. (a) I_0: solar radiation, (b) T_1: sea water temperature in Box 1 and T_2: pore water temperature in Box 2, (c) S_1 and S_4: salinity in Box 1 and Box 4, respectively, (d) R: river discharge, (e) DIN_3 (left axis) and DIN_4 (right axis) : DIN concentration in Box 3 and Box 4, respectively, (f) PHY_4: PHY concentration in Box 4, (g) U_{14}: horizontal advection velocity, (h) Kh_{14}: horizontal eddy diffusivity, (i) w_{2d}: soft-body dry weight per individual of deposit feeder and w_{2s}: soft-body dry weight per individual of suspension feeder, (j) W: monthly averaged wind speed.

Table 1 Parameters used in the model and their references.

	symbol	definition	value	unit	reference
⊿t	dt	time step	100	s	1)
physics	V_1, V_{21}, V_{22}	volume	148×10^{6}, 0.74×10^{6}, 14.8×10^{6}	L	—
	A_{12}・A_{23}, A_{14}	sectional area	148×10^{3}, 530	m^2	—
	L_{12}, L_{23}, L_{14}	distance	50.25×10^{-2}, 10^{-2}, 3750	m	—
	Kv_{12}, Kv_{23}	eddy diffusivity	7.9×10^{-6}, 6.8×10^{-8} (9.8×10^{-10})	$m^2\ s^{-1}$	tuning (2))
DET_1	W_d	sinking speed of detritus	1.0	$m\ d^{-1}$	2)
phytoplankton	Vm_1	maximum photosynthetic speed	1.0	d^{-1}	5)
	Kn_1	half saturation constant for DIN	0.16	$mgN\ L^{-1}$	4)
	k_1	temperature dependency of photosynthesis	0.063	$℃^{-1}$	5)
	$Iopt_1$	optimum light intensity for photosynthesis	50×10^{5}	$cal\ m^{-2}\ d^{-1}$	—
	$A2_1$	ratio of extracellular excertion of DON	0.135	—	5)
	Mpo_1	mortality rate at 0℃	8.15 (2.0)	$L\ mgN^{-1}\ d^{-1}$	tuning (5))
	Kmp_1	temperature coefficient for mortality	0.069	$℃^{-1}$	5)
zooplankton	α_G	maximum grazing speed at 0 ℃	0.4	d^{-1}	6)
	λ	Ivlev' s constant	99.9	$(mgN\ L^{-1})^{-1}$	5)
	PHY^*	threshold of grazing	6.02×10^{-4}	$mgN\ L^{-1}$	5)
	k_g	temperature dependency of grazing	0.069	$℃^{-1}$	5)
	α_1	excretion generation speed	0.4	—	5)
	β_1	egestion generation speed	0.3	—	5)
	Mzo_1	mortality rate at 0℃	4.15	$L\ mgN^{-1}\ d^{-1}$	5)
	Kmz_1	temperature coefficient for mortality	0.069	$℃^{-1}$	5)
microphytobenthos	Vm_2	maximum photosynthetic speed	1.68	d^{-1}	3)
	Kn_2	half saturation constant for DIN	0.16	$mgN\ L^{-1}$	4)
	$A2_2$	ratio of extracellular excertion of DON	0.135	—	5)
	Mpo_2	mortality rate at 0℃	1.0×10^{-3}	$L\ mgN^{-1}\ d^{-1}$	tuning
	Kmp_2	temperature coefficient for mortality	0.069	$℃^{-1}$	5)
deposit feeder	α_{2d}	excretion generation speed	0.4	—	5)
	β_{2d}	egestion generation speed	0.3	—	5)
	Mzo_{2d}	mortality rate at 0℃	1.5×10^{-3}	$L\ mgN^{-1}\ d^{-1}$	tuning
	Kmz_{2d}	temperature coefficient for mortality	0.069	$℃^{-1}$	5)
suspension feeder	α_{2s}	excretion generation speed	0.4	—	5)
	β_{2s}	egestion generation speed	0.3	—	5)
	Mzo_{2s}	mortality rate at 0℃	1.43×10^{-4}	$L\ mgN^{-1}\ d^{-1}$	tuning
	Kmz_{2s}	temperature coefficient for mortality	0.069	$℃^{-1}$	5)
Box1 and Box2	$Vni_{1\ or\ 2}$	decomposition speed of detritus to DIN at 0℃	0.03	d^{-1}	5)
	$Kvni_{1\ or\ 2}$	temperature dependency of decomposition of detritus to DIN	0.069	$℃^{-1}$	5)
	$Vno_{1\ or\ 2}$	decomposition speed of detritus to DON at 0℃	0.03	d^{-1}	5)
	$Kvno_{1\ or\ 2}$	temperature dependency of decomposition of detritus to DON	0.069	$℃^{-1}$	5)
	$Vdi_{1\ or\ 2}$	decomposition speed of DON to DIN at 0℃	0.03	d^{-1}	5)
	$Kvdi_{1\ or\ 2}$	temperature dependency of decomposition of DON to DIN	0.069	$℃^{-1}$	5)

1) Onitsuka *et al.* (2002), 2) Hata *et al.* (1995), 3) Montani *et al.* (2003), 4) Nishijima *et al.* (1990), 5) Kawamiya *et al.* (1995), 6) Fujii *et al.* (2002)

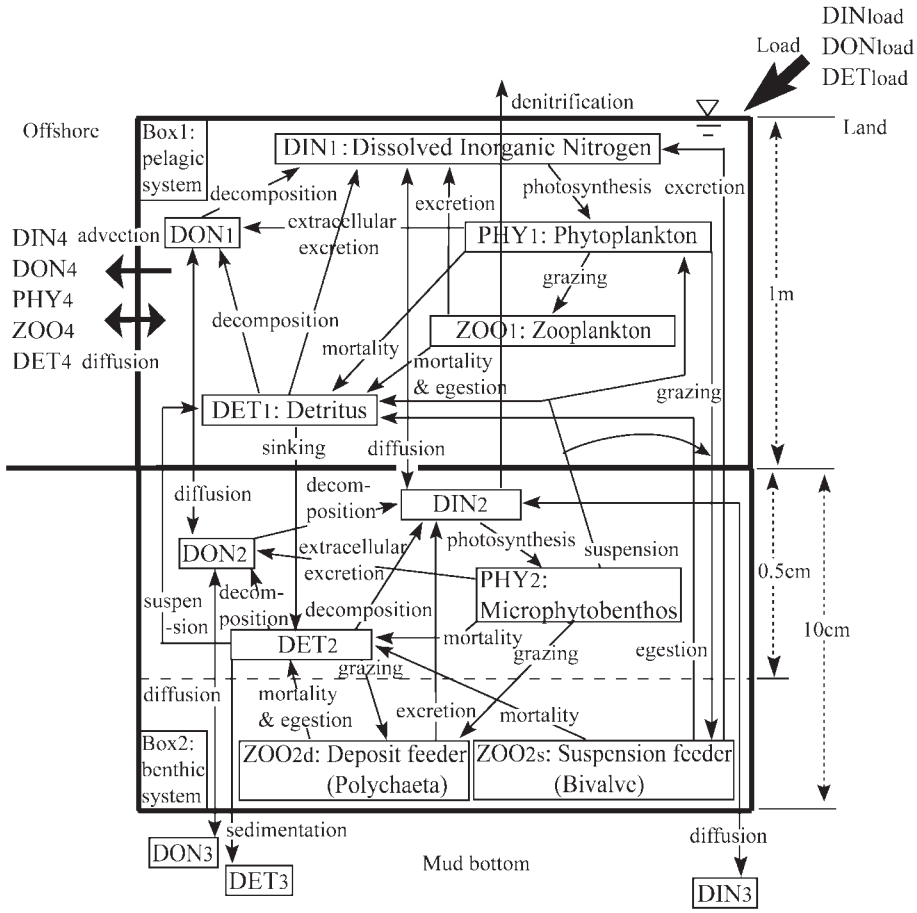

Fig. 4 Schematic diagram of nitrogen cycling in the numerical ecosystem model.

4. Ecosystem models

In the boxes of Box 1 and Box 2 (Fig. 2), a physical, biological and chemical processes concerning the nitrogen cycling shown in Fig. 4 are considered.

The compartments of Box 1 are Dissolved Inorganic Nitrogen (DIN_1), Dissolved Organic Nitrogen (DON_1), phytoplankton (PHY_1), zooplankton (ZOO_1) and detritus (DET_1) within 1 m water column. The compartments of Box 2 are Dissolved Inorganic Nitrogen (DIN_2), Dissolved Organic Nitrogen (DON_2), microphytobenthos (PHY_2) and detritus (DET_2) within 0.5 cm sediment depth, and deposit feeder "polychaeta" (ZOO_{2d}) and suspension feeder "bivalve" (ZOO_{2s}) within 10 cm sediment depth. Reproduction of seasonal variations in DIN_1, PHY_1, PON_1 (particulated organic nitrogen in Box 1 $=PHY_1+ZOO_1+DET_1$), DIN_2, PHY_2, ZOO_{2d} and ZOO_{2s} concentrations at Box 1 and Box 2 is tried in this numerical experiment.

The temporal variations in 9–compartemnt concentrations at Box 1 and Box 2 are given by the following equations, based on KAWAMIYA *et al.* (1995).

$$V_1\frac{dDIN_1}{dt}$$
$$=\text{Load from rivers } (DIN_{LA1})$$
$$-\text{Photosynthesis } (PHY_1)$$
$$+\text{Excretion } (ZOO_1)$$
$$+\text{Decomposition } (DET_1\rightarrow DIN_1)$$
$$+\text{Decomposition } (DET_1\rightarrow DON_1)$$
$$+\text{Excretion } (ZOO_{2s})$$
$$-\text{Vertical Diffusion } (DIN_1, DIN_2)$$
$$-\text{Horizontal Diffusion } (DIN_1, DIN_4)$$
$$-\text{Horizontal Advection } (DIN_1) \qquad (3)$$

$$V_1\frac{d\mathrm{DON_1}}{dt}$$
$$=\mathrm{Load\ from\ rivers\ (DON_{LA1})}$$
$$+\mathrm{Extracellular\ excretion\ (PHY_1)}$$
$$+\mathrm{Decomposition\ (DET_1\rightarrow DON_1)}$$
$$-\mathrm{Decomposition\ (DON_1\rightarrow DIN_1)}$$
$$-\mathrm{Vertical\ Diffusion\ (DON_1,\ DON_2)}$$
$$-\mathrm{Horizontal\ Diffusion\ (DON_1,\ DON_4)}$$
$$-\mathrm{Horizontal\ Advection\ (DON_1)} \quad (4)$$

$$V_1\frac{d\mathrm{PHY_1}}{dt}$$
$$=\mathrm{Photosynthesis\ (PHY_1)}$$
$$-\mathrm{Extracellular\ excretion\ (PHY_1)}$$
$$-\mathrm{Mortality\ (PHY_1)}$$
$$-\mathrm{Grazing\ (PHY_1\rightarrow ZOO_1)}$$
$$-\mathrm{Grazing\ (PHY_1\rightarrow ZOO_{2s})}$$
$$-\mathrm{Horizontal\ Diffusion\ (PHY_1,\ PHY_4)}$$
$$-\mathrm{Horizontal\ Advection\ (PHY_1)}$$
$$+\mathrm{Suspension\ (PHY_2)} \quad (5)$$

$$V_1\frac{d\mathrm{ZOO_1}}{dt}$$
$$=\mathrm{Grazing\ (PHY_1\rightarrow ZOO_1)}$$
$$-\mathrm{Excretion\ (ZOO_1)}$$
$$-\mathrm{Egestion\ (ZOO_1)}$$
$$-\mathrm{Mortality\ (ZOO_1)}$$
$$-\mathrm{Horizontal\ Diffusion\ (ZOO_1,\ ZOO_4)}$$
$$-\mathrm{Horizontal\ Advection\ (ZOO_1)} \quad (6)$$

$$V_1\frac{d\mathrm{DET_1}}{dt}$$
$$=\mathrm{Load\ from\ rivers\ (DET_{LA1})}$$
$$+\mathrm{Mortality\ (PHY_1)}$$
$$+\mathrm{Egestion\ (ZOO_1)}$$
$$+\mathrm{Mortality\ (ZOO_1)}$$
$$-\mathrm{Decomposition\ (DET_1\rightarrow DIN_1)}$$
$$-\mathrm{Decomposition\ (DET_1\rightarrow DON_1)}$$
$$-\mathrm{Horizontal\ Diffusion\ (DET_1,\ DET_4)}$$
$$-\mathrm{Horizontal\ Advection\ (DET_1)}$$
$$-\mathrm{Sinking\ (DET_1)}$$
$$+\mathrm{Suspension\ (PHY_2)}$$
$$+\mathrm{Suspension\ (DET_2)}$$
$$+\mathrm{Egestion\ (ZOO_{2s})} \quad (7)$$

$$V_{21}\frac{d\mathrm{DIN_2}}{dt}$$
$$=-\mathrm{Photosynthesis\ (PHY_2)}$$
$$+\mathrm{Decomposition\ (DET_2\rightarrow DIN_2)}$$
$$+\mathrm{Decomposition\ (DON_2\rightarrow DIN_2)}$$
$$+\mathrm{Excretion\ (ZOO_{2d})}$$
$$-\mathrm{Vertical\ Diffusion\ (DIN_2,\ DIN_3)}$$
$$-\mathrm{Horizontal\ Diffusion\ (DIN_2,\ DIN_1)}$$
$$-\mathrm{Nitrification\ (DIN_2)} \quad (8)$$

$$V_{21}\frac{d\mathrm{DON_2}}{dt}$$
$$=\mathrm{Extracellular\ excretion\ (PHY_2)}$$
$$+\mathrm{Decomposition\ (DET_2\rightarrow DON_2)}$$
$$-\mathrm{Decomposition\ (DON_2\rightarrow DIN_2)}$$
$$-\mathrm{Vertical\ Diffusion\ (DON_2,\ DON_3)}$$
$$-\mathrm{Vertical\ Diffusion\ (DON_2,\ DON_1)} \quad (9)$$

$$V_{21}\frac{d\mathrm{PHY_2}}{dt}$$
$$=\mathrm{Photosynthesis\ (PHY_2)}$$
$$-\mathrm{Extracellular\ excretion\ (PHY_2)}$$
$$-\mathrm{Mortality\ (PHY_2)}$$
$$-\mathrm{Suspension\ (PHY_2)}$$
$$-\mathrm{Grazing\ (PHY_2\rightarrow ZOO_{2d})} \quad (10)$$

$$V_{22}\frac{d\mathrm{ZOO_{2d}}}{dt}$$
$$=\mathrm{Grazing\ (PHY_2\rightarrow ZOO_{2d})}$$
$$+\mathrm{Grazing\ (DET_2\rightarrow ZOO_{2d})}$$
$$-\mathrm{Excretion\ (ZOO_{2d})}$$
$$-\mathrm{Egestion\ (ZOO_{2d})}$$
$$-\mathrm{Mortality\ (ZOO_{2d})} \quad (11)$$

$$V_{22}\frac{d\mathrm{ZOO_{2s}}}{dt}$$
$$=\mathrm{Grazing\ (PHY_1\rightarrow ZOO_{2s})}$$
$$+\mathrm{Grazing\ (PHY_2\rightarrow ZOO_{2s})}$$
$$-\mathrm{Excretion\ (ZOO_{2s})}$$
$$-\mathrm{Egestion\ (ZOO_{2s})}$$
$$-\mathrm{Mortality\ (ZOO_{2s})} \quad (12)$$

$$V_{21}\frac{d\mathrm{DET_2}}{dt}$$
$$=\mathrm{Mortality\ (PHY_2)}$$
$$-\mathrm{Decomposition\ (DET_2\rightarrow DIN_2)}$$
$$-\mathrm{Decomposition\ (DET_2\rightarrow DON_2)}$$
$$-\mathrm{Suspension\ (DET_2)}$$
$$-\mathrm{Grazing\ (DET_2\rightarrow ZOO_{2d})}$$
$$+\mathrm{Egestion\ (ZOO_{2d})}$$
$$+\mathrm{Mortality\ (ZOO_{2d})}$$
$$+\mathrm{Mortality\ (ZOO_{2d})}$$
$$+\mathrm{Sinking\ (DET_1)}$$
$$-\mathrm{Sediment\ (DET_2)} \quad (13)$$

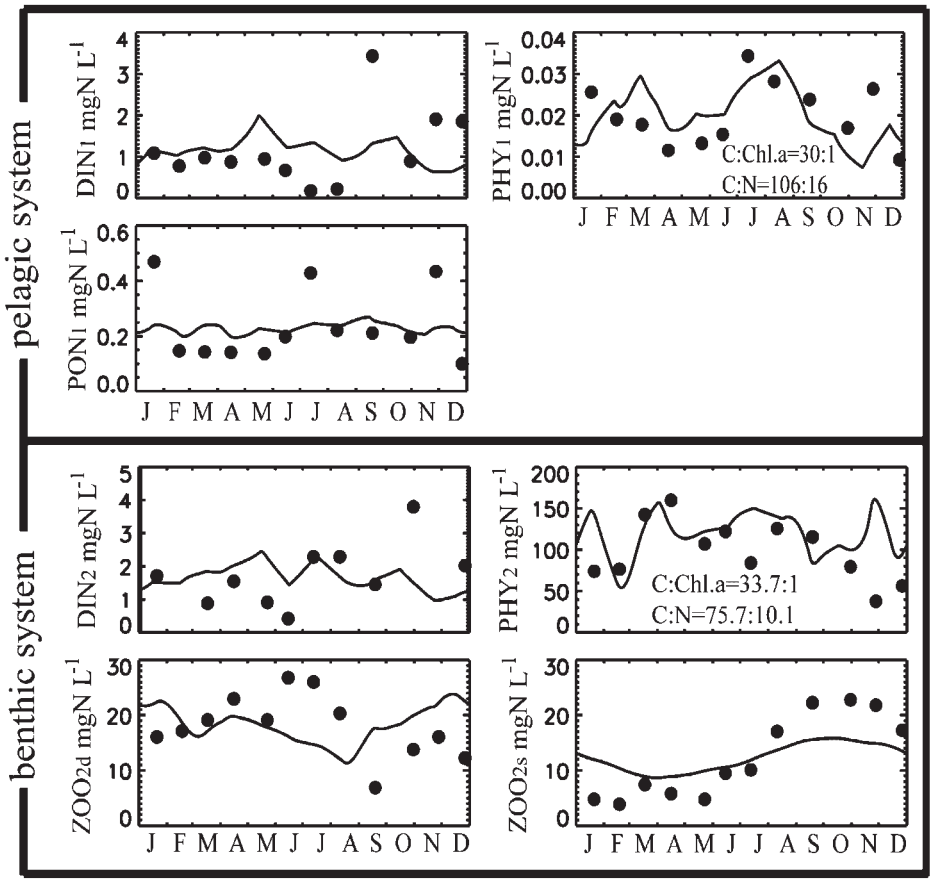

Fig. 5. Seasonal variations in calculated (full line) and observed (dot) values of DIN_1, PHY_1, PON_1, DIN_2, PHY_2, ZOO_{2d}, and ZOO_{2s} in the tidal flat of the Seto Inland Sea.

The details of each term are described in Appendix.

Parameters used in this numerical experiment are shown in Table 1. Almost all parameters are the values referred from the references. The major differences between our parameters and those of references are 1) the vertical eddy diffusivity between Box 2 and Box 3 ($Kv_{23}=6.8\times10^{-8}$ m^2 s^{-1}), that is, vertical eddy diffusivity for the pore water in our model is larger than that of HATA *et al.* (1995) (9.8×10^{-10} m^2 s^{-1}), 2) the sinking speed of detritus and mortality of phytoplankton at 0 ℃ are larger than those from the references. Tuning 1) is necessary for reproducing DIN_2 concentration and 2) for reproducing PON_1 and PHY_1 concentrations. While the mortalities of microphytobenthos (PHY_2), deposit feeder (ZOO_{2d}) and suspension feeder (ZOO_{2s}) are tuned to reproduce their observed concentrations because there is no reference on these parameters.

Figure 3 shows the input data and boundary conditions for the model calculation. We assume that Dissolved Organic Nitrogen in Box 3 (DON_3), that in Box 4 (DON_4), zooplankton in Box 4 (ZOO_4) and detritus in Box 4 (DET_4) concentrations are equal to DIN in Box 3 (DIN_3), that in Box 4 (DIN_4), 0.1 times phytoplankton in Box 4 (PHY_4) and DIN_4, respectively. The loads of DIN, DON and DET from rivers are given as 45, 22 and 33 % of TN load from three rivers, respectively, based on the results of field observation (Dr. K. ICHIMI, personal communication).

The initial conditions for model compartments are given by setting the annually

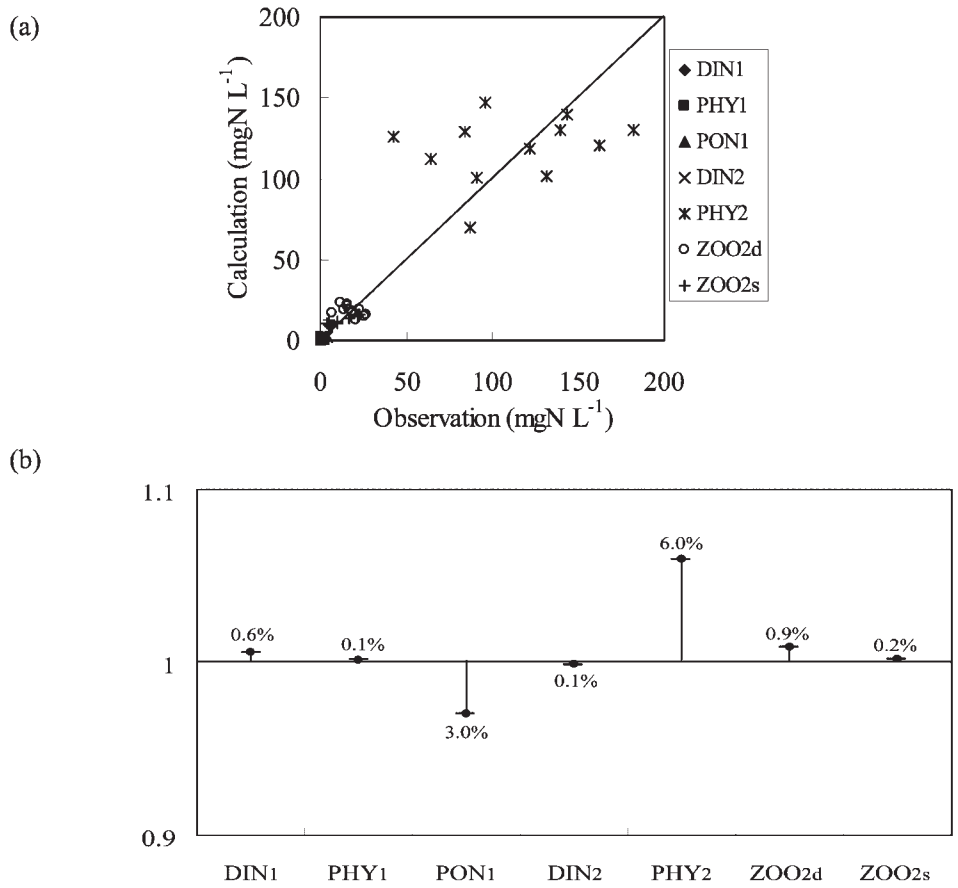

Fig. 6. (a) Correlation between observed and calculated values of nitrogen concentration. (b) Ratio of the annually averaged calculated value and the annually averaged observed value.

averaged values of observed data in the tidal flat. The integration was carried out with a time step of 100 seconds and quasi–steady seasonal variations were obtained 3 years after the start of the calculation. The seasonal variations in the fourth year were analyzed.

5. Results and Discussion

Verification of calculation

Figure 5 shows the seasonal variations in calculated (full line) and observed (dot) DIN_1, PHY_1, PON_1, DIN_2, PHY_2, ZOO_{2d} and ZOO_{2s} concentrations at the tidal flat. The observed DIN_2 concentrations in February and November were missing. The details of seasonal variations are not reproduced enough, but the annually averaged values and phases of seasonal variations are roughly reproduced by our model. Therefore we may consider that this model results reproduce the annually averaged situation of this tidal flat.

Figure 6 (a) shows a correlation between observed and calculated values of nitrogen concentration. Only PHY_2 values are very high because they are concentrated at the surface of bottom mud of tidal flat. The correlation coefficient and the root mean squared error are 0.93 and 15.9 $mgNL^{-1}$, respectively. Fig. 6 (b) shows the ratio of the annually averaged calculated value to the annually averaged observed value of each compartment. We can understand that the differences between the calculated and observed values of each compartment are less than 6.0 % from Fig. 6 (b). After this, our discussion will be focused on the annually averaged values.

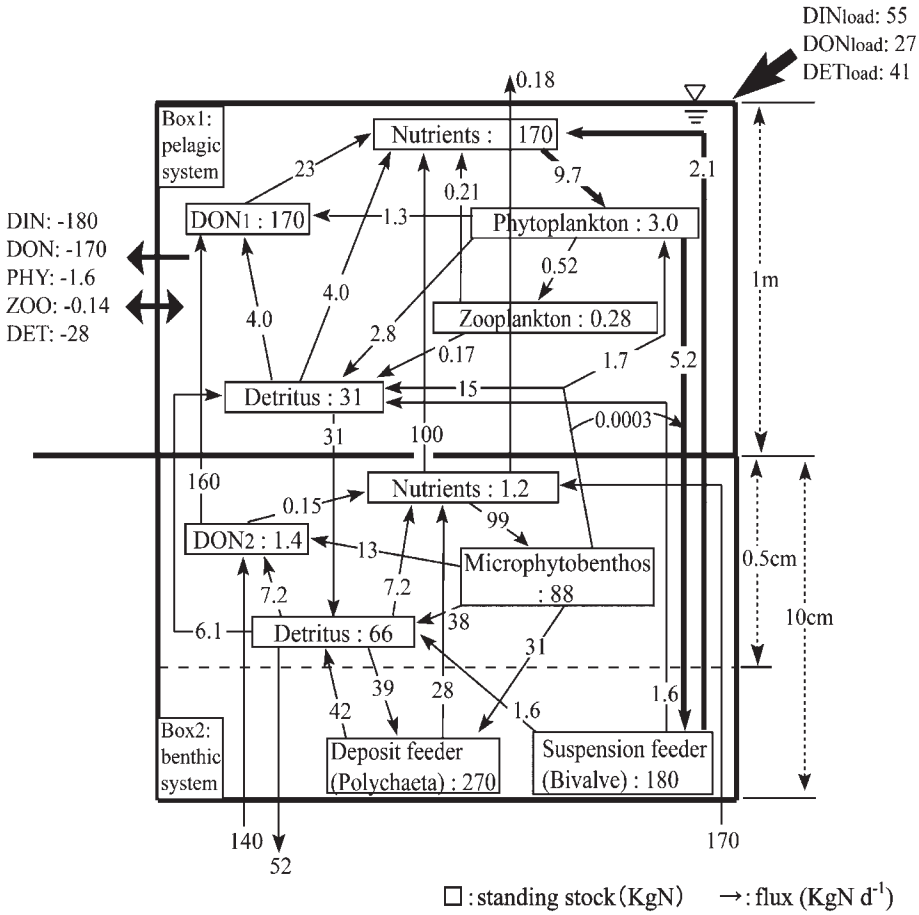

Fig. 7. Annually averaged values of nitrogen standing stocks (KgN) and their fluxes (KgN d^{-1}) in the tidal flat of the Seto Inland Sea. Thick arrows show the main pathway.

Present case and the case where there is no suspension feeder (bivalve)

Figure 7 shows the annually averaged values of nitrogen standing stocks and their fluxes in the present case with the suspension feeder (bivalve) at the tidal flat. The numbers in the small box show the standing stocks with the unit of KgN. The numbers on the arrow show the fluxes with the unit of KgN d^{-1}. The main pathway of the nitrogen cycling in the tidal flat was nutrients in Box 1 (DIN_1) →phytoplankton (PHY_1) →suspension feeder (ZOO_{2s}) → nutrients in Box 1 (DIN_1). The suspension feeder plays an important role in the exchange of nitrogen between the pelagic and benthic ecosystems in the tidal flat.

In recent years, the standing stock of suspension feeder has dramatically decreased while the number of red tide occurrence has increased in Japanese coastal seas with tidal flats though the nutrient load from the river has not increased (e.g. TSUTUMI *et al.*, 2003). We pay our attention to the role of suspension feeder, which is known to have the water quality purification capability by filtration of suspended matter, and want to predict the phytoplankton concentration in the case where there is no suspension feeder.

Figure 8 shows the seasonal variations of calculated values in the present case with the suspension feeder (solid line) and in the case where there is no suspension feeder (broken line). When there is no suspension feeder (ZOO_{2s}) in the tidal flat, the nitrogen concen-

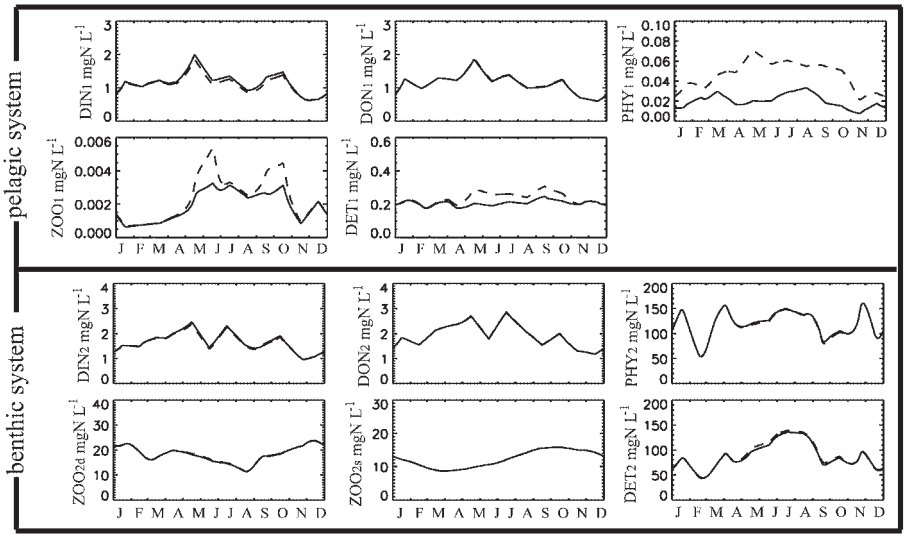

Fig. 8. Seasonal variations of calculated values in the present case with the suspension feeder (solid line) and the case where there is no suspension feeder (broken line).

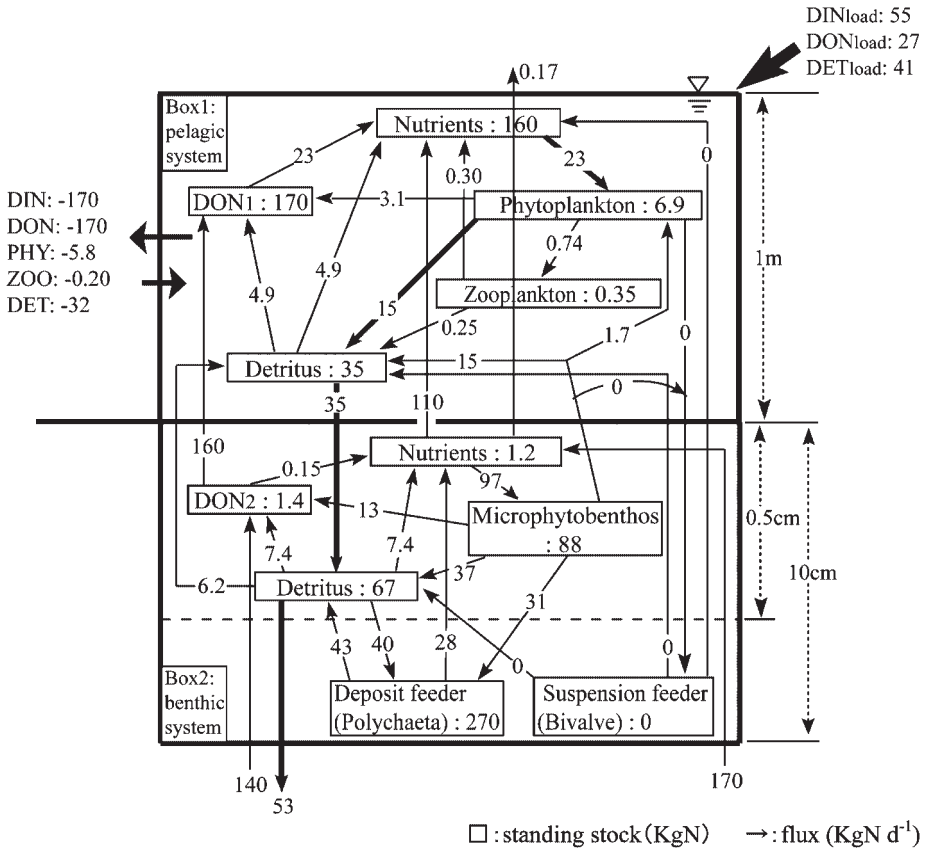

Fig. 9. Annually averaged values of nitrogen standing stocks (KgN) and their fluxes (KgN d^{-1}) in the case where there is no suspension feeder at the tidal flat. Thick arrows show the main pathway.

trations of phytoplankton (PHY_1), zooplankton (ZOO_1) and detritus (DET_1) in Box 1, and detritus (DET_2) in Box 2 increase and the nitrogen concentration of nutrient in Box 1 (DIN_1) decreases.

The nitrogen concentration of phytoplankton (PHY_1) in Box 1 is about 2.3 times as high as the present case because of the vanishing of

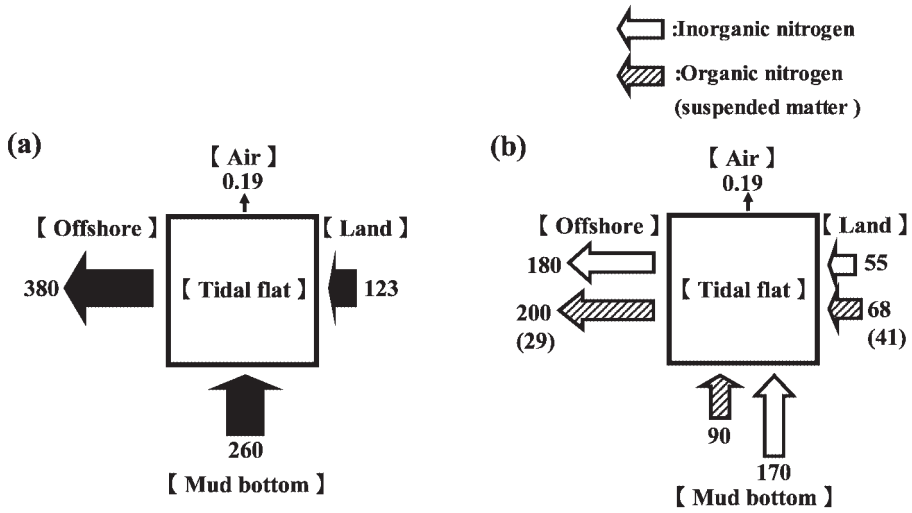

Fig. 10. Annually averaged values of nitrogen budget (a) and inorganic and organic nitrogen budgets (b) in the present case with the suspension feeder.

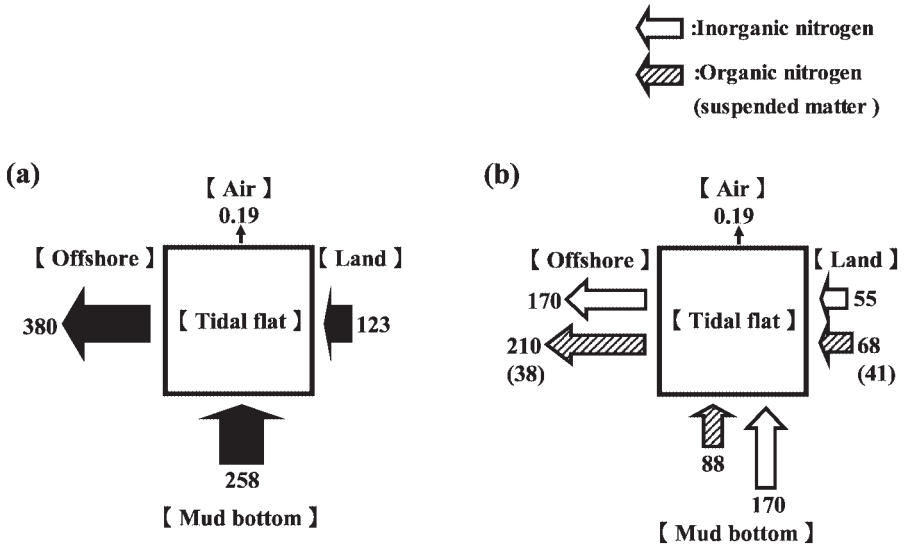

Fig. 11. Annually averaged values of nitrogen budget (a) and inorganic and organic nitrogen budgets (b) in the case where there is no suspension feeder (bivalve) .

grazing pressure and the red tide (PHY_1 concentration of 0.053 mgN L^{-1} corresponds to 10 μgChl. a L^{-1} which is the red tide concentration of diatom) may occur.

Figure 9 shows the annually averaged values of nitrogen standing stocks and their fluxes in the case where there is no suspension feeder at the tidal flat. The main pathway of the nitrogen cycling becomes nutrients in Box 1 (DIN_1) →phytoplankton (PHY_1) →detritus in Box 1 (DET_1) →detritus in Box 2 (DET_2).

Water quality purification capability

There are various viewpoints about the purification capability in the coastal sea (e.g. NAKATA and HATA, 1994; HATA *et al.*, 1995; 1996; 2004; SUZUKI *et al.*, 1997). In this paper, we define the purification capability as follows. One is the conversion from organic nitrogen to inorganic nitrogen (that is, mineralization). The other is the reduction of suspended matter being transported offshore (that is, removal capability of the suspended matter from the water column). In order to evaluate the purification capability of the tidal flat, we pay attention to the nitrogen budget in this tidal flat (Fig. 10 (a) and Fig. 11 (a)), and divide their budgets into inorganic nitrogen and organic nitrogen in this tidal flat (Fig. 10 (b) and Fig. 11 (b)). Figures 10 and 11 are made from Fig. 7 and Fig. 9, and they show the annually averaged values of nitrogen budget (a) and inorganic and organic nitrogen budgets (b) in the present case with the suspension feeder (Fig. 10) and the case where there is no suspension feeder (Fig. 11) at the tidal flat, respectively.

From the comparison of Fig. 10 (a) with Fig. 11 (a), we can understand that, in the case where there is no suspension feeder (Fig. 11 (a)), the nitrogen flux from the tidal flat to the mud bottom is smaller than that in the present case because the increase of detritus deposition. The detritus which is deposited to the mud bottom causes the degradation of the marine environment in this tidal flat.

To evaluate the water quality purification capability, we pay attention to the nitrogen fluxes from the land to the tidal flat (inflow) and from the tidal flat to the offshore (outflow) in Figs.10 and 11.

From the comparison of Fig. 10 (b) and Fig. 11 (b), the water quality purification capability of the tidal flat in the case where there is no suspension feeder is lower because the outflow of organic nitrogen increases and that of inorganic nitrogen decreases compared to those in the present case.

6. Conclusion

A simple tidal flat model with pelagic and benthic ecosystems was developed in order to analyze the nitrogen cycling in an inter–tidal flat of the Seto Inland Sea, Japan. The main pathway of the nitrogen cycling in the present tidal flat with the suspension feeder is nutrients in the pelagic system →phytoplankton → suspension feeder (bivalve) →nutrients in the pelagic system. When there is no suspension feeder in the tidal flat, the main pathway of the nitrogen cycling in the tidal flat changes into nutrients in the pelagic system →phytoplankt on →detritus in the pelagic system →detritus in the benthic system, and the concentration of phytoplankton is about 2.3 times as high as that in the present case with the suspension feeder. It results in the occurrence of red tide in the tidal flat. From the view point of the water quality purification capability of tidal flat, the water quality purification capability of the tidal flat becomes lower in the case without the suspension feeder in the tidal flat because the outflow of organic nitrogen increases compared to that in the present case.

The material cycling in the tidal flat is greatly changed by the change of benthic communities there and at the same time, the water purification capability of the tidal flat will be changed. The suspension feeder plays a very important role in the water purification capability of tidal flat.

Appendix

The seasonal variations in 9–component concentrations (mgN L^{-1} except g L^{-1} of ZOO_{2d}* and ZOO_{2s}* which are a soft–body dry weight) at Box 1 and Box 2 are given by the following equations. Governing equations and ecosystem processes are based on KAWAMIYA *et al.* (1995).

$$V_1\frac{d\mathrm{DIN}_1}{dt}$$
$$=\text{Load from rivers }(\mathrm{DIN}_{LA1})$$
$$-\text{Photosynthesis }(\mathrm{PHY}_1)$$
$$+\text{Excretion }(\mathrm{ZOO}_1)$$
$$+\text{Decomposition }(\mathrm{DET}_1\rightarrow \mathrm{DIN}_1)$$
$$+\text{Decomposition }(\mathrm{DET}_1\rightarrow \mathrm{DON}_1)$$
$$+\text{Excretion }(\mathrm{ZOO}_{2s})$$
$$-\text{Vertical Diffusion }(\mathrm{DIN}_1,\ \mathrm{DIN}_2)$$
$$-\text{Horizontal Diffusion }(\mathrm{DIN}_1,\ \mathrm{DIN}_4)$$
$$-\text{Horizontal Advection }(\mathrm{DIN}_1)$$
$$=DIN_{LA1}$$
$$+V_1\ (-A1_1\ \mathrm{PHY}_1+B2_1\ \mathrm{ZOO}_1$$
$$+C1_1\ \mathrm{DET}_1+D1_1\ \mathrm{DON}_1)$$
$$+V_{22}\ B2_{2s}\ \mathrm{ZOO}_{2s}$$
$$-A_{12}\frac{Kv_{12}}{L_{12}}\ (\mathrm{DIN}_1-\mathrm{DIN}_2)$$
$$-A_{14}\frac{Kh_{14}}{L_{14}}\ (\mathrm{DIN}_1-DIN_4)$$
$$-A_{14}\ U_{14}\ \mathrm{DIN}_1 \qquad \text{(A1)}$$

$$V_1\frac{d\mathrm{DON}_1}{dt}$$
$$=\text{Load from rivers }(\mathrm{DON}_{LA1})$$
$$+\text{Extracellular excretion }(\mathrm{PHY}_1)$$
$$+\text{Decomposition }(\mathrm{DET}_1\rightarrow \mathrm{DON}_1)$$
$$-\text{Decomposition }(\mathrm{DON}_1\rightarrow \mathrm{DIN}_1)$$
$$-\text{Vertical Diffusion }(\mathrm{DON}_1,\ \mathrm{DON}_2)$$
$$-\text{Horizontal Diffusion }(\mathrm{DON}_1,\ \mathrm{DON}_4)$$
$$-\text{Horizontal Advection }(\mathrm{DON}_1)$$
$$=DON_{LA1}$$
$$+V_1\ (A1_1\ A2_1\ \mathrm{PHY}_1$$
$$+C2_1\ \mathrm{DET}_1-D1_1\ \mathrm{DON}_1)$$
$$-A_{12}\frac{Kv_{12}}{L_{12}}\ (\mathrm{DON}_1-\mathrm{DON}_2)$$
$$-A_{14}\frac{Kh_{14}}{L_{14}}\ (\mathrm{DON}_1-DON_4)$$
$$-A_{14}U_{14}\ \mathrm{DON}_1 \qquad \text{(A2)}$$

$$V_1\frac{d\mathrm{PHY}_1}{dt}$$
$$=\text{Photosynthesis }(\mathrm{PHY}_1)$$
$$-\text{Extracellular excretion }(\mathrm{PHY}_1)$$
$$-\text{Mortality }(\mathrm{PHY}_1)$$
$$-\text{Grazing }(\mathrm{PHY}_1\rightarrow \mathrm{ZOO}_1)$$
$$-\text{Grazing }(\mathrm{PHY}_1\rightarrow \mathrm{ZOO}_{2s})$$
$$-\text{Horizontal Diffusion }(\mathrm{PHY}_1,\ \mathrm{PHY}_4)$$
$$-\text{Horizontal Advection }(\mathrm{PHY}_1)$$
$$+\text{Suspension }(\mathrm{PHY}_2)$$
$$=V_1\ (A1_1\ \mathrm{PHY}_1-A1_1\ A2_1\ \mathrm{PHY}_1-A3_1\ \mathrm{PHY}_1^2$$
$$-B1_1\ \mathrm{ZOO}_1)$$
$$-V_{22}\ B1_{2s-1}\ \mathrm{ZOO}_{2s}$$
$$-A_{14}\frac{Kh_{14}}{L_{14}}\ (\mathrm{PHY}_1-PHY_4)$$
$$-A_{14}\ U_{14}\ \mathrm{PHY}_1$$
$$+b\times\ c\times\ V_{21}\ A4_2\ \mathrm{PHY}_2 \qquad \text{(A3)}$$

$$V_1\frac{d\mathrm{ZOO}_1}{dt}$$
$$=\text{Grazing }(\mathrm{PHY}_1\rightarrow \mathrm{ZOO}_1)$$
$$-\text{Excretion }(\mathrm{ZOO}_1)$$
$$-\text{Egestion }(\mathrm{ZOO}_1)$$
$$-\text{Mortality }(\mathrm{ZOO}_1)$$
$$-\text{Horizontal Diffusion }(\mathrm{ZOO}_1,\ \mathrm{ZOO}_4)$$
$$-\text{Horizontal Advection }(\mathrm{ZOO}_1)$$
$$=V_1\ (B1_1\ \mathrm{ZOO}_1-B2_1\ \mathrm{ZOO}_1-B3_1\ \mathrm{ZOO}_1$$
$$-B4_1\ \mathrm{ZOO}_1^2)$$
$$-A_{14}\frac{Kh_{14}}{L_{14}}\ (\mathrm{ZOO}_1-ZOO_4)$$
$$-A_{14}\ U_{14}\ \mathrm{ZOO}_1 \qquad \text{(A4)}$$

$$V_1\frac{d\mathrm{DET}_1}{dt}$$
$$=\text{Load from rivers }(\mathrm{DET}_{LA1})$$
$$+\text{Mortality }(\mathrm{PHY}_1)$$
$$+\text{Egestion }(\mathrm{ZOO}_1)$$
$$+\text{Mortality }(\mathrm{ZOO}_1)$$
$$-\text{Decomposition }(\mathrm{DET}_1\rightarrow \mathrm{DIN}_1)$$
$$-\text{Decomposition }(\mathrm{DET}_1\rightarrow \mathrm{DON}_1)$$
$$-\text{Horizontal Diffusion }(\mathrm{DET}_1,\ \mathrm{DET}_4)$$
$$-\text{Horizontal Advection }(\mathrm{DET}_1)$$
$$-\text{Sinking }(\mathrm{DET}_1)$$
$$+\text{Suspension }(\mathrm{PHY}_2)$$
$$+\text{Suspension }(\mathrm{DET}_2)$$
$$+\text{Egestion }(\mathrm{ZOO}_{2s})$$
$$=DET_{LA1}$$
$$+V_1\ (A3_1\ \mathrm{PHY}_1^2+B3_1\ \mathrm{ZOO}_1$$
$$+B4_1\ \mathrm{ZOO}_1^2-C1_1\ \mathrm{DET}_1-C2_1\ \mathrm{DET}_1)$$
$$-A_{14}\frac{Kh_{14}}{L_{14}}\ (\mathrm{DET}_1-DET_4)$$
$$-A_{14}\ U_{14}\ \mathrm{DET}_1$$
$$-A_{12}\ w_d\ \mathrm{DET}_1$$
$$+\ (1-b)\ \times\ c\times\ V_{21}\ A4_2\ \mathrm{PHY}_2$$
$$+V_{21}\ A4_2\ \mathrm{DET}_2$$
$$+V_{22}\ B3_{2s}\ \mathrm{ZOO}_{2s} \qquad \text{(A5)}$$

$$V_{21}\frac{d\mathrm{DIN}_2}{dt}$$
$$=\text{Photosynthesis }(\mathrm{PHY}_2)$$
$$+\text{Decomposition }(\mathrm{DET}_2\rightarrow \mathrm{DIN}_2)$$
$$+\text{Decomposition }(\mathrm{DON}_2\rightarrow \mathrm{DIN}_2)$$

$$
\begin{aligned}
&+\text{Excretion } (ZOO_{2d})\\
&-\text{Vertical Diffusion } (DIN_2, DIN_3)\\
&-\text{Horizontal Diffusion } (DIN_2, DIN_1)\\
&-\text{Nitrification } (DIN_2)\\
=\ & V_{21}\,(-A1_2\ PHY_2+C1_2\ DET_2+D1_2\ DON_2)\\
&+V_{22}\,(B2_{2d}\ \ ZOO_{2d})\\
&-A_{23}\frac{Kv_{23}}{L_{23}}\,(DIN_2-DIN_3)\\
&-A_{12}\frac{Kv_{12}}{L_{12}}\,(DIN_2-DIN_1)\\
&-A_{12}\,E1_2\ DIN_2 \qquad \text{(A6)}
\end{aligned}
$$

$$
\begin{aligned}
&V_{21}\frac{dDON_2}{dt}\\
=\ &\text{Extracellular excretion } (PHY_2)\\
&+\text{Decomposition } (DET_2\rightarrow DON_2)\\
&-\text{Decomposition } (DON_2\rightarrow DIN_2)\\
&-\text{Vertical Diffusion } (DON_2, DON_3)\\
&-\text{Vertical Diffusion } (DON_2, DON_1)\\
=\ & V_{21}\,(A1_2\ A2_2\ PHY_2+C2_2\ DET_2-D1_2\ DON_2)\\
&-A_{23}\frac{Kv_{23}}{L_{23}}\,(DON_2-DON_3)\\
&-A_{12}\frac{Kv_{12}}{L_{12}}\,(DON_2-DON_1) \qquad \text{(A7)}
\end{aligned}
$$

$$
\begin{aligned}
&V_{21}\frac{dPHY_2}{dt}\\
=\ &\text{Photosynthesis } (PHY_2)\\
&-\text{Extracellular excretion } (PHY_2)\\
&-\text{Mortality } (PHY_2)\\
&-\text{Suspension } (PHY_2)\\
&-\text{Grazing } (PHY_2\rightarrow ZOO_{2d})\\
=\ & V_{21}\,(A1_2\ PHY_2-A1_2\ A2_2\ PHY_2-A3_2\ PHY_2^2\\
&-A4_2\ PHY_2)\\
&-V_{22}\,(B1_{2d-1}\ ZOO_{2d}) \qquad \text{(A8)}
\end{aligned}
$$

$$
\begin{aligned}
&V_{22}\frac{dZOO_{2d}}{dt}\\
=\ &\text{Grazing } (PHY_2\rightarrow ZOO_{2d})\\
&+\text{Grazing } (DET_2\rightarrow ZOO_{2d})\\
&-\text{Excretion } (ZOO_{2d})\\
&-\text{Egestion } (ZOO_{2d})\\
&-\text{Mortality } (ZOO_{2d})\\
=\ & V_{22}\,(B1_{2d-1}\ ZOO_{2d}{}^*+B1_{2d-2}\ ZOO_{2d}{}^*\\
&-B2_{2d}\ ZOO_{2d}{}^*-B3_{2d}\ ZOO_{2d}{}^*-B4_{2d}\ ZOO_{2d}{}^2)\\
& \qquad \text{(A9)}
\end{aligned}
$$

$$
\begin{aligned}
&V_{22}\frac{dZOO_{2s}}{dt}\\
=\ &\text{Grazing } (PHY_1\rightarrow ZOO_{2s})\\
&+\text{Grazing } (PHY_2\rightarrow ZOO_{2s})\\
&-\text{Excretion } (ZOO_{2s})\\
&-\text{Egestion } (ZOO_{2s})\\
&-\text{Mortality } (ZOO_{2s})\\
=\ & V_{22}\,(B1_{2s-1}\ ZOO_{2s}{}^*+B1_{2s-2}\ ZOO_{2s}{}^*-B2_{2s}\ ZOO_{2s}{}^*\\
&-B3_{2s}\ ZOO_{2s}{}^*-B4_{2s}\ ZOO_{2s}{}^2) \qquad \text{(A10)}
\end{aligned}
$$

$$
\begin{aligned}
&V_{21}\frac{dDET_2}{dt}\\
=\ &\text{Mortality } (PHY_2)\\
&-\text{Decomposition } (DET_2\rightarrow DIN_2)\\
&-\text{Decomposition } (DET_2\rightarrow DON_2)\\
&-\text{Suspension } (DET_2)\\
&-\text{Grazing } (DET_2\rightarrow ZOO_{2d})\\
&+\text{Egestion } (ZOO_{2d})\\
&+\text{Mortality } (ZOO_{2d})\\
&+\text{Mortality } (ZOO_{2s})\\
&+\text{Sinking } (DET_1)\\
&-\text{Sediment } (DET_2)\\
=\ & V_{21}\,(A3_2\ PHY_2^2-C1_2\ DET_2\\
&-C2_2\ DET_2-0.5\ A4_2\ DET_2)\\
&+V_{22}\,(-B1_{2d-2}\ ZOO_{2d}+B3_{2d}\ ZOO_{2d}\\
&+B4_{2d}\ ZOO_{2d}{}^2+B4_{2s}\ ZOO_{2s}{}^2)\\
&+A_{12}\ w_d\ DET_1\\
&-A_{23}\ S_d\ DET_2 \qquad \text{(A11)}
\end{aligned}
$$

Here dt is the time step in second. V is the volume in liter, subscript 1, 21 and 22 denote 0 to 1 m water depth in Box 1, 0 to 0.5 cm sediment depth in Box 2 and 0 to 10 cm sediment depth in Box 2, respectively. A is the sectional area in m^2, L is the distance in meter, U is the current velocity in m s^{-1}, Kh is the horizontal eddy diffusivity in m^2 s^{-1}, Kv is the vertical eddy diffusivity in m^2 s^{-1}, subscript 12 denotes between Box 1 and Box 2, subscript 23 denotes between Box 2 and Box 3, subscript 14 denotes between Box 1 and Box 4. w_d is the sinking speed of detritus in m s^{-1}, s_d is the sedimentation speed of detritus in m s^{-1}. Subscript LA1 denotes the load from rivers.

$A1$ is photosynthesis by primary producer and is represented by the following equation:

$$
\begin{aligned}
A1_1 = Vm_1\left(\frac{DIN_1}{DIN_1+Kn_1}\right)\times\exp\,(k_1T_1)\\
\times\frac{I_1}{Iopt_1}\exp\left(1-\frac{I_1}{Iopt_1}\right) \qquad \text{(A12)}
\end{aligned}
$$

$$
A1_2 = Vm_2\left(\frac{DIN_2}{DIN_2+Kn_2}\right)\times\frac{(0.081\times T_2+1.48)}{3.83}
$$

$$\times\frac{(7.85-\mathrm{TANH}(\frac{0.0785-I_2}{7.85}))}{8.84} \quad \text{(A13)}$$

where subscripts 1 and 2 denote Box 1 (or phytoplankton in Box 1) and Box 2 (or microphytobenthos in Box 2), respectively. The function of temperature and light in the photosynthesis equation by microphytobenthos (that is, the second and third term in right-hand side of Eq. (A13)) is experimental equation of MONTANI *et al.* (2003). Vm (d^{-1}) is the maximum photosynthesis speed of primary producer, Kn (mgN L^{-1}) is a half saturation constant for DIN, k_1 ($℃^{-1}$) is the temperature dependency of photosynthesis, T (℃) is water temperature, I is the average light intensity and $Iopt_1$ (cal m^{-2} d^{-1}) is optimum light intensity for photosynthesis. I_1 (converted into cal m^{-2} d^{-1}; 1 J m^{-2} d^{-1}=1/4.1868 cal m^{-2} d^{-1}) and I_2 (converted into μE m^{-2} d^{-1}; 1 MJ m^{-2} d^{-1} =4.52 E m^{-2} d^{-1}) are the average light intensity reaching the Box 1 and Box 2, respectively. They were calculated using the following equation:

$$I_1=I_0\times d \quad \text{(A14)}$$
$$I_2=I_0\times d\times r \quad \text{(A15)}$$

where I_0 (MJ m^{-2} d^{-1}) is the total surface radiation observed at the Takamatsu Meteorological Observatory. d is the percentage of irradiance reduction through the water column and is calculated using the following exponential equation (MONTANI *et al.*, 2003) :

$$d=\frac{95.2}{H_1}\int_0^{H_1}10^{(-0.143Z_1)}\,dZ_1 \quad \text{(A16)}$$

where H_1 (m) is the water depth. r is the percentage of light reduction through the sediments and is calculated using the following exponential equation (MONTANI *et al.*, 2003) :

$$r=\frac{100}{H_2}\int_0^{H_2}10^{(-1.49Z_2)}\,dZ_2 \quad \text{(A17)}$$

where H_2 (mm) is the sediment depth.

$A2$ is the ratio of extracellular excertion of DON accompanying photosynthesis and is given by the constant value (Table 1). Subscripts 1 and 2 denote phytoplankton in Box 1 and microphytobenthos in Box 2, respectively.

$A3$ is the mortality of primary producer and is represented by the following equation:

$$A3_1=Mpo_1\exp(kmp_1\,T_1) \quad \text{(A18)}$$
$$A3_2=Mpo_2\exp(kmp_2\,T_2) \quad \text{(A19)}$$

where subscripts 1 and 2 denote Box 1 (or phytoplankton in Box 1) and Box 2 (or microphytobenthos in Box 2), respectively. Mpo (L mgN^{-1} d^{-1}) is the mortality rate of primary producer at 0℃, kmp ($℃^{-1}$) is temperature coefficient for mortality.

$A4$ is the suspension speed of microphytobenthos and detritus caused by wind waves and is represented by the following equation:

$$A4=a\times W^2 \quad \text{(A20)}$$

where a is coefficient, W (m s^{-1}) is the wind speed. b and c are a coefficient about suspension of microphytobenthos (PHY_2). The suspended PHY_2 is assumed as follows. All of the suspended PHY_2 becomes a target as food of suspension feeder ZOO_{2s}, however, the suspended PHY_2 not eaten by suspension feeder ZOO_{2s} becomes PHY_1 (b percent) and DET_1 (1–b percent). c is a coefficient and is represented by the following equation:

$$c=1-\frac{0.5\times V_{22}\,CR_{2s}\,ZOO_{2s}}{V_1} \quad \text{(A21)}$$

$B1$ is the grazing by secondary producer. $B1_1$ is the grazing PHY_1 by zooplankton and is represented by the following equation:

$$B1_1=\alpha_G\left\{1-\exp(\lambda(PHY^*-PHY_1))\right\}\exp(k_gT_1) \quad \text{(A22)}$$

where subscript 1 denote Box 1 (or zooplankton in Box 1). α_G (d^{-1}) is the maximum grazing speed at 0 ℃, λ (($mgN\ L^{-1}$) $^{-1}$) is Ivlev's constant, PHY* (mgN L^{-1}) is the threshold of grazing (that is, when the concentration of phytoplankton is lower than PHY*, the grazing by zooplankton becomes zero). k_g ($℃^{-1}$) denotes the temperature dependency of grazing. The PHY_2 and DET_2 grazing by deposit feeder are based on the grazing by suspension feeder (NAKAMURA, 2004) and are represented by the

following equation, respectively:

$$B1_{2d-1} = 0.5 \times CR_{2d} \times \mathrm{PHY}_2 \quad \text{(A23)}$$
$$B1_{2d-2} = 0.5 \times CR_{2d} \times \mathrm{DET}_2 \quad \text{(A24)}$$

where subscripts 2, 2d, 2d–1 and 2d–2 denote Box 2, deposit feeder in Box 2, the PHY_2 grazing by deposit feeder in Box 2, the DET_2 grazing by deposit feeder in Box 2, respectively. CR_{2d} is the clearance rate by deposit feeder and is represented by the following equation:

$$CR_{2d} = 2.41 \times w_{2d}^{-0.32} \times f(T_2) \quad \text{(A25)}$$

$$f(T_2) = \frac{-0.0549 \times T_2^2 + 2.67 \times T_2 - 11.2}{18.9} \quad \text{(A26)}$$

where w_{2d} (g ind.$^{-1}$) is soft–body dry weight of deposit feeder, f is the function of temperature. The PHY_1 and $PHY_2{}^{\dagger}$ grazing by suspension feeder are represented by the following equation (NAKAMURA, 2004), respectively:

$$B1_{2s-1} = 0.5 \times CR_{2s} \times \mathrm{PHY}_1 \quad \text{(A27)}$$
$$B1_{2s-2} = 0.5 \times CR_{2s} \times \mathrm{PHY}_2{}^{\dagger} \quad \text{(A28)}$$

$$\mathrm{PHY}_2{}^{\dagger} = \frac{V_{21} \times A4_2 \times \mathrm{PHY}_2}{V_1} \quad \text{(A29)}$$

where subscripts 2s, 2s–1 and 2s–2 denote suspension feeder in Box 2, the PHY_1 and $PHY_2{}^{\dagger}$ grazing by suspension feeder in Box 2, respectively. $\mathrm{PHY}_2{}^{\dagger}$ is the suspended PHY_2 in Box 1. CR_{2s} is the clearance rate by suspension feeder and is represented by the following equation:

$$CR_{2s} = 2.41 \times w_{2s}^{-0.32} \times f(T_1) \quad \text{(A30)}$$

$$f(T_1) = \frac{-0.0549 \times T_1^2 + 2.67 \times T_1 - 11.2}{18.9} \quad \text{(A31)}$$

where w_{2d} is soft–body dry weight of suspension feeder, f is the function of temperature.

$B2$ is the excretion generation speed of secondary producer and is represented by the following equation:

$$B2_1 = \alpha_1 B1_1 \quad \text{(A32)}$$
$$B2_{2d} = \alpha_{2d} (B1_{2d-1} + B1_{2s-2}) \quad \text{(A33)}$$
$$B2_{2s} = \alpha_{2s} (B1_{2s-1} + B1_{2s-2}) \quad \text{(A34)}$$

where subscripts 1, 2d and 2s denote zooplankton in Box 1, deposit feeder in Box 2 and suspension feeder in Box 2, respectively. α is assumed to be proportional to the grazing $B1$.

$B3$ is the egestion generation speed of secondary producer and is represented by the following equation:

$$B3_1 = \beta_1 B1_1 \quad \text{(A35)}$$
$$B3_{2d} = \beta_{2d} (B1_{2d-1} + B1_{2d-2}) \quad \text{(A36)}$$
$$B3_{2s} = \beta_{2s} (B1_{2s-1} + B1_{2s-2}) \quad \text{(A37)}$$

where subscripts 1, 2d and 2s denote zooplankton in Box 1, deposit feeder in Box 2 and suspension feeder in Box 2, respectively. β is assumed to be proportional to the grazing $B1$.

$B4$ is the mortality speed of secondary producer at 0℃ and is represented by the following equation:

$$B4_1 = Mzo_1 \exp(kmz_1 T_1) \quad \text{(A38)}$$
$$B4_{2d} = Mzo_{2d} \exp(kmz_{2d} T_2) \quad \text{(A39)}$$
$$B4_{2s} = Mzo_{2s} (8.5 - \exp(kmz_{2s} T_1)) \quad \text{(A40)}$$

where subscripts 1, 2d and 2s denote zooplankton in Box 1, deposit feeder in Box 2 and suspension feeder in Box 2, respectively. Mzo (L mgN^{-1} d^{-1}) is the mortality of secondary producer at 0℃, kmz (℃$^{-1}$) is the temperature dependency of mortality of secondary producer.

$C1$ and $C2$ are decomposition of detritus to give DIN and DON, respectively. $C1$ and $C2$ are represented by the following equation:

$$C1_1 = Vni_1 \exp(kvni_1 T_1) \quad \text{(A41)}$$
$$C1_2 = Vni_2 \exp(kvni_2 T_2) \quad \text{(A42)}$$
$$C2_1 = Vno_1 \exp(kvno_1 T_1) \quad \text{(A43)}$$
$$C2_2 = Vno_2 \exp(kvno_2 T_2) \quad \text{(A44)}$$

where subscripts 1 and 2 denote Box 1 and Box 2. Vni (d^{-1}) is decomposition speed of detritus to DIN at 0℃, Vno (d^{-1}) is decomposition speed of detritus to DON at 0℃, $kvni$ (℃$^{-1}$) is temperature dependency of decomposition of detritus to DIN, $kvno$ is temperature dependency of decomposition of detritus to DON.

$D1$ is decomposition of DON to DIN and is represented by the following equation:

$$D1_1 = Vdi_1 \exp(kvdi_1 T_1) \quad \text{(A45)}$$
$$D1_2 = Vdi_2 \exp(kvdi_2 T_2) \quad \text{(A46)}$$

where subscripts 1 and 2 denote Box 1 and Box 2. Vdi (d^{-1}) is decomposition speed of DON to DIN at 0℃, $kvdi$ (℃$^{-1}$) is temperature dependency of decomposition of DON to DIN.

$E1$ is denitrification speed from Box 2 and is

represented by the following equation, based on KOIKE (1991) :

$$E1 = Vde_2 \exp(kvde_2 T_1) \qquad (A47)$$

where Vde_2 (d^{-1}) is denitrification speed, $kvde_2$ ($℃^{-1}$) is temperature dependency of denitrification.

References

BARETTA, J. W. and P. RUARDIJ (1988) : Tidal Flat Estuaries. Simulation and Analysis of the Ems Estuary. Ecological Studies, **71**. Springer–Verlag, Berlin, 353pp.

FUJII, M., Y. NOJIRI, Y. YAMANAKA and M. J. KISHI (2002) : A one–dimensional ecosystem model applied to time series Station KNOT. Deep–Sea Res., II, **49**, 5441–5461.

HATA, K., I. OSHIMA and K. NAKATA (1995) : Evaluation of the Nitrogen Cycle in a Tidal Flat. Estuarine and Coastal Modeling, **4**, 542–554.

HATA, K., I. OSHIMA and K. NAKATA (1996) : Evaluation of near–shore benthic nitrogen cycle using benthic ecosystem model. J. Adv. Mar. Sci. Tech. Soci, **2** (2), 31–50. (in Japanese with English abstract and captions)

HATA, K., K. NAKATA and T. SUZUKI (2004) : The nitrogen cycle in tidal flats and eelgrass beds of Ise Bay. Journal of Marine Systems, **45**, 237–253.

KAWAMIYA, M., M. KISHI, Y. YAMANAKA and N. SUGINOHARA (1995) : An ecological–physical coupled model applied to Station Papa. Journal of Oceanography, **51**, 635–664.

KOIKE, I. (1993) : Microorganisms. *In* Tokyo Bay: Its Environmental Change for Recent 100 Years. Norio Ogura (ed.), Kouseisha Kouseikaku, Tokyo, p. 102–117. (in Japanese)

MONTANI, S., P. MAGNI and N. ABE (2003) : Seasonal and interannual patterns of intertidal microphytobenthos in combination with laboratory and areal production estimates. Mar. Eco. Prog. Ser. **249**, 79–91.

NAKAMURA, K. (2004) : Suspension feeding and growth of juvenile Manila clam Ruditapes philippinarum reared in the laboratory. Fish. Sci., **70**, 215–222.

NAKATA, K. and K. HATA (1994) : Evaluation of nutrient cycle in tidal flat. J. Jpn. Soc. Water Environ, **17** (3), 158–166. (in Japanese)

NISHIJIMA, T., A. YAMATO and Y. HATA (1990) : AGP test to Skeletonema. Water Pollution Research, **13**, 173–179.

ONITSUKA, G., T. YANAGI, S. MONTANI, M. YAMADA, N. UEDA and M. SUZUKI (2002) : An Attempt to Purify Water by Culturing Mussels in Dokai Bay, Japan. Oceanography in Japan, **11** (3), 403–417. (in Japanese with English abstract and captions)

PARSONS, T. R., M. TAKAHASHI, and B. HARGRAVE (1984) : Biological Oceanographic Processes 3rd edition. Pergamon Press, 330pp.

REDFIELD, A. C., B. H. KECHUM, and F. A. RICHARDS (1963) : The influence of organisms on the composition of sea water. *In* The Sea, M. N. Hill (ed.), Interscience Pub., New York, **2**, 26–77.

SASAKI, K. (2001) : Water purification capacity of tidal flat and shallow coastal sea. Kagaku, **71**, 902–911, (in Japanese).

SOHMA, A., T. SATO and K. NAKATA (2000) : New numerical model study on a tidal flat system seasonal, daily and tidal variations. Spill Science and Technology Bulletin, **6** (2), 173–185.

SUZUKI, T., H. AOYAMA and K. HATA (1997) : The quantification of Nitrogen cycle on tidal flat by ecosystem model－In the case of Isshiki tidal flat in Mikawa bay–, J.Adv.Mar.Sci.Tech.Soci, **3** (1), 63–80. (in Japanese with English abstract and captions)

TSUTSUMI, H., E. OKAMURA, M. OGAWA, T. TAKAHASHI, K. YAMAGUCHI, S. MONTANI, N. OHASHI, T. ADACHI and T.KOMATSU (2003) : Rekations among the oxygen deficient water mass, red tide and marine structure in the head of Ariake Bay in recent years. Oceanography in Japan, **12**, 85–96 (in Japanese with English abstract and captions).

Received November 9, 2006
Accepted October 19, 2007

La mer 45 : 135-147, 2007
Société franco-japonaise d'océanographie, Tokyo

Growth and reproduction of the pilumnid crab *Benthopanope indica* (Decapoda: Brachyura) in Tateyama Bay, Japan

Wataru DOI, Masashi YOKOTA and Seiichi WATANABE

Abstract: The growth and reproduction of the pilumnid crab, *Benthopanope indica*, were examined from April 2001 to March 2002 in Tateyama Bay, central Japan. Ovigerous females were mainly observed from June to August, whereas small juveniles were recruited from August to January. After settlement, juveniles (carapace width, CW, of less than 2 mm) grew to and exceeded the mature size (CW 5.80 mm in males and 4.54 mm in females) by the following April. Although large males had considerably larger major chelipeds, their relative growth did not correspond to sexual maturity. The relative growth rate of the male abdominal width decreased at the puberty molt. Enlargement of the abdomen occurred in the mature females, but it was difficult to distinguish postpubertal females from prepubertal females on the basis of abdominal width only, because some females had intermediate abdominal widths, between those of pre – and postpubertal females. Brood size correlated positively with CW, ranging from 120 to 1,700 eggs. After the reproductive season, many large individuals died of senescence, with a longevity of almost one year. However, from size frequency distributions and growth rate analysis, it is likely that some individuals survived until the next reproductive season.

Keywords: *Benthopanope indica*, Pilumnidae, growth, reproduction

1. Introduction

The pilumnid crab *Benthopanope indica* (Decapoda, Brachyura) is a small species that attains a carapace width (CW) of approximately 11 mm. It inhabits the branches or roots of the brown alga *Sargassum thunbergii* and under calcareous algae in the intertidal zone. It has been recorded from the temperate to subtropical region of the Indo–West Pacific Ocean (SAKAI, 1976; MIYAKE, 1998). DAVIE (1989) transferred this species from the genus *Pilumnopeus* (SAKAI, 1976; MIYAKE, 1998) to the new genus *Benthopanope* established by him. *Benthopanope* is distinguished from other genera by its postlarval morphological characteristics. KO (1995) described the complete larval development of *B. indica* and confirmed DAVIE's classification. The crab of this genus recorded in Japan is *B. indica* only (DAVIE, 1989).

Faculty of Marine Science, Tokyo University of Marine Science and Technology
4–5–7 Konan, Minato–ku, Tokyo 108–8477, Japan

The growth and reproduction of Xanthoidea have frequently been investigated, especially those of Menippidae (*e.g.*, TWEEDALE *et al.*, 1993), Xanthidae (*e.g.*, KNUDSEN, 1960), Panopeidae (*e.g.*, MCDONALD, 1982), and Eriphiidae (*e.g.*, TOMIKAWA and WATANABE, 1992). No such studies of the Pilumnidae have been performed until recently, although there are 400 pilumnid species all over the world (NG and HUANG, 2002). The limited references to the Pilumnidae include reports of their embryonic and postembryonic development (WEAR, 1967; CLARK and NG, 2004), agonistic behavior (LINDBERG and FRYDENBERG, 1980), fecundity (ALMAÇA, 1987), size at sexual maturity (KUHLMANN and WALKER II, 1999), feeding (KYOMO, 1999), reproductive behavior (KYOMO, 2001), reproductive cycle (KYOMO, 2002; LITULO, 2005a), and population structure (LITULO, 2005a, b).

The mouth of Tokyo Bay is by the side of the Kuroshio Current and many aquatic organisms exist in this coastal area. Various crab species including warm–water species, also live on the

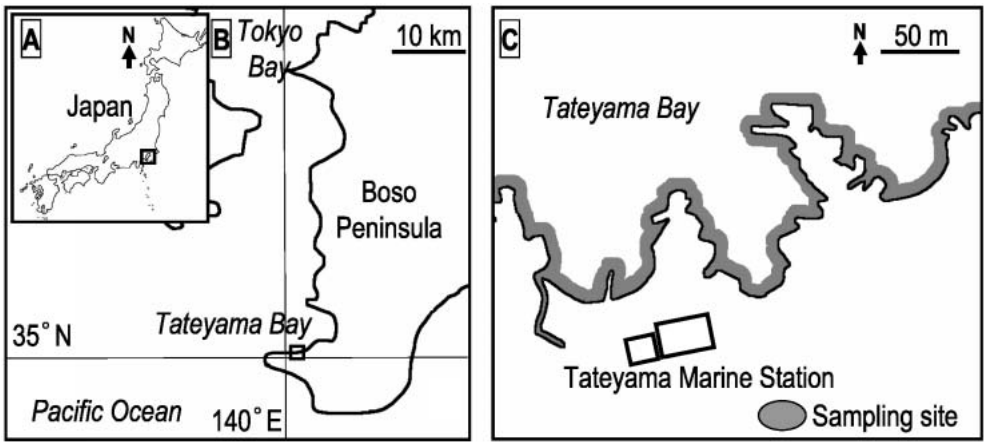

Fig. 1. Maps showing sampling site in Tateyama Bay. (A) – (C) show the site in increasing detail. Sampling of *Benthopanope indica* was carried out on the intertidal rock along the shoreline shown in (C).

reef. Therefore, basic ecological studies of these crabs have been undertaken: the majids *Tiarinia cornigera* (TSUCHIDA and WATANABE, 1991) and *Pugettia quadridens quadridens* (FUSEYA and WATANABE, 1993; FUSEYA *et al.*, 2001), the xanthid *Leptodius exaratus* (WATANABE *et al.*, 1990), the eriphiid *Eriphia smithii* (TOMIKAWA and WATANABE, 1992), the plagusiid *Plagusia dentipes* (TSUCHIDA and WATANABE, 1997; SAMSON *et al.*, 2007), the hymenosomatid *Rhynchoplax coralicola* (GAO *et al.*, 1994), the portunids *Thalamita sima* (NORMAN, 1996) and *Thalamita pelsarti* (as *T. prymna*; NORMAN *et al.*, 1997). Although *B. indica* is one of the dominant crabs in this area (personal observation), its life history has not yet been investigated.

In this study, monthly sampling over one year and the morphometric analysis of several body parts of the collected samples were used to clarify the patterns of growth and reproduction and size at sexual maturity. The life history of *B. indica* was inferred from the data.

2. Materials and Methods

Samples were collected monthly between April 2001 and March 2002 at upper intertidal zone on the rocky shore near the Tateyama Marine Station, Field Science Center of Tokyo University of Marine Science and Technology, located near the tip of Boso Peninsula, Chiba Prefecture, Japan (Fig. 1). Crabs attached to the roots of the brown alga *S. thunbergii* or hidden below the calcareous algae were collected by hand and forceps during the day (April–October) or at night (November–March) during low tide. Sampling was performed in those algae associations randomly selected until up to about one hundred individuals were collected but the sample size could not reach the purpose in April and May in 2001. The specimens were preserved in 10% formaldehyde–sea water. The crabs were sexed based on the form of the pleopods and the location of the gonopores. The females were checked for the presence or absence of attached eggs in the pleopods. Ovigerous females were separated into those bearing early developing (nonpigmented–eyed) eggs and those with pigmented–eyed eggs. Carapace width (CW) to the nearest 0.01 mm was measured with digital calipers in all specimens and CW frequency distributions by sex for 1 mm intervals were constructed for each month.

Carapace width and the following body parts were measured to the nearest 0.01 mm with digital calipers and under a stereomicroscope using a micrometer: propodus length (PL) and height (PH) of the major chelipeds and the width of the fifth abdominal segment (AW). Cheliped handedness was determined by the size and dentition of the cheliped.

To detect quantitative morphological changes, the growth of some body parts

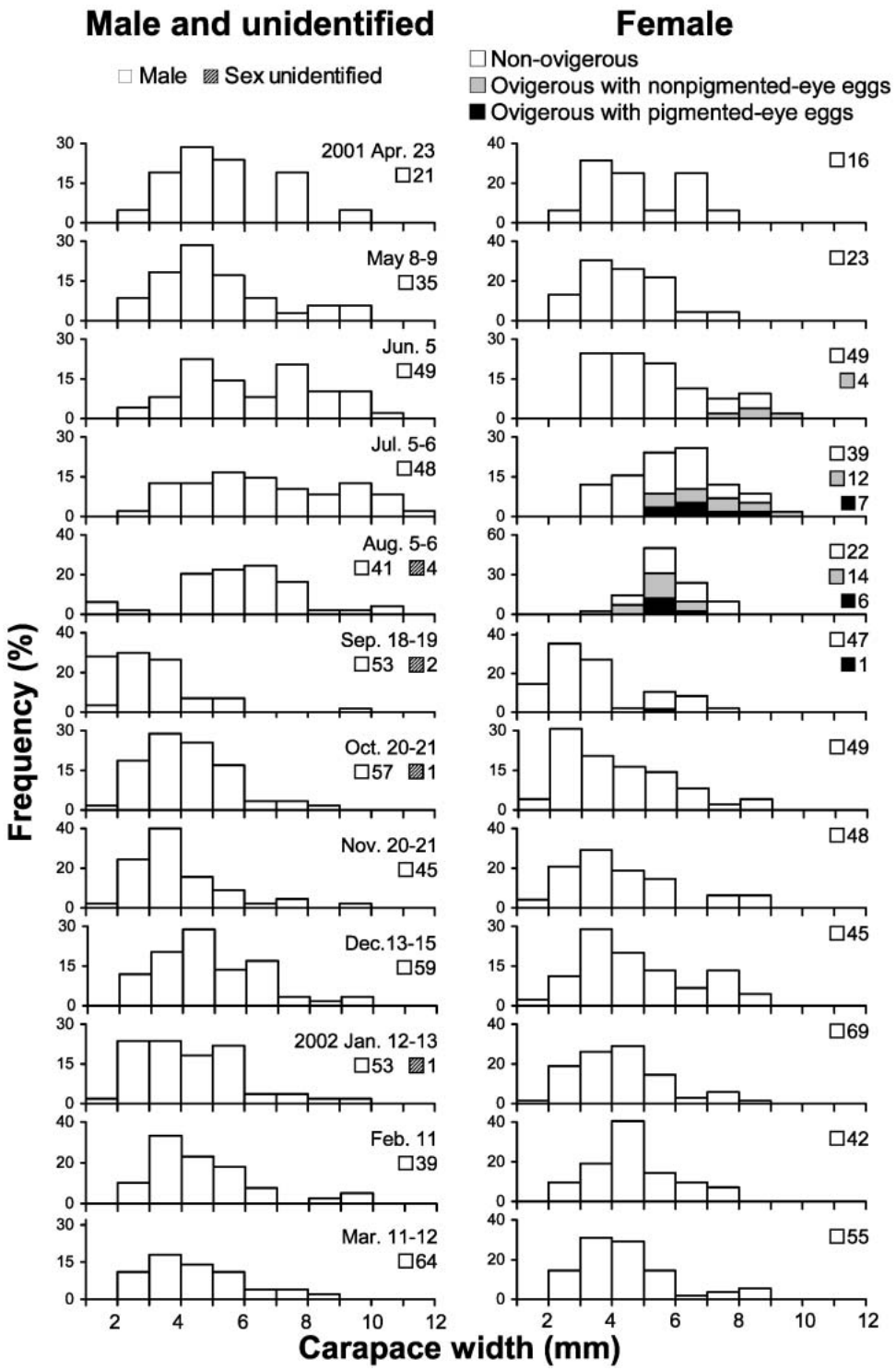

Fig. 2. Monthly changes in the size frequency distribution of *Benthopanope indica* from April 2001 to March 2002. Figures at the right side of each box indicate the number of individuals in each category.

relative to the CW was analyzed with regression lines. If a morphological change in a body part does not occur during growth, the relationship between the body part and CW is usually described by a single regression line. Conversely, when a morphological change occurs in a body part, two or more regression lines are possible. If the ranges of CW of the two regression lines do not overlap, we can estimate the parameter of the regression lines by searching statistically for the inflection point. We used the Akaike's information criterion (AIC) method (AKAIKE, 1973) as the criterion for detecting the best-fit inflection point between two regression lines (see DOI *et al.*, 2007). The inflection point was estimated by the stepwise calculation of each 0.10 mm. In the case of overlapping CW ranges in the regression lines, we tried to distinguish them using the body part/CW ratio.

The total numbers of external eggs (NE) attached to the pleopods of all ovigerous females were counted under a stereomicroscope. To evaluate the relationship between CW and NE, a power function was fitted by the nonlinear least square methods using Solver, a nonlinear optimization tool in Excel 2003 (Microsoft, Tokyo, Japan). To estimate mean egg diameter, the longest and shortest diameters closest to 0.025 mm were measured using a micrometer under a binocular microscope.

3. Results

Growth

The total number of crabs sampled was 1,128, consisting of 572 males, 548 females, eight small individuals of unidentified sex, and two intersex individuals. The CW ranged from 1.29 to 11.32 mm for males and from 1.32 to 9.51 mm for females. The CW frequencies were relative uniformly distributed over the entire size range from April to July (Fig. 2). The size frequency distribution showed that the population was composed of two size groups larger and smaller than ca 7.00 mm CW in June and July. The small crabs (CW $<$ 7.00 mm) grew during this period. Whereas those adults comprised the main group in August, they almost disappeared and juveniles (CW $<$ 4.00 mm) became the main group in September. The recruits began to occur in August and comprised most of the population from September to March. Although alteration of the cohorts (year class) was clearly observed between August and September, few larger crabs of the previous cohort were observed to have survived.

Reproduction

A total of 44 ovigerous females were collected during the study and their sizes ranged from 4.54 to 9.51 mm CW (mean $\pm$ SD, 6.37 $\pm$ 1.26) (Fig. 2). Ovigerous females were found from June to September. Their frequency was low in June (7.6%), but increased abruptly to $>$ 30% in July (32.8%) and August (47.6%). Only one specimen was sampled in September (2.1%). Females bearing eyed eggs were collected except in June and their frequencies were 12.1% and 14.3% in July and August, respectively. The mean CW ($\pm$ SD) of ovigerous females in those months were 8.30 $\pm$ 0.93 mm, 6.82 $\pm$ 1.23 mm, and 5.63 $\pm$ 0.50 mm in June, July, and August, respectively, and the CW of one ovigerous female in September was 5.06 mm.

Relative growth

AIC analysis of two relative size relations (PL to CW, PH to CW) produced two regression lines in males (Fig. 3, Table 1). The inflection points of PL and PH were at CW values of 7.50 mm and 7.60 mm, respectively. The secondary sexual characteristic, elongation of the cheliped, was more clearly observed in the PL value. The relative growth of AW in males was divided into two lines at the CW value of 5.80 mm (Fig. 4; Table 1). The gradient of the upper line was smaller than that of the lower line.

There was no marked increase of the cheliped in females. The increase in both PL and PH relative to CW was fitted to a single straight line (Table 1). The female abdominal segment showed considerable enlargement by the puberty molt (Fig. 5). An overlap of the mature, immature, and transition groups was observed from CW larger than 3.00 mm. Therefore, a single straight line representing the growth of AW relative to CW was fitted only for ovigerous females (Fig. 5, Table 1).

The minimum AW/CW value in ovigerous females was 0.293. Assuming this value to be the

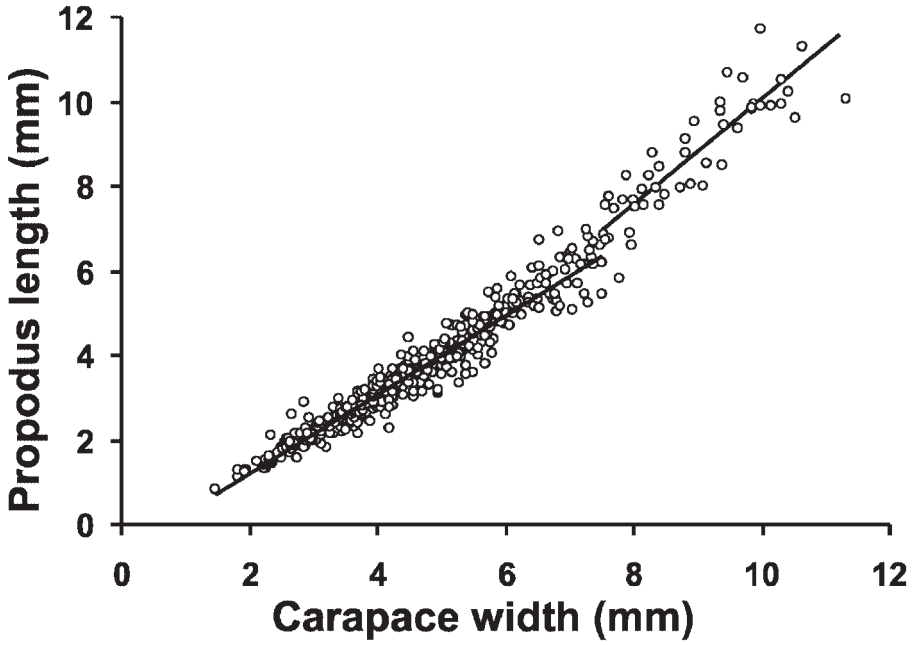

Fig. 3. Growth of propodus length relative to carapace width in male *Benthopanope indica*.

Table 1. Regression lines $y = a + bx$ for the morphometric analysis of *Benthopanope indica*. Asterisk indicates that the slope (b) is significant (t test; * $P<0.001$). Dagger indicates that the slope (b) is significantly different between sexes (ANCOVA; † $P<0.001$). AIC, Akaike's information criterion; AW, fifth abdominal segment width; CW, carapace width; IP, inflection point; NA, not applicable; PH, propodus height of the major cheliped; PL, propodus length of the major cheliped.

Sex	Dependent variables	No. regression lines	AIC	IP (mm, CW)	CW range	Parameter		N	R	Significance	
						Intercept (a)	Slope (b)			b	Between sexes
Male	PL	1	536	NA	1.47–11.32	−1.150	1.057	480	0.979	NA	†
		2	442	7.50	1.47–7.47	−0.675	0.939	431	0.970	NA	†
					7.50–11.32	−2.372	1.247	49	0.879	NA	†
	PH	1	−54	NA	1.47–11.32	−0.541	0.573	480	0.979	NA	†
		2	−113	7.60	1.47–7.57	−0.363	0.529	435	0.967	NA	†
					7.61–11.32	−0.432	0.580	45	0.846	NA	†
	AW	1	−1374	NA	1.29–11.32	0.094	0.181	570	0.980	NA	†
		2	−1447	5.80	1.29–5.79	0.004	0.205	421	0.965	NA	†
					5.81–11.32	0.205	0.165	149	0.933	NA	†
Female	PL	1	NA	NA	1.32–9.41	−0.232	0.803	459	0.973	*	NA
	PH	1	NA	NA	1.32–9.41	−0.124	0.459	460	0.970	*	NA
	AW	1	NA	NA	4.54–9.51	−0.270	0.367	44	0.975	*	NA

puberty point, we distinguished nonovigerous females at two stages: postpuberty ≥ 0.293 and prepuberty < 0.293 (Fig. 6). There were not only postpubertal females with broad abdomens, but also those with extremely narrow abdomens between June and September. Although the change of generations occurred after the main reproductive season (June to August), postpubertal and mature-sized females were found with a mean CW that was greater than that of ovigerous females (6.37 mm CW). Whereas the postpubertal females were included in the group with large CW in most months, females at the postpuberty that were smaller than the smallest ovigerous female (4.54 mm CW) were found in December,

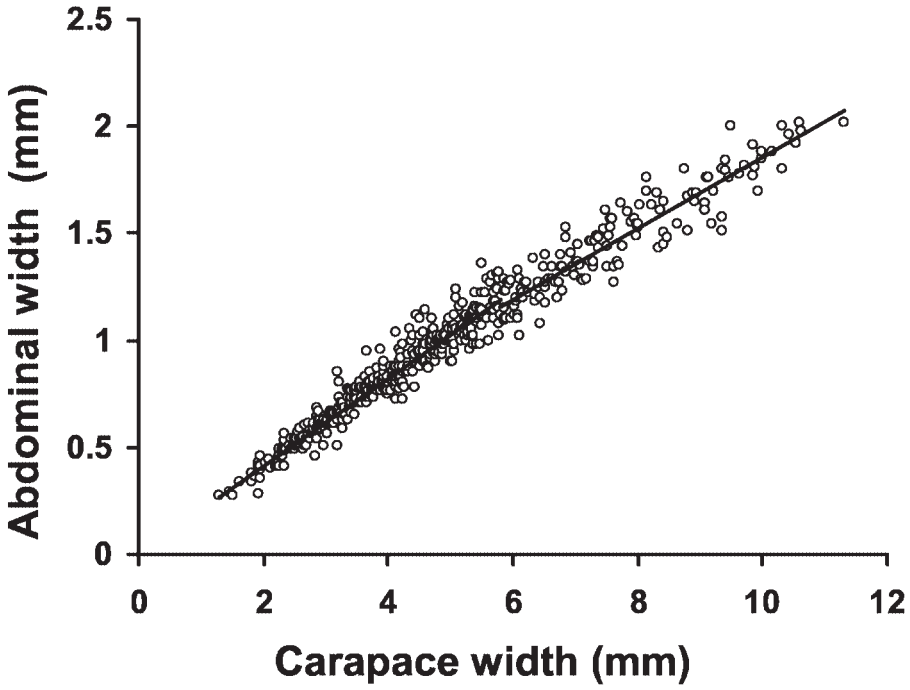

Fig. 4. Growth of fifth abdominal segment width relative to carapace width in male *Benthopanope indica*.

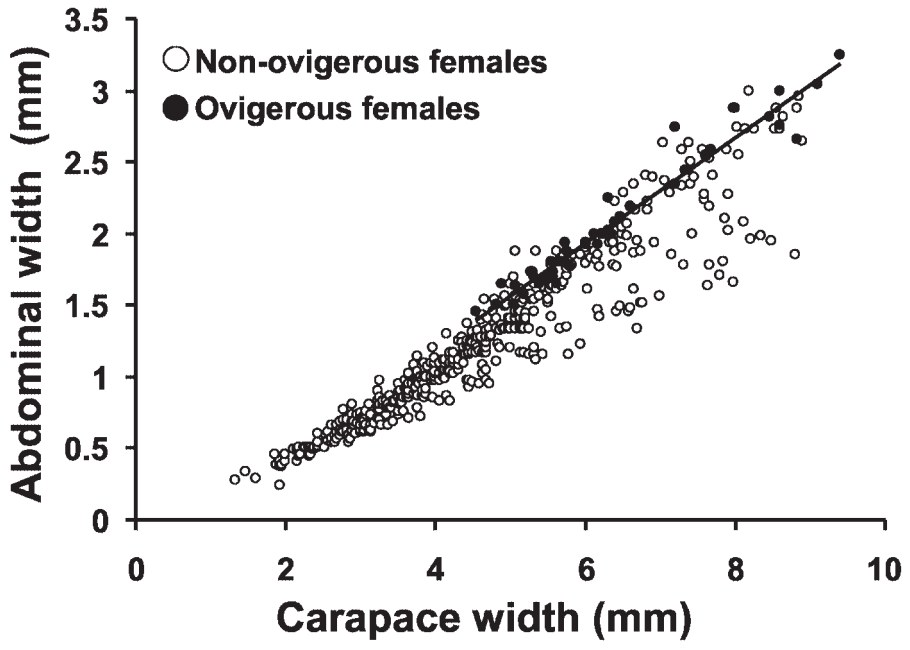

Fig. 5. Growth of fifth abdominal segment width relative to carapace width in female *Benthopanope indica*. Open and closed circles indicate nonovigerous and ovigerous females, respectively.

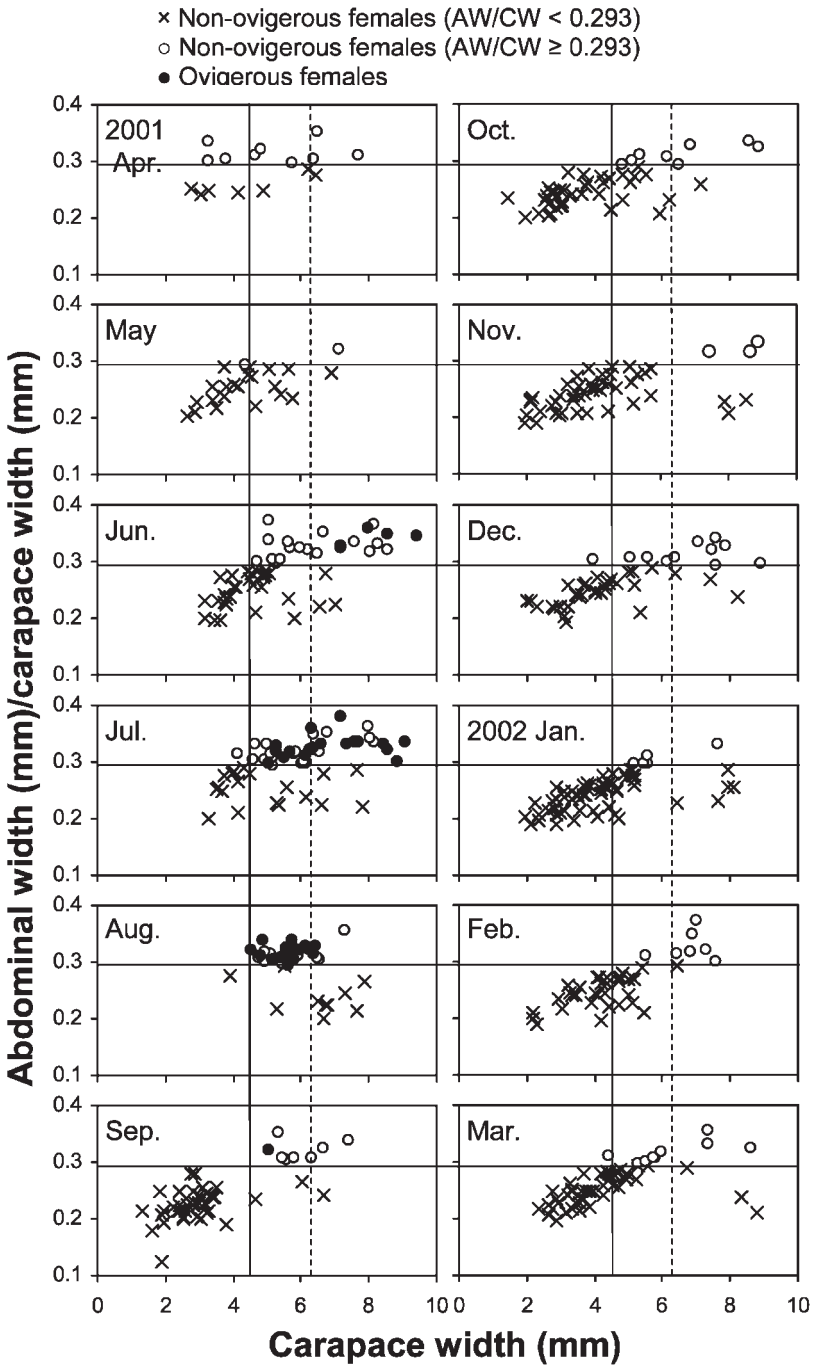

Fig. 6. Monthly changes in the relationship between carapace width (CW) and abdominal width (AW), AW/CW, in female *Benthopanope indica* from April 2001 to March 2002. Closed circles, open circles, and crosses indicate ovigerous females, nonovigerous females with wide abdomens (AW/CW $\geq$ 0.293), and nonovigerous females with narrow abdomens (AW/CW $<$ 0.293), respectively. Solid and dashed vertical lines indicate the smallest (4.54 mm) and mean CW of ovigerous females (6.37 mm), respectively. Horizontal lines indicate the puberty point (AW/CW = 0.293).

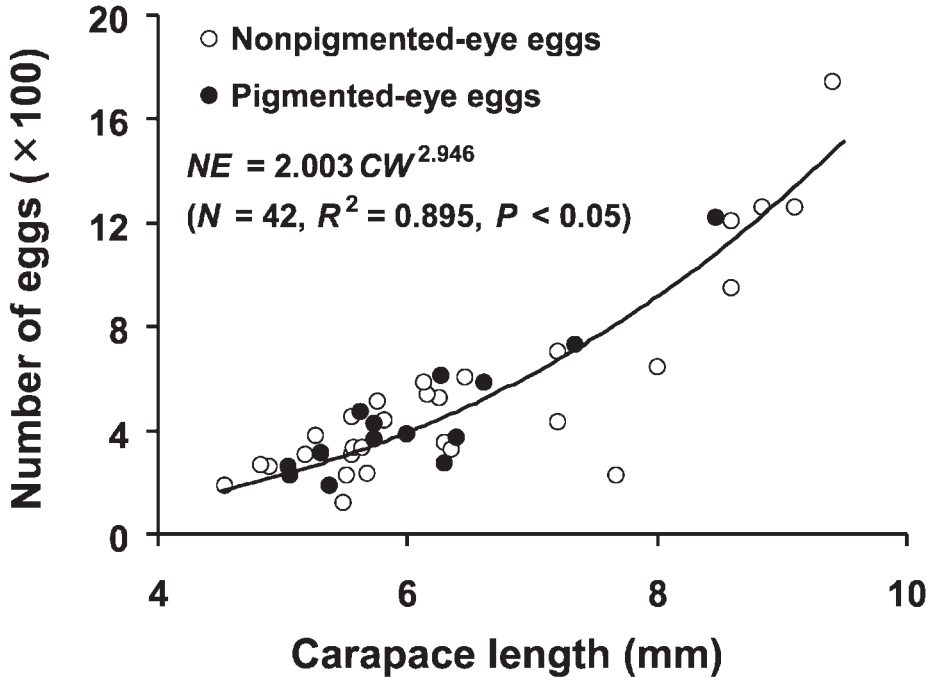

Fig. 7. Relationship between carapace width and number of eggs in the pleopods of *Benthopanope indica* females. Open and closed circles indicate noneyed and eyed eggs, respectively.

March, and especially in April. Sexual dimorphism in growth rates relative to CW was found for all parameters evaluated (Table 1).

Brood size and egg size

The numbers of eggs of the 44 ovigerous females (4.54–9.51 mm CW) ranged from 120 to 1,739. Egg number increased with CW (Fig. 7), and large females had large numbers of eggs. The relationship between brood size (number of eggs, NE) and CW is described as follows: $NE = 2.003CW^{2.946}$ ($N = 44$, $R^2 = 0.895$, $P < 0.05$). The mean diameter of noneyed eggs was 0.38 $\pm$ 0.03 mm ($N = 300$, 10 broods), and was significantly smaller than that of eyed eggs, with a mean diameter of 0.42 $\pm$ 0.03 mm ($N = 360$, 12 broods) (t test, $P < 0.01$).

4. Discussion

Newly settled crabs (CW < 2.00 mm) were found from August, and the smallest males and females (CW 1.32 mm and CW 1.29 mm, respectively) were collected in September. From these results, we infer that the beginning of recruitment of the small crabs occurred in August or early September. Ko (1995) reported that the period from the first zoea to the first juvenile crab of *B. indica* was at least 24–28 days (20–25 ℃) and that the size of the megalopa was 0.87 mm. Quintana (1986) showed that the CWs of the megalopa and the first–, second–, and third –stage crabs in the related pilumnid, *Parapilumnus trispinosus*, were 0.83, 1.28, 1.58, and 1.77 mm, respectively. Therefore, these small crabs of *B. indica* might constitute the first postlarval stage one month after hatching, and the earliest hatching females might be from the preceding June or early July. This corresponds to the earliest month (June) in which we collected ovigerous females (Fig. 2).

It is difficult to estimate the final reproductive season from our current data because of inconsistencies in the results. Ovigerous females were collected until September, whereas several crabs of the small size group were sampled in January (Fig. 2). If the period from hatching to recruitment was also one month in the final reproductive season, the small crabs of the final season would have been born around December or late November. However, it was only

three months before we collected the final ovigerous females. This inconsistency is remarkable. There are three possible explanations of this discrepancy. First, the recruits could be transported from the southern populations with the longer reproductive season through the warm oceanic current. For instance, the tropical and sub-tropical hermit crabs, *Calcinus* spp., could be collected in this area (MURATA *et al.*, 1991). The larval transportation through the oceanic current would play an important role in the source of the recruits of *B. incica* in this area. Second, the actual pelagic larval period could be longer because the described period was measured in the warmer season. Further research into the relationship between larval development and environmental conditions should clarify this. Third, samples of ovigerous females would not have been caught later in the reproductive season because the main reproductive season had already finished. As we will explain in a later section, this species has two forms of life history. Thus, several mature or mature-like females do not die out, but live beyond the main reproductive season. Occasionally, the surviving females produce eggs until the end of autumn. These results lead us to hypothesize that the reproductive season of this species extends at least from June to September (three months), or slightly longer, until October or November in this area. This seasonality and the duration of the reproductive period are similar to those of the xanthid crab *Leptodius exaratus* (WATANABE *et al.*, 1990), the eriphiid crab *Eriphia smithii* (TOMIKAWA and WATANABE, 1992), the majid crab *Tiarinia cornigera* (TSUCHIDA and WATANABE, 1991), the portunid crab *Thalamita pelsarti* (NORMAN *et al.*, 1997), and the hymenosomatid crab *Rhynchoplax coralicola* (GAO *et al.*, 1994) in the same study area. *B. indica* and these five species are warm-water species and the present study area is the northern limit in their distributions except for *R. coralicola* (SAKAI, 1976; MIYAKE, 1998). The reproductive season of all warm-water species are limited in about three warmer months in this area. In contrast, other temperate species with the northward distribution have longer reproductive period and/or different seasonality in this area: February-August in the majid crab *Pugettia quadridens quadridens* (FUSEYA and WATANABE, 1993), October-December in the plagusiid crab *Plagusia dentipes* (TSUCHIDA and WATANABE, 1997). These patterns of reproductive seasons are possibly related to physiological difference between warmer and temperate species.

In September 2001, a considerable number of small crabs appeared and grew. In the same month, the number of large crabs decreased, although they had comprised the major proportion of the population in previous months. Most individuals that have completed their reproductive activity probably die from senescence. Therefore, their longevity is almost one year. However, some crabs might live for more than one year. From September onwards, a few large crabs were distinguishable from the juveniles recruited in August. To confirm the age of those large crabs, we analyzed their growth rates as follows. We assumed that all the crabs settled on September 1 and calculated the growth rate (ΔCW),

Table 2. Growth rate (ΔCW) analysis based on the assumption that all crabs were recruited on September 1, 2001, in *Benthopanope indica*. ΔCW_{it} was calculated as follows, $\Delta CW_t = CW_{it} - \overline{CW}_{t-1}$, where ΔCW_{it} and CW_{it} are the growth rate and carapace width of individual i in month t, respectively. $\overline{CW}_{t-1}$ is the mean carapace width in month $t-1$. Individuals with $-\Delta CW_{it}$ were excluded from the analysis because they hatched after September 1, 2001.

Month	Male ΔCW_i (> 0)			Female ΔCW_i (> 0)		
	Mean	Range	*N*	Mean	Range	*N*
Oct.	1.61	0.04−5.70	47	1.88	0.19−5.40	26
Nov.	1.35	0.01−4.79	14	1.69	0.07−4.74	21
Dec.	1.57	0.01−5.43	43	1.73	0.02−4.60	24
Jan.	1.25	0.06−4.22	19	1.29	0.13−3.36	19
Feb.	1.50	0.13−5.03	28	1.17	0.05−3.34	25
Mar.	1.25	0.19−3.98	28	1.37	0.05−4.31	23

$$\Delta CW_{it} = CW_{it} - \overline{CW}_{t-1},$$

where ΔCW_{it} and CW_{it} are the growth rate and CW of individual i in month t. $\overline{CW}_{t-1}$ is the mean CW in month t–1. ΔCW_{it} values that were <0 were excluded from the analysis because those individuals had hatched after September 1, 2001. Although the mean ΔCW ranged from 1.17 to 1.88, the maximum ΔCW showed a considerably higher value (3.34–5.70) in each month (Table 2). Individuals with extremely high ΔCW could have been members of the previous year class that had survived after the reproductive season. However, their size frequency distributions were unclear because the sample size was small. The presence of two longevity forms is similar to those of the majid crabs *T. cornigera* (TSUCHIDA and WATANABE, 1991) and *P. quadridens quadridens* (FUSEYA and WATANABE, 1993) in the same study area.

The relative growth rates of male PL and PH increased at the inflection points of 7.50 mm and 7.60 mm CW, respectively. Although both inflection points were close, it is doubtful that these changes reflect physiological maturity. The growth of Brachyura displays two patterns relative to the timing of the puberty molt: one in which the puberty molt is the terminal molt and the other in which molts occur more than once after the puberty molt (HARTNOLL, 1985). In the former type, considerable changes in relative growth were observed at the puberty molt, but in the latter type, these changes are not clear. *Benthopanope indica* is the latter type, like most xanthoid crabs (HARTNOLL, 1985), because the ovigerous females molt after larval hatching in captivity.

In panopeid crabs such as the male *Panopeus austrobesus*, the growth of the cheliped dimensions relative to CW provides a much higher estimate of the mature sizes than that calculated with gonad analysis. The measurement of the length of the first gonopod is consistent with gonad development (NEGREIROS–FRANSOZO and FRANSOZO, 2003). Moreover, the pattern of relative growth of the first gonopod length corresponds to the relative increase in AW (HARTNOLL, 1974). Therefore, the inflection point for the male AW (5.80 mm CW) probably indicates the size at physiological maturity in *B. indica* males.

For the relative growth of female AW, a straight line could only be fitted to data from ovigerous females. It was difficult to rigidly divide nonovigerous females into immature and mature groups because many females had a transitional AW.

Morphologically mature females with broad abdomens were found throughout the year. However, our limited data do not show whether the females that survived into the second reproductive season had already spawned in the first reproductive season. We did not examine their ovaries because their body size was small. In future studies, histological observation will be required to confirm their reproductive cycle. Females with narrow abdomens were observed, which exceeded the mean CW of ovigerous females during and after the reproductive season. These females may not have attained sexual maturity. A parasitic epicaridean isopod, *Xanthion spadix*, causes the narrowing of the abdomen of female *L. exaratus* and inhibits their reproductive ability (MIZOGUCHI *et al.*, 2002). It must be confirmed in a future study whether *B. indica* females with narrow abdomens are parasitized by epicaridean isopods. Some small females with broad abdomens were found in December, March, and April, indicating that the puberty molt also occurs during winter and spring, before the reproductive season in females.

Our study area is located at the extreme northern limit of the distribution of *B. indica* (SAKAI, 1976; MIYAKE, 1998). In female *Panopeus herbstii*, the size at sexual maturity, the mean size of the mature crabs, and the proportion of large crabs were less in the northern part of its distribution than in southern areas (HINES, 1989). HINES (1989) attributed this to the cessation of the molt during the cold season. This interpretation may explain why there are two longevity forms and so much variation in size at maturity in *B. indica* .

Brood size was positively related to body size. The relationship between the number of the eggs per brood and CW in crabs that have the same reproductive season as *B. indica* at Banda are as follows: 610–10,110 (11.80–26.20

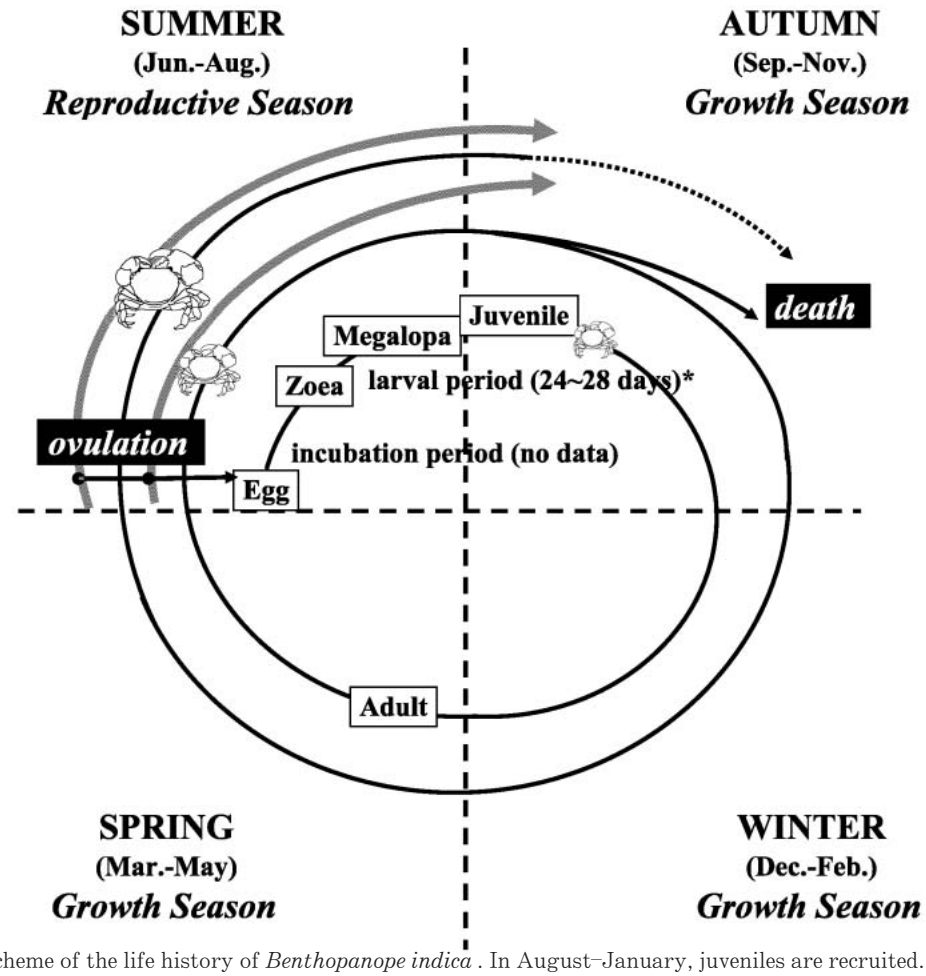

Fig. 8. Scheme of the life history of *Benthopanope indica* . In August–January, juveniles are recruited. The carapace width of juveniles increases to above 6.00 mm by June. From June to early September, these crabs start to spawn and incubate their eggs. After the reproductive season, most individuals die. Part of the population survives until the next reproductive season. (* Ko (1995))

mm) in *L. exaratus* (Watanabe *et al.*, 1990), 5,293–73,501 (25.10–52.60 mm) in *E. smithii* (Tomikawa and Watanabe, 1992), 1,000–2,000 (17.00–25.00 mm) in *T. cornigera* (Tsuchida and Watanabe, 1991), and 23–230 (2.65–3.90 mm) in *R. coralicola* (Gao *et al.*, 1994), respectively. The mean number of eggs of *B. indica* is relatively smaller than that of these species because its body size is smaller (Hines, 1982; Reid and Corey, 1991). *B. indica* and the latter two species with the relative smaller brood size inhabit in colonies of the algae, while the former two species occur under cobbles and inside crevices. The habitat stability (Fukui and Wada, 1986) and complexity (Lohrer *et al.*, 2000) are related to the different reproductive effort of the brachyurans and opportunistic species adapt unstable and low complex habitats (Fukui and Wada, 1986; Lohrer *et al.*, 2000). The habitat characteristic of the colonies of the algae is still unknown, but they may contribute to the low mortality of crabs inhabiting them. It is necessary to investigate the survival rates of such crabs living in the algae. The accurate number of spawnings per female in the annual reproductive season is still unknown, and must be clarified before the reproductive efforts of these species can be compared. *B. indica* has relative small brood size and restricted spawning season in this area. Further studies are

needed to clarify that how degree do the population of Tateyama Bay and that of the southern area contribute to the maintenance of the population of this area.

The life history of *B. indica* can be deduced from previously published data and the results of this study (Fig. 8). In August–January, the juveniles appear after the larval stage in the colony of brown algae and under calcareous algae. Juveniles with CWs of around 3 mm reach the size of morphological maturity for males (CW 5.80 mm) and the minimum size of ovigerous females (CW 4.54 mm) by the following April. During the reproductive season, from June to early September, the mature females spawn 127–1,739 eggs at a time. Thereafter, most individuals die out, but a few survive into the second year after recruitment and reproduce.

Acknowledgements

The authors would like to thank the staff of the Field Science Center, Tateyama Station (Banda), Tokyo University of Marine Science and Technology for their kind support during field sampling.

References

AKAIKE, H. (1973) : Information theory and an extension of the maximum likelihood principle. *In* 2nd International Symposium on Information Theory. Petrov, B.N. and F. Csáki (eds.), Akdémiai Kiadó, Budapest, p.267–281.

ALMAÇA, C. (1987) : Crabs of the *Sabellaria alveolata* (Linnaeus, 1767) community. Egg number and population size in *Pilumnus hirtellus* (Linnaeus, 1761) and *Porcellana platycheles* (Pennant, 1777). Arq. Mus. Bocage, **1**, 19–32.

CLARK, P.F. and P.K.L. NG (2004) : The larval development of *Actumnus setifer* (de Haan, 1835) (Brachyura: Xanthoidea: Pilumnidae) described from laboratory reared material. Crust. Res., **33,** 27–50.

DAVIE, P.J.F. (1989) : A re–appraisal of *Heteropanope* Stimpson, and *Pilumnopeus* A. Milne Edwards (Crustacea: Decapoda: Pilumnidae) with descriptions of new species and new genera. Mem. Queensland Mus., **27**, 129–156.

DOI, W., T.T. LWIN, M. YOKOTA, C.A. STRÜSSMANN and S. WATANABE (2007) : Maturity and reproduction of goneplacid crab *Carcinoplax vestita* (Decapoda, Brachyura) in Tokyo Bay. Fish. Sci., **73**, 331–340.

FUKUI, Y. and K. WADA (1986) : Distribution and reproduction of four intertidal crabs (Crustacea, Brachyura) in the Tonda River Estuary, Japan. Mar. Ecol. Prog. Ser., **30**, 229–241.

FUSEYA, R. and S. WATANABE (1993) : Growth and reproduction of the spider crab, *Pugettia quadridens quadridens* (De Haan) (Brachyura: Majidae). Crust. Res., **22**, 75–81.

FUSEYA, R., K. YOKOKURA and S. WATANABE (2001) : Morphology and distribution of setae used for decorating on the dorsal carapace of the spider crab, *Pugettia quadridens quadridens* (De Haan) (Brachyura: Majidae). Crust. Res., **30**, 154–159.

GAO, T., S. TSUCHIDA and S. WATANABE (1994) : Growth and reproduction of *Rhynchoplax coralicola* Rathbun (Brachyura: Hymenosomatidae). Crust. Res., **23**, 108–116.

HARTNOLL, R.G. (1974) : Variation in growth pattern between some secondary sexual characters in crabs (Decapoda Brachyura). Crustaceana, **27**, 131–136.

HARTNOLL, R.G. (1985) : Growth, sexual maturity and reproductive output. *In* Crustacean Issue 3: Factors in adult growth. Wernner, A. M. (ed.), A. A. Balkema, Rotterdam, p.101–128.

HINES, A.H. (1982) : Allometric constraints and variables of reproductive effort in brachyuran crabs. Mar. Biol., **69**, 309–320.

HINES, A.H. (1989) : Geographic variation in size at maturity in brachyuran crabs. Bull. Mar. Sci., **45**, 356–368.

KNUDSEN, J.W. (1960) : Reproduction, life history, and larval ecology of the California Xanthidae, the pebble crabs. Pac. Sci., **14**, 3–17.

KO, H.S. (1995) : Larval development of *Benthopanope indica* (de Man, 1887) (Decapoda: Brachyura: Pilumnidae) in the laboratory. J. Crust. Biol., **15**, 280–290.

KUHLMANN, M.L. and R.E. WALKER II (1999) : Geographic variation in size structure and size at maturity in the crab *Pilumnus sayi* (Crustacea: Decapoda: Xanthidae) in the northern Gulf of Mexico. Bull. Mar. Sci., **64**, 535–541.

KYOMO, J. (1999) : Feeding patterns, habits and food storage in *Pilumnus vespertilio* (Brachyura: Xanthidae). Bull. Mar. Sci., **65**, 381–389.

KYOMO, J. (2001) : Reproductive behavior of the play –dead hairy *Pilumnus vespertilio* (Crustacea: Brachyura: Pilumnidae) with respect to carapace size. Bull. Mar. Sci., **68**, 37–46.

KYOMO, J. (2002) : Timing and synchronization of the breeding period in *Pilumnus vespertilio* (Crustacea: Pilumnidae) in subtropical Okinawa, Japan. Pac. Sci., **56**, 317–328.

LINDBERG, W.J. and R.B. FRYDENBERG (1980) : Resource centered agonism of *Pilumnus sayi* (Brachyura, Xanthidae), an associate of the

bryozoan *Schizoporella pungeus*. Behaviour, **75**, 235–250.

LITULO, C. (2005a) : Reproductive biology of the hairy crab *Pilumnus vesperitilio* (Brachyura: Pilumnidae) in the East African region. J. Mar. Biol. Assoc. UK, **85**, 877–881

LITULO, C. (2005b) : Population structure and breeding biology of the hairy crab *Pilumnus vespertilio* (Fabricius, 1793) (Crustacea: Brachyura: Pilumnidae) in southern Mozambique. J. Nat. Hist., **39**, 1359–1366.

LOHRER, A.M., Y. FUKUI, K. WADA and R.B. WHITLATCH (2000) : Structural complexity and vertical zonation of intertidal crabs, with focus on habitat requirements of the invasive Asian shore crab, *Hemigrapsus sanguineus* (de Haan). J. Exp. Mar. Biol. Ecol., **244**, 203–217.

MCDONALD, J. (1982) : Divergent life history patterns in the co–occurring intertidal crabs *Panopeus herbstii* and *Eurypanopeus depressus* (Crustacea: Brachyura: Xanthidae). Mar. Ecol. Prog. Ser., **8**, 173–180.

MIYAKE, S. (1998) : Japanese Crustacean Decapods and Stomatopods in Color, Vol. 2. Brachyura (crabs). Hoikusha, Osaka, 277pp. (in Japanese).

MIZOGUCHI, K., Y. HENMI and T. YAMAGUCHI (2002) : Parasitic status of epicaridean isopods (Crustacea: Malacostraca) and the effects on their brachyuran crab hosts. Jap. J. Benthol., **57,** 79–84 (in Japanese with English abstract).

MURATA, K., S. WATANABE and A. ASAKURA (1991) : Hermit crabs of genus *Calcinus* (Crustacea: Decapoda: Anomura) from Boso Peninsula. J. Nat. Hist. Mus. Inst., Chiba., **1**, 21–23 (in Japanese with English abstract).

NEGREIROS–FRANSOZO, M.L. and V. FRANSOZO (2003): A morphometric study of the mud crab, *Panopeus austrobesus* Williams, 1983 (Decapoda, Brachyura) from a subtropical mangrove in South America. Crustaceana, **76**, 281–294.

NG, P.K.L. and J.–F. HUANG (2002) : The Indo–Pacific Pilumnidae XV. On two rare species of Rhizopinae (Decapoda, Brachyura) from Taiwan. Crustaceana, **74**, 1379–1385.

NORMAN, C.P. (1996) : Reproductive biology and evidence for hard–female mating in the brachyuran crab *Thalamita sima* (Portunidae). J. Crust. Biol., **16**, 656–662.

NORMAN, C.P., Y.J. HIRANO and T. MIYAZAKI (1997): Hard–female mating in the brachyuran crab *Thalamita prymna* (Portunidae). Crust. Res., **26**, 62–69.

QUINTANA, R. (1986) : On the megalopa and early crab stages of *Parapilumnus trispinosus* SAKAI, 1965 (Decapoda, Brachyura, Xanthidae). Proc. Japan. Soc. Syst. Zool., **34**, 1–17.

REID, D.M. and S. COREY (1991) : Comparative fecundity of decapod crustacean, II The fecundity of fifteen species of anomuran and brachyuran crabs. Crustaceana, **61**, 175–189.

SAKAI, T. (1976) : Crabs of Japan and the adjacent seas. Kodanshya, Tokyo, 773pp.

SAMSON, A.S., M. YOKOTA, C.A. STRÜSSMANN and S. WATANABE (2007) : Natural diet of grapsoid crab *Plagusia dentipes* De Haan (Decapoda: Brachyura: Plagusiidae) in Tateyama Bay, Japan. Fish. Sci., **73**, 171–177.

TOMIKAWA, N. and S. WATANABE (1992) : Reproductive ecology of the xanthid crab *Eriphia smithii* McLeay. J. Crust. Biol., **12**, 57–67.

TSUCHIDA, S. and S. WATANABE (1991) : Growth and reproduction of the spider crab, *Tiarina cornigera* (Latreille) (Brachyura: Majidae). Res. Crust., **20**, 43–55.

TSUCHIDA, S. and S. WATANABE (1997) : Growth and reproduction of the grapsid crab *Plagusia dentipes* (Decapoda: Brachyura). J. Crust. Biol., **17**, 90–97.

TWEEDALE, W.A., T.M. BERT and S.D. BROWN (1993): Growth of postsettlement juveniles of the Florida stone crab, *Menippe mercenaria* (Say) (Decapoda: Xanthidae), in the laboratory. Bull. Mar. Sci., **52**, 873–885.

WATANABE S., H. YAMANA and N. TOMIKAWA (1990) : Reproduction of the xanthid crab, *Leptodius exaratus* (H. Milne Edwards). Res. Crust., **19**, 73 –78.

WEAR, R.G. (1967) : Life–history studies on New Zealand Brachyura 1. Embryonic and post–embryonic development of *Pilumnus novaezealandiae* Filhol, 1886, and of *P. lumpinus* Bennett, 1964 (Xanthidae, Pilumninae). N.Z. J. Mar. Freshwat. Res., **1**, 482–535.

Received July 25, 2007
Accepted December 4, 2007

La mer 45 : 149-158, 2007
Société franco-japonaise d'océanographie, Tokyo

Distribution of the density ratio in the North Pacific

Keishi SHIMADA*, Masao NEMOTO and Jiro YOSHIDA

Abstract: We estimated the spatial distribution of the density ratio (R_ρ) in the upper 1000 db of the North Pacific from the WOCE data set. The mode value of R_ρ was equivalent to those reported in former studies (3〜4), meaning that the double diffusive convection is moderate or weak; however, the "hot spots" of double diffusive convection were found off eastern Hokkaido and at the formation region of the ESTMW (Eastern Subtropical Mode Water). The vertical eddy double diffusive flux of the density there is up-gradient, where the eddy diffusivity was negative: $-(9\text{〜}8)\times10^{-5}$m^2/s in the area off eastern Hokkaido and $-(8\text{〜}4)\times10^{-5}$m^2/s in the ESTMW region. This result means the importance of double diffusive convection to the water mass formation in certain regions. While lower R_ρ of the ESTMW region is related to the lateral mixed layer density ratio (R_L) estimated in the former studies, the mechanism maintaining large R_ρ in other regions still remains to be a topic of future study.

Keywords: *Density ratio, Mode Water, Vertical eddy diffusivity, Water mass structure*

1. Introduction

World ocean density ratio distributions were first investigated by INGHAM (1966). Here, the density ratio is defined as $R_\rho=\alpha\overline{\theta_z}/\beta\overline{S_z}$, where $\overline{\theta_z}$ and $\overline{S_z}$ are mean vertical gradients of potential temperature and salinity, respectively. $\alpha=\frac{1}{\rho}\frac{\partial\rho}{\partial\theta}$ and $\beta=\frac{1}{\rho}\frac{\partial\rho}{\partial S}$ are the thermal expansion and the haline contraction coefficients, respectively. The TURNER angle (Tu) is defined as a function of R_ρ, *i.e.*, $Tu=\tan^{-1}\left(\frac{R_\rho+1}{R_\rho-1}\right)$ (RUDDICK, 1983). When R_ρ is larger than 1 (Tu ranges between 45° and 90°), the salt finger convection occurs, and when R_ρ ranges between 1 and 0 (Tu ranges between −45° and −90°), the diffusive convection occurs. The activity of both type of convection is intensified as R_ρ becomes closer to unity. Especially when R_ρ ranges between 1 and 2, the salt finger convection is so active that salt and heat are efficiently transported downwards and that for R_ρ ranging between 0.5 and 1, the diffusive convection is active to transport heat and salt upward.

INGHAM (1966) showed that R_ρ is constant (≈ 2) in the main thermocline of the Central Waters in world ocean subtropical gyres. SCHMITT (1981, 1990) explained that salt finger convection is a major mechanism of the formation of the Atlantic Central Water maintaining such a constant value. Later on, mapping of R_ρ in the world ocean has been tried by FIGUEROA (1996) and YOU (2002) using the Levitus data set. FIGUEROA (1996) then pointed out that R_ρ in the main thermocline is less than 2 in most of the ocean except in the Central Waters in the North Pacific where R_ρ is larger than 3〜4.

The double diffusive convection occurs when relatively warm and salty water overlies cooler and fresher water, or vice versa. Such areas are generally found in various oceans; if a certain oceanic area has such lower values of R_ρ around unity, it should be called as a "hot spot" of double diffusive convection, where effective vertical mixing should take place.

It has been suggested that enhanced vertical

Department of Ocean Sciences, TokYOUniversity of Marine Science and Technology, 4-5-7 Konan, Minato-ku, Tokyo 108-8477, Japan
E-mail: d0402010@kaiyodai.ac.jp
* Corresponding author

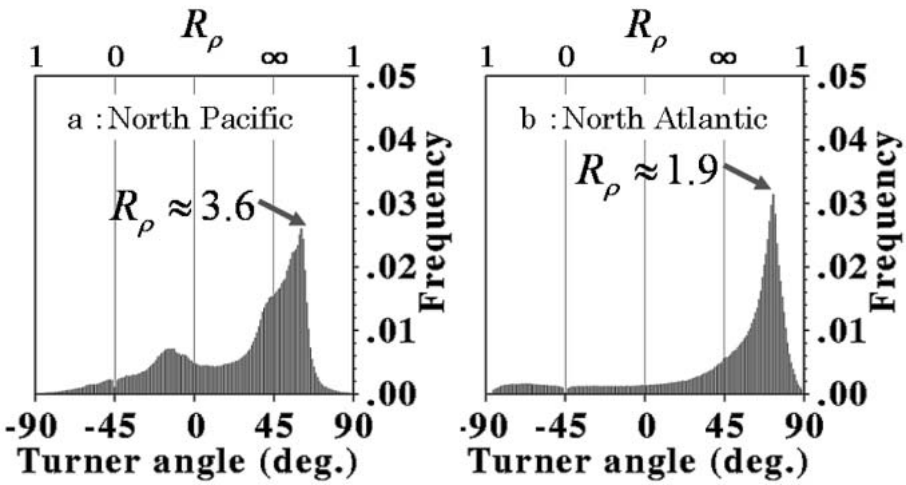

Fig. 1. The occurrence frequency of R_ρ in the upper 1000 db (a) in the North Pacific and (b) in the North Atlantic Oceans estimated from the WOCE data set.

mixing can produce significant effects on various large scale features of the ocean, and such effects have driven active studies and researches on this subject. BRYAN (1987) investigated the sensitivity of meridional overturning (MOT) and associated meridional heat flux by using a coarse resolution basin–scale model to K_V (the vertical eddy diffusivity of density). By varying K_V from 1×10^{-5} to $5 \times 10^{-4} m^2/s$, he reported that the magnitude of meridional mass transport in the model increased by an order of 4–fold. If, however, "hot spot" of double diffusive convection is ubiquitous in the world ocean, the effect of associated differential flux of heat and salt and negative flux of density may not be negligible. GARGETT and HOLLOWAY (1992) used the same model domain and forcing used by BRYAN (1987), but taking such a differential flux into account, with heat (T) and salinity (S) as separate fields having different diffusivities. By varying the ratio of diffusivity of S and T defined as $d = K_S/K_T$, they showed that the magnitude and the direction of MOT and the mean steady state distribution of T and S are sensitive to this parameter d.

Recent observations, however, revealed the enhanced vertical diffusivities over rough topography (*e.g.*, POLZIN *et al.*, 1997) due to the tidal effects near the boundary regions. If turbulent diffusivities are indeed enhanced in the deep ocean, such boundary mixing processes might affect the modification of water masses and the circulation pattern of world oceans (SAENKO and MERRYFIELD, 2005), and the relative importance of double diffusive convection will be smaller, given that R_ρ in the deep ocean are not significantly smaller than those in the upper ocean (YOU, 2002). The result of these observations may limit the effect of double diffusive convection in the deep ocean, but the double diffusive convection still remains important in the upper ocean where turbulent diffusivities are only of the order of $10^{-5} m^2/s$ and the diffusivities of T and S differ significantly (ST. LAURENT and SCHMITT, 1998).

Recently, the concept of lateral mixed layer density ratio (hereafter referred to as $R_L = \alpha \Delta T_L / \beta \Delta S_L$, where ΔT_L and ΔS_L are the horizontal temperature and salinity differences between the successive mixed layers several tens of kilometers apart) is introduced to explain the mechanism maintaining the main thermocline R_ρ value through the salt finger convection. These studies are motivated by the regulator theory proposed by STOMMEL (1993) and STOMMEL and YOUNG (1993). They found R_L over the basin scale is close to 2 in the temperature range between 7 and 17 °C and assumed a certain process, such as a random rainfall at sea surface controls the temperature and salinity field in the mixed layer to maintain this particular temperature and salinity

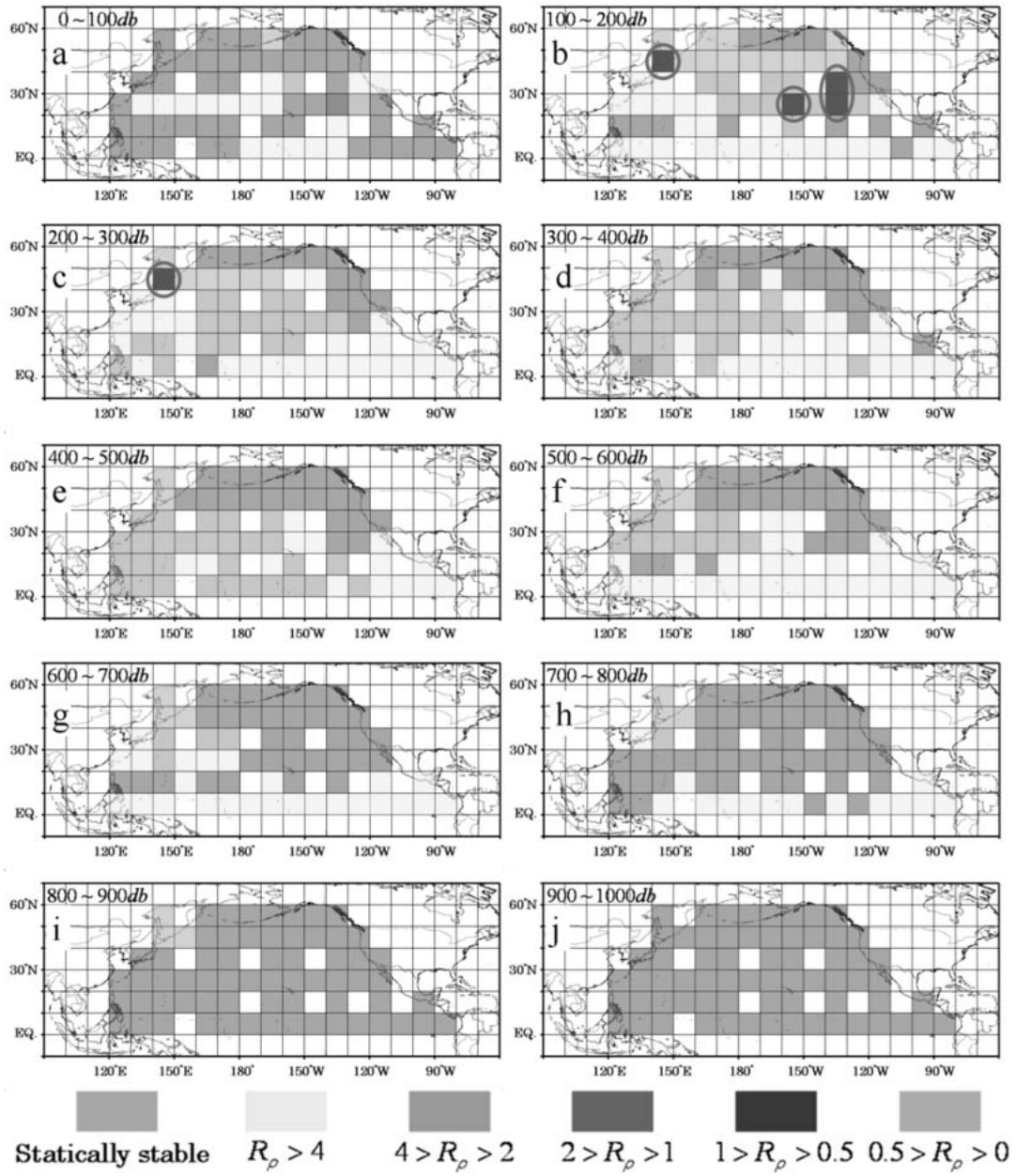

Fig. 2. Horizontal distributions of mode value of R_ρ in 10 degree boxes between the pressure surfaces. Open circles indicate the hot spots.

relation. Subsequently, CHEN (1995) used the Levitus climatological data set to show R_L in the same temperature range is less than 2 which supports the STOMMEL's idea (STOMMEL, 1993). RUDNICK and FERRARI (1999) investigated this lateral changes of temperature and salinity in the mixed layer in more detail in the Northeast Pacific, and obtained a surprising result that lateral changes in temperature and salinity are compensated in density at scales less than O (100 km), and a resulting R_L is close to unity. FERRARI and YOUNG (1997)

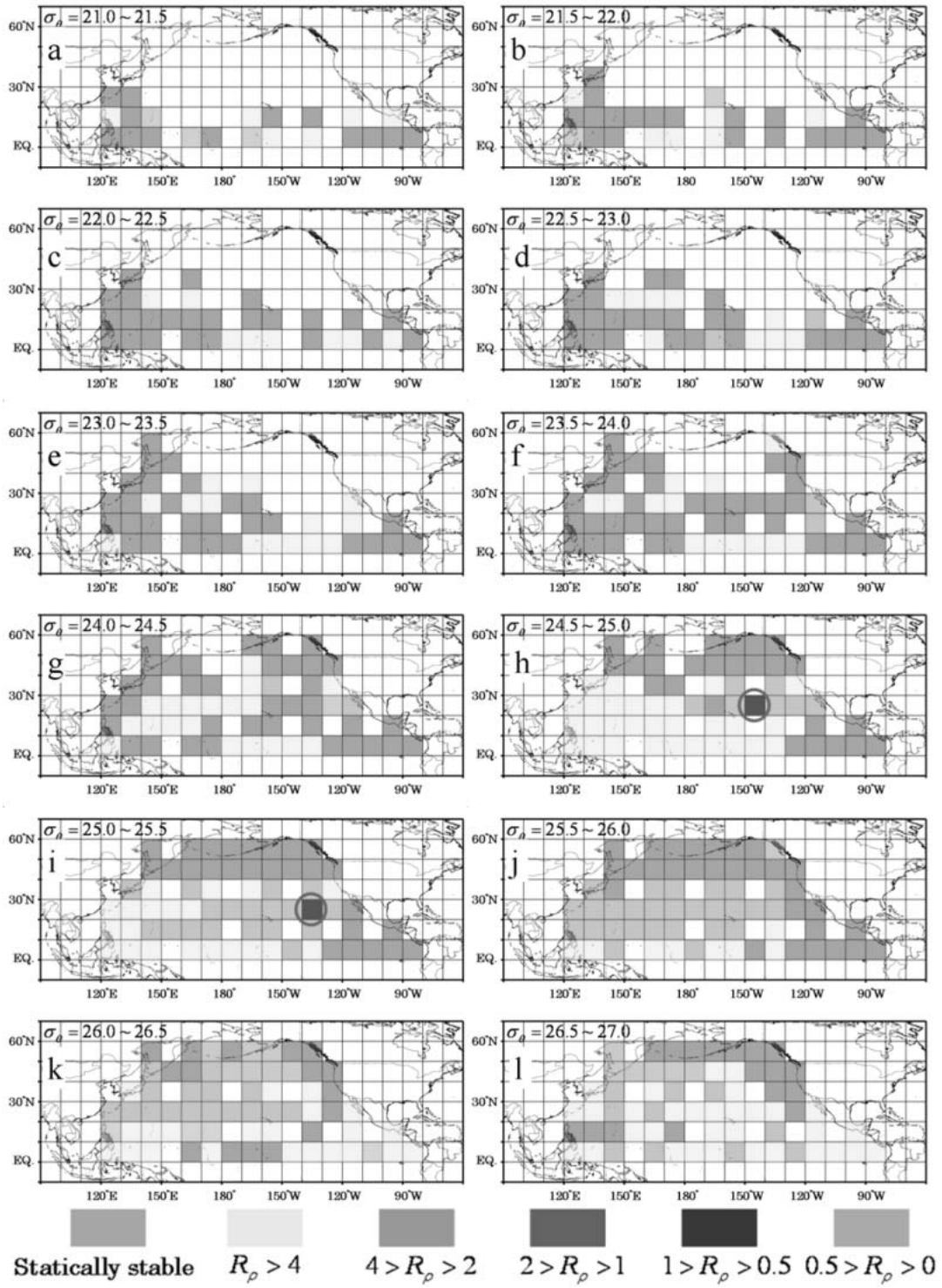

Fig. 3. Same as in Fig. 2, but for the designated sigma-theta surfaces. Open circles indicate the hot spots.

explained this low R_L by the slumping of slightly dense water in a surface layer of less dense water, and in the course of this slumping, horizontal density differences are easily disappeared to have R_L close to unity. This model, however, cannot explain the large scale R_L having the value of 2, and the R_ρ value also having 2 in the main thermocline. Recent idea of explaining this contradiction is given by SCHMITT (1999) that such density compensating temperature–salinity anomaly called as "spice" is consumed by the salt finger convection while the upper layer water being subducted, and the R_ρ is kept 2 in the main thermocline.

The problem raised here is the difference in the mode of R_ρ values between the North Pacific and the other oceans. The examples are shown in Fig. 1 for the WOCE data set (WOCE Global Data Ver.3, 2002, upper 1000 db) in the North Pacific (Fig. 1a) and in the North Atlantic (Fig. 1b). The mode in the North Atlantic is close to 2, while that in the North Pacific is larger than 3. This means that the salt finger convection is not so active in the North Pacific. Is this right? Are there no "hot spots" of double diffusive convection in the North Pacific? This higher value of R_ρ is usually explained by the fact that average salinity near a surface layer in the North Pacific is lower than that in the North Atlantic caused by strong evaporation over the entire Atlantic. However, this higher value of R_ρ could not be maintained by the mechanisms explained by the theories above. To solve this problem, we must know the basic water mass structures in the North Pacific through observing the detailed R_ρ distribution pattern. In the present study, the activity of double diffusive convection in the North Pacific is investigated through the R_ρ distribution in the upper 1000 db WOCE data set because, below this level, the stratification is usually highly stable.

2. Data processing

Before calculating R_ρ and Tu, all the WOCE CTD casts underwent several processes. Firstly, potential temperature (θ) and salinity were calculated and linearly interpolated at 1 db intervals. The CTD data sets stored at more than 2 db interval were removed for consistency of the quality of data. Secondly, temperature and salinity were vertically smoothed by 11 points (10 db) running mean. Lastly, vertical gradients were calculated by a 10 db least square fit. The α and β were calculated by differentiating equation of state (UNESCO, 1981) by temperature and salinity respectively. The occurrence frequencies of R_ρ values are estimated at each pressure interval (*e.g.*, 0〜100 db) or at each designated sigma–theta (hereafter σ_θ) interval (*e.g.*, 21.0〜21.5 σ_θ) and the peak values of the R_ρ are plotted at each 10 degree box in latitude and longitude to analyze the most favorable mode of double diffusive convection.

3. The horizontal distribution at the constant pressure and density surfaces

Shown in Fig. 2 are the horizontal distributions of R_ρ on pressure surfaces. In higher latitude region beyond 40°N, most fluid columns are stably stratified. In lower latitude region between the equator and 20°N in the layer from the surface to 800 db, the mode values exceed 4, suggesting the salt finger convection is not so active. On the other hand, in the mid–latitude (Subtropical Gyre) between 200 and 500 db, the mode values were between 2 and 4, suggesting the existence of weak salt finger convection. This is in contrast to the North Atlantic where the mode of R_ρ is less than 2.

Looking at the mode value distributions more precisely, we can see that the salt finger convection is active (R_ρ<2) in the shallower layer between 100 and 300 db in the area off eastern Hokkaido (40〜50°N, 140〜150°E) and in the eastern sub–tropical North Pacific (20〜30°N, 150〜130°W). These regions correspond to the region where the North Pacific Intermediate Water (NPIW) and the Eastern Subtropical Mode Water (ESTMW) are formed, respectively. The NPIW is defined as a thick salinity minimum around 26.7〜26.9 σ_θ in the western North Pacific (*e.g.*, QIU and JOYCE, 1992). The ESTMW is defined as a pycnostad (a minimum of potential vorticity) water around 24.0〜25.4 σ_θ in the eastern North Pacific (*e.g.*, HANAWA and TALLEY, 2001). Strong modification/formation of water masses are

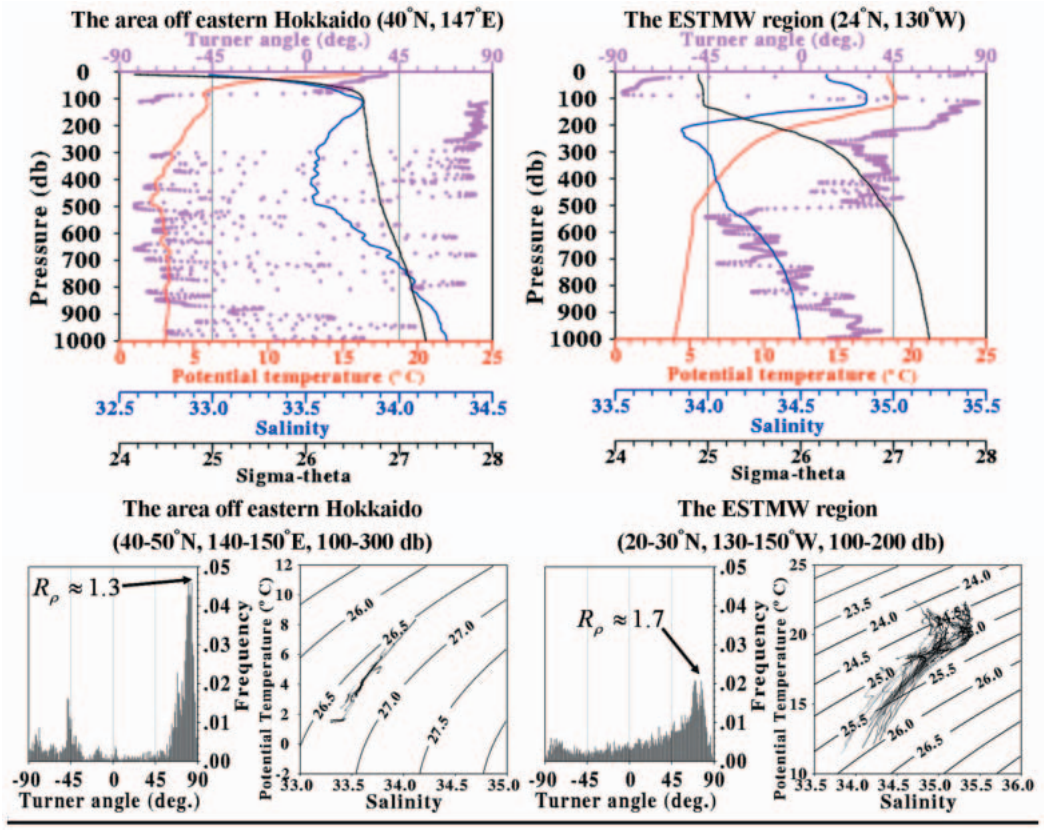

Fig. 4. (Upper two panels) : Examples of vertical profiles of potential temperature (red), salinity (blue), sigma-theta (black), and the TURNER angle (pink) at hot spots. (Bottom four panels) : Histograms of TURNER angle and -*S* diagrams plotted for the encircled regions shown in Figs. 2 and 3. Left two panels for the area off eastern Hokkaido (40–50° N, 140–150° E. 100–300 db), and right two for the ESTMW region (20–30°N, 130–150°W. 100–200 db).

anticipated in these regions; then, these regions should be "hot spots" of salt finger convection, which should have an important role in the modification formation of these waters. In the area off eastern Hokkaido, weak diffusive convection is expected to occur in the layer below 300 db to 900 db.

R_ρ distributions on σ_θ surfaces (Fig. 3) show slight changes in the mode distribution from Fig. 2. In the shallower layers with σ_θ being less than 24.0, fluid layers are almost statically stable; however, the layers where σ_θ ranges between 25.0 and 26.5 in the sub–tropical gyre ($2< R_\rho <4$) suggest existence of weak salt finger convection. On the other hand, in the deeper layers in the high latitude, weak diffusive convection is anticipated.

Hot spots found in Fig. 2 are also found in density layers with σ_θ ranging between 24.5 and 25.0 in the eastern sub–tropical North Pacific, but as for in the area off eastern Hokkaido, hot spots become rather ambiguous and undetectable in presented density surfaces. The reason for this phenomenon will be discussed in the next section.

4. Hot spots

To see the vertical profile of R_ρ together with θ and S in the area off eastern Hokkaido (Fig. 4, top–left), in the layer between 100 and 300 db (at the top of thermocline), R_ρ is close to unity (Tu is close to 90°) suggesting the existence of strong salt fingering. However, in the layers deeper than 300 db, salt fingering and diffusive

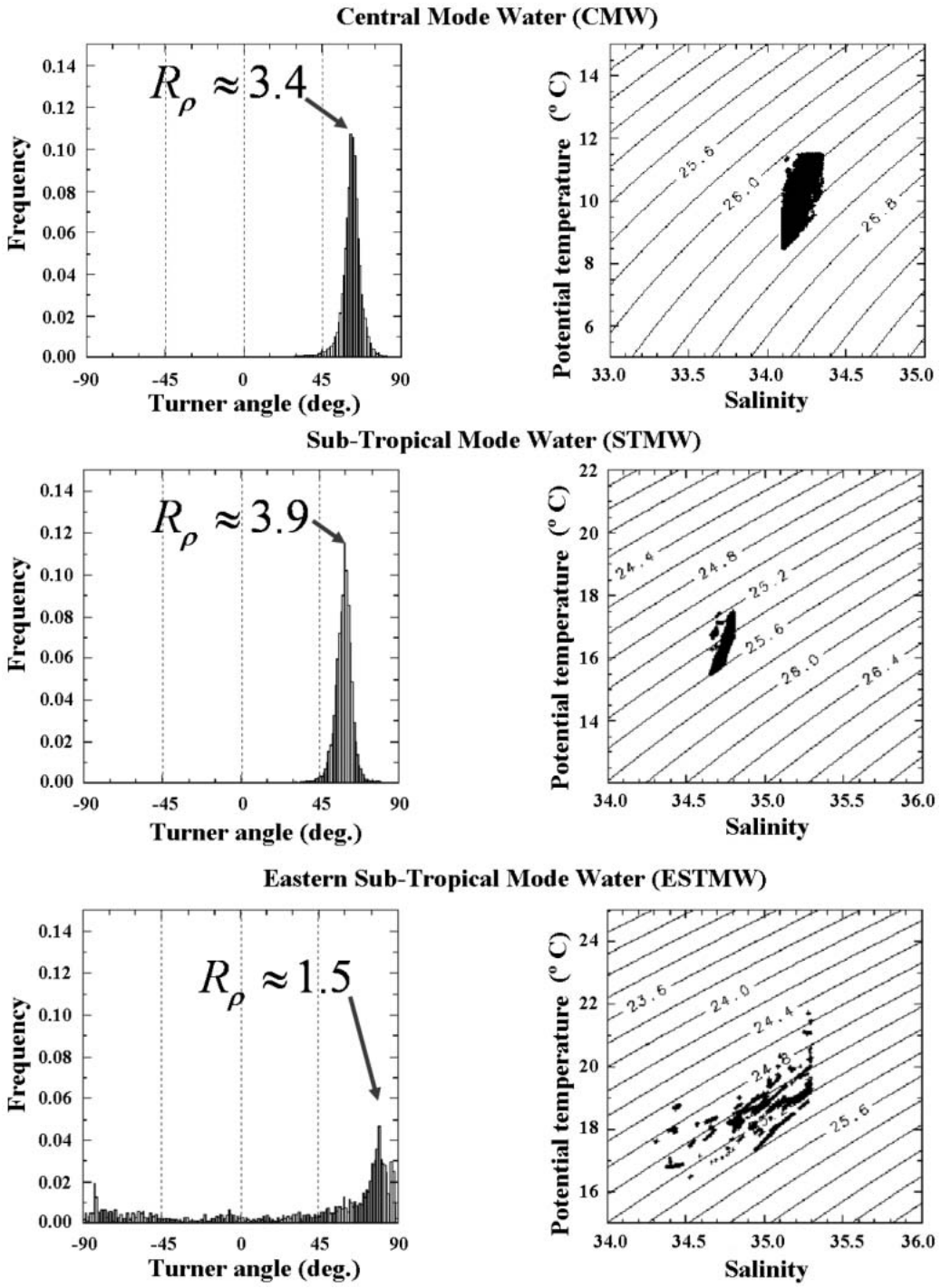

Fig. 5. Histograms of TURNER angle and θ-S relationship for Central Mode Water (33～40° N, 170～150° W), for Subtropical Mode Water (20～35° N, 120～180° E) and for Eastern Subtropical Mode Water (20～40° N, 120～160° W). All of these Mode Waters are specified by core temperatures, salinities, and by potential vorticity ($<2.0\times10^{-10}m^{-1}s^{-1}$).

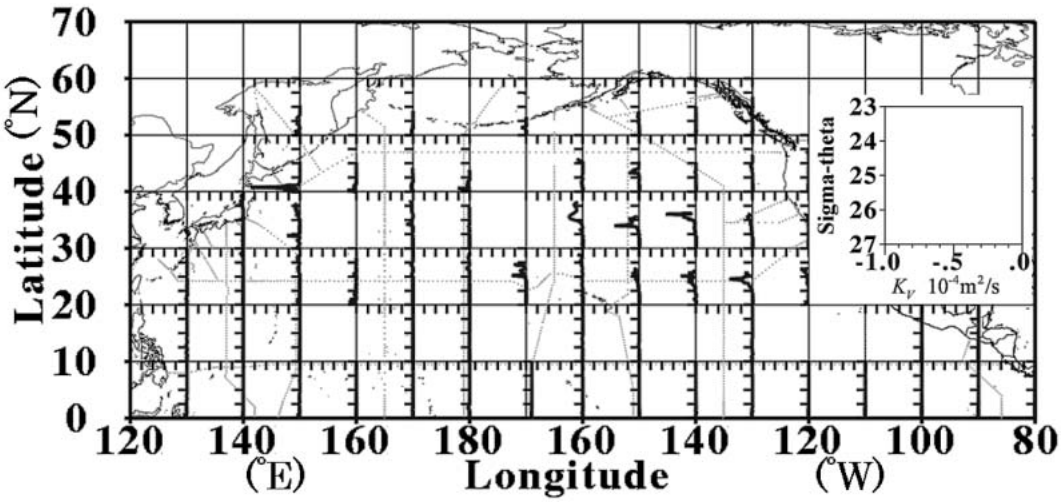

Fig. 6. Horizontal distributions of vertical eddy diffusivity of density in 10 degree boxes taking σ_θ for the vertical axis. See the inserted figure on the top right for reference.

convection layers are piled up alternatively suggesting the intrusive features possibly created by double diffusive convection (*e.g.*, RUDDICK and TURNER, 1979). Contrary to this, in the ESTMW region (Fig. 4, right), the salt finger convection favorable layer is found only in the layer between 100 and 200 db (at the top of thermocline), and in the deeper layers, the entire fluid column is stably stratified.

The occurrence frequency of R_ρ and θ–S relations in the area off eastern Hokkaido (Fig. 4, bottom– left) shows a sharp pointed peak in the salt finger convection regime ($45° < Tu < 90°$, $R_\rho \approx 1.3$). The θ–S relations aligned along an isopycnal line ($26.7\,\sigma_\theta$) also supports this low R_ρ value and it is showing that favorable layers of salt finger convection are confined to a narrow band in the density coordinate (around $26.6 \sim 26.7\,\sigma_\theta$) than in the pressure coordinate (100～300 db). It is, thus reasonable that hot spots found in pressure surfaces were rather ambiguous in density surfaces taking interval of $0.5\,\sigma_\theta$. A relatively small peak is found in the diffusive regime. This should be caused by the temperature inversions commonly observed in this region. As for in the ESTMW region (Fig. 4, bottom–right), a peak value of R_ρ is about 1.7, and this also suggests the occurrence of strong salt finger convection; however, the peak is not clearly defined but shows a flat distribution. The θ–S relations show a complicated structure contaminated by a certain surface process.

5. Mode Waters in the North Pacific

Two hot spots for double diffusive convection in the North Pacific show different features. Especially at the formation region of ESTMW, the θ–S relationship showed a complicated structure. It is thus worth comparing this region with other typical Mode Waters in the North Pacific, such as the Central Mode Water (CMW) and the Subtropical Mode Water (STMW), and discussing the processes to maintain the thermocline in the North Pacific in this section. The CMW is characterized as a pycnostad (minimum of potential vorticity) water centered at $26.2\,\sigma_\theta$ surface found at the western coast of the Kuril Islands to 150°W and between the Kuroshio Extension Front (approx. 33°N) and the Kuroshio Bifurcation Front (approx. 40°N) (SUGA *et al.*, 1997). The STMW is also a pycnostad water centered at $25.2\,\sigma_\theta$ surface found in the Kuroshio region to the International Date Line and is limited between 20°N and 40°N. As shown in Fig. 5, the mode values of R_ρ are 3.4 for the CMW and 3.9 for the STMW, respectively, suggesting the salt finger convection is not active. However, in the ESTMW region, the mode value is less than

2 (=1.5). This suggests that the mechanism proposed by SCHMITT (1999) works here indicating the importance of salt finger convection to form the ESTMW. This point is noted by FERRARI and RUDNICK (2000) at the same observation site, however, the mechanism of maintaining such large R_ρ in the other Mode Waters in the North Pacific is unclear. The salt finger convection is too weak in these locations to maintain large scale constant R_ρ values larger than 2 in the thermocline (FIGUEROA, 1996 also pointed out this).

6. Vertical diffusivity of density deduced by the formulation by ZHANG *et al.* (1998)

The important effect of double diffusive convection is the effective downward transport of density. In both types of convection, density gradient is intensified, that is, the sign of eddy diffusivity becomes negative. ZHANG *et al.* (1998) investigated this effect through parameterizing eddy diffusivities by R_ρ, and pointed out that meridional overturning cell was weakened and deeper temperature and salinity increased in the presence of double diffusive convection. Here, we use their parameterization, and show the horizontal distribution of vertical eddy diffusivity in Fig. 6. Profiles shown here are the averages of vertical diffusivity of density within each σ_θ surface (K_V) in respective boxes. "Hot spots" can be found in the σ_θ layer around 26.7 in the area off eastern Hokkaido and between in the ESTMW area, respectively. K_V was estimated as $(9\sim8)\times10^{-5}\mathrm{m^2/s}$ in the area off eastern Hokkaido and $-(8\sim4)\times10^{-5}\mathrm{m^2/s}$ in the ESTMW area. These magnitudes are larger than the typical K_V value $1\times10^{-5}\mathrm{m^2/s}$ in the thermocline (ST. LAURENT and SCHMITT, 1998) by about an order, showing the importance of double diffusive convection to the water mass formation in respective region.

7. Summary and discussion

We investigated the water mass structure and detailed R_ρ distribution in the upper 1000 db of the North Pacific by using the WOCE data set. The "hot spots" of double diffusive convection were found in the area off eastern Hokkaido and in the Eastern North Pacific where the NPIW and the ESTMW are formed. Mode values of R_ρ in these regions are 1.3 and 1.7, respectively. The salt finger convection must be an important process for water mass madification formation in these regions. Although the favorable condition for the onset of salt finger convection was satisfied in most of the mid–latitude (the subtropical gyre) between 200〜500 db or between 25.0〜26.5 σ_θ including the CMW and the STMW, the modes of R_ρ in these regions lie between 3 and 4, suggesting salt finger convection is not so active. The mechanism of maintaining large value of R_ρ in these regions is still unclear. This higher value of density ratio is usually explained by the fact that the average salinity near the surface layer in the North Pacific is lower than that in the Atlantic where the evaporation is so strong.

The subduction process causing inflow to the main thermocline occurs in winter when the surface mixed layers deepened through surface cooling. In this case, R_L estimated from the Levitus annual mean could not have direct connection with thermocline R_ρ, and the explanation presented by SCHMITT's idea of "spice" holds true for the Atlantic, but not for the North Pacific except for ESTMW region as was shown in the present study. The observation field in the ESTMW region by RUDNICK and FERRARI (1999) was too limited to discuss the whole basin of the North Pacific; however, RUDNICK and MARTIN (2002) extended their analysis including the Indian and the Atlantic Oceans and concluded that this low value of R_L (≈ 1) is a common feature of all the oceans at the scales about O (3〜4km) where the mixed layer depth exceeds about 75 m. Therefore, in order to clarify the maintenance mechanism of thermocline R_ρ in the North Pacific, we must investigate winter time distribution of R_L more precisely in relation to the mixed layer depth. This problem will remain to be a topic of the future work.

Acknowledgements

The authors would like to express their sincere thanks to Drs. R. INOUE and Y. TANAKA for their discussion and kind supports throughout this study. We thank the

anonymous referees for their helpful comments. This work is supported by the Ministry of Education, Culture, Sports, Science and Technology of the Japanese Government, and is a part of the Ph.D. thesis of K. SHIMADA.

References

BRYAN, F. (1987) : On the parameter sensitivity of primitive equation ocean general circulation models. J. Phys. Oceanogr., **17**, 970–985.

CHEN, L. G. (1995) : Mixed layer density ratio from the Levitus data. J. Phys. Oceanogr., **25**, 691–701.

FERRARI, R. and D. L. RUDNICK (2000) : Thermohaline variability in the upper ocean. J. Geophys. Res., **105**, 16,857–16,883.

FERRARI, R. and W. R. YOUNG (1997) : On the development of thermohaline correlations as a result of nonlinear diffusive parameterizations. J. Mar. Res., **55**, 1069–1101.

FIGUEROA, H. A. (1996) : World ocean density ratios. J. Phys. Oceanogr., **26**, 267–275.

GARGETT, A. E. and G. HOLLOWAY (1992) : Sensitivity of the GFDL ocean model to different diffusivities for heat and salt. J. Phys. Oceanogr., **22**, 1158–1177.

HANAWA, K. and L. D. TALLEY (2001) : Mode Waters. *In* Ocean Circulation and Climate, (*eds.*) G. Siedler and J. Church, International Geophysics Series, Academic Press, 373–386.

INGHAM, M. C. (1966) : The salinity extrema of the world ocean. Ph.D. dissertation, Oregon State University, 63pp.

POLZIN, K. L., J. M. TOOLE, J. R. LEDWELL and R. W. SCHMITT (1997) : Spatial variability of turbulent mixing in the abyssal ocean. Science, **276**, 93–96.

QIU, B. and T. M. JOYCE (1992) : Interannual variability in the mid– and low–latitude western North Pacific. J. Phys. Oceanogr., **22**, 1092–1079.

RUDDICK, B. R. (1983) : A practical indicator of the stability of the water column to double–diffusive activity. Deep–Sea Res., **30**, 1105–1107.

RUDDICK, B. R. and J. S. TURNER (1979) : The vertical length scale of double–diffusive intrusions. Deep–Sea Res., **26**, 903–913.

RUDNICK, D. L. and R. FERRARI (1999) : Compensation of horizontal temperature and salinity gradients in the ocean mixed layer. Science, **283,** 526–539.

RUDNICK, D. L. and J. P. MARTIN (2002) : On the horizontal density ratio in the upper ocean. Dyn. Atmos. Oceans, **36**, 3–21.

SAENKO, O.A. and W. J. MERRYFIELD (2005) : On the effect of topographically enhanced mixing on the global ocean circulation. J. Phys. Oceanogr., **35**, 826–834.

SCHMITT, R. W. (1981) : Form of the temperature–salinity relationship in the Central Water: evidence for double–diffusive mixing. J. Phys. Oceanogr., **11**, 1015–1026.

SCHMITT, R. W. (1990) : On the density ratio balance in the Central Water. J. Phys. Oceanogr., **20**, 900–906.

SCHMITT, R. W. (1999) : Spice and the Demon. Science, **283**, 498–499.

ST. LAURENT, L. and R.W. SCHMITT (1998) : The contribution of salt fingers to vertical mixing in the North Atlantic tracer release experiment. J. Phys. Oceanogr., **29**, 1404–1424.

STOMMEL, H. M. (1993) : A conjectural regulating mechanism for determining the thermohaline structure of the oceanic mixed layer. J. Phys. Oceanogr., **23**, 142–148.

STOMMEL, H. M. and W. R. YOUNG (1993) : The average T–S relation of a stochastically forced box model. J. Phys. Oceanogr., **23**.151–158.

SUGA, T., Y. TAKEI and K. HANAWA (1997) : Thermostad distribution in the North Pacific subtropical gyre: the Central Mode Water and the Subtropical Mode Water. J. Phys. Oceanogr., **27**, 140–152.

UNESCO (1981) : Tenth report of the joint panel on oceanographic tables and standards. UNESCO Tech. Paper in Marine Science, **36**, 25 pp.

WOCE GLOBAL DATA PRODUCTS COMMITTEE (2002) : WOCE Global Data Version 3. WOCE International Project Office WOCE report No.180/02, Southampton, UK.

YOU, Y. (2002) : A global ocean climatological atlas of the TURNER angle: implications for double–diffusion and water–mass structure. Deep–Sea Res., **49**, 2075–2093.

ZHANG, J., R. W. SCHMITT and R. X. HUANG (1998) : Sensitivity of the GFDL modular ocean model to parameterization of double–diffusive processes. J. Phys. Oceanogr., **28**, 589–605.

Received October 3, 2007
Accepted December 7, 2007

La mer 45 : 159-160, 2007
Société franco-japonaise d'océanographie, Tokyo

資　料

第 45 巻第 3 号掲載欧文論文の和文要旨

野村英明[1*]、豊田圭太[2]、山田美穂子[3]、岡本研[3]、和田実[1]、西村昌彦[1]、吉田明弘[1]、柴田晃[1]、高田秀重[3]、大和田紘一[4]：石油および石油と分散型油処理剤添加後にみられた中規模半閉鎖型海洋生態系における植物プランクトン群集の遷移

メソコスム（中規模半閉鎖型疑似現場海洋生態系）を用いて、海産植物プランクトン群集に及ぼす低濃度のA重油（水溶性画分）の影響を調べた。実験は2001年 5 月23日から 6 月 2 日にかけて行った。海水に重油を添加した石油区、海水に重油と分散型油処理剤を添加した石油分散剤区、および油を加えていない海水のみの海水区において、植物プランクトンの出現量、種組成、沈降粒子束、水中石油成分濃度及び水温・塩分などの環境因子をモニターした。実験開始当初は珪藻、主に*Chaetoceros*属や*Skeletonema costatum*を主体とした群集構造が形成されていたが、それは最終的には鞭毛藻主体の群集に遷移した。こうした遷移はどのメソコスムタンクにも共通した現象であった。しかし、ゆるやかに遷移した海水区と異なり、油の混入した二つのタンクの珪藻個体群は、添加後4日内に大きく減衰しそれ以後珪藻の増加は見られない一方、鞭毛藻は急速に増加し、海水区に比べると高密度になった。また、海水区では実験の後半にも珪藻がマイナ-なピ-クを形成したのに対し、石油の混入したタンクではそれが見られないことに加えて、沈降粒子束中の珪藻細胞は海水区の20%以下と少なかった。珪藻個体群の減衰は、石油成分に暴露されたことによる成長阻害と考えられた。珪藻個体群の縮小は、生食食物網を変質させると共に、底層への有機物フラックスを減ずるため浮遊系と底生系のカップリングを弱めることになる。メソコスム実験系では、自然では水中に存在する物理学的属性である微小な乱流が抑制されることで、植物プランクトン種それぞれの生理的活性状況の違いが感知しやすくなる。おそらく湾奥港湾水域のような閉鎖あるいは半閉鎖条件の現場で起こっているであろう低濃度の石油汚染による基礎生産者への影響は、天然では様々な要因が複雑に反映して明らかにならない。こうした低濃度な石油汚染でも基礎生産者に影響を与えることが、乱流のようないくつかの環境因子を人為的に取り除くことのできるメソコスム実験系では観察することができる。

（[1] 東京大学海洋研究所　[2] 株式会社水圏科学コンサルタント　[3] 東京農工大学大学院共生科学技術研究部　[4] 熊本県立大学環境共生学部　*164-8639 中野区南台1-15-1　電話：03-5351-6483、ファックス：03-5351-6482　電子郵便住所：nmr@ori.u-tokyo.ac.jp）

屋良由美子*、柳哲雄、門谷茂、多田邦尚：沿岸海域における物質循環に対する干潟の機能

浮遊・底生結合生態系モデルの簡単な干潟生態系モデルを構築し、瀬戸内海の干潟において窒素循環過程を解析した。干潟における観測項目は水質や底生生物に関する項目があり、観測値の季節変動を本モデルの計算結果は再現したため、モデルを用いて、干潟の機能を水質浄化機能の観点から評価した。その結果、干潟に懸濁物食者（二枚貝）が存在する現在の干潟は有機物の無機化の割合が大きいことが分かった。さらに、干潟に懸濁物食者が全く存在しないと仮定した場合、有機窒素の流出が現在よりも増加するため、干潟の水質浄化能力は低下し、植物プランクトンによる摂食圧の現象により赤潮の発生することが分かった。

（※〒060-0810 札幌市北区北十条西 5 丁目　北海道大学大学院地球環境科学研究院地球圏科学部門気候力学分野
〒816-8580 福岡県春日市春日公園6-1　九州大学応用力学研究所力学シミュレーション研究センター野外計測分野
tel. and fax: 092-583-7492　E-mail: yara@riam.kyushu-u.ac.jp）

土井　航・横田賢史・渡邊精一：館山湾におけるトラノオガニの成長と繁殖

ケブカガニ科のトラノオガニの成長と繁殖を明らかにするために、2001年 4 月から2002年 3 月までの間、千葉県の館山湾で月例採集を行なった。抱卵雌は主に 6 月から 8 月にかけて出現し、稚ガニの加入は 8 月から 1 月にかけてみられた。稚ガニは着底後に成長し、翌年の 4 月には成熟サイズを超える。大型の雄は特に大きな鉗脚を有するが、その相対成長は性成熟には一致しなかった。その一方で、雄の腹節幅の成長率は成熟脱皮後に減少した。雌では成熟個体で腹節幅の増大がみられた。しかし、成熟脱皮前後の中間的な腹節をもつ雌がいるために、腹節幅によって未成熟、成熟個体を区別することはできなかった。一腹卵数は甲幅とともに増大し、その範囲は120粒から1､700粒であった。繁殖期後、大型個体のほとんどは老衰によって死滅し、本種の寿命は約 1 年と推定された。しかし、甲幅頻度分布と成長率の解析から、翌年の繁殖期まで生存する個体もいると考えられる。

（東京海洋大学海洋生物資源学科　〒108-8477　東京都港区港南4－5－7、TEL 03-5463-0535、FAX 03-5463-0684、E-mail：Watanabe@kaiyodai.ac.jp）（渡邊）

嶋田啓資、根本雅生、吉田次郎：北太平洋における密度比の空間分布

北太平洋の上層1000 dbにおける密度比（R_ρ）の空間分布をWOCEデータセットから見積もった。これまでの研究と同様にR_ρのモード値は3～4で、二重拡散対流は不活発であることが示されたが、北海道東部沖の海域及び、東部亜熱帯モード水（ESTMW）形成域において二重拡散対流が活発な「hot spot」が存在することが分かった。密度の鉛直渦拡散係数はそれぞれ－（9～8）$\times10^{-5}m^2/s$（北海道東部沖）、－（8～4）$\times10^{-5}m^2/s$（ESTMW形成域）と見積もられた。これらのことから二重拡散対流が水塊の形成に重要な役割を果たしている海域が存在することが示された。ESTMW形成域の低い密度比は、これまでの研究で見積もられた表層混合層の密度比との間に関連があることが示されたが、その他の海域の温度躍層に見られる大きな密度比を維持する機構は未だ不明であり、今後の課題として挙げられる。

（東京海洋大学海洋環境学科　〒108-8477　東京都港区港南4-5-7　Eメール：d042010@kaiyodai.ac.jp）

La mer 45 : 161-163, 2007
Société franco-japonaise d'océanographie, Tokyo

学　会　記　事

1. 2007年 6 月 9 日（土）日仏会館会議室において，平成19年度学術研究発表が開かれ発表題目と発表者は次のとおり

平成19年度日仏海洋学会学術研究発表会

期日：平成19年 6 月 9 日（土）

場所：日仏会館会議室（501号室）東京都渋谷区恵比寿31−9−25

電話03-5421-7641

プ　ロ　グ　ラ　ム

午前（10：00−12：00）

1．内浦湾における内部潮汐の反射・散乱
……○川村有二・北出裕二郎・松山優治（海洋大）

2．長崎県形上湾における水温鉛直分布の連続観測
……○小林雅人（横商大・農林産研）・早川康博（水大校）・山口仁士・川井仁（長崎環保研セ）

3．2006年 4 月に駿河湾で発生した急潮
…○永井美雪（海洋大）・久保田雅久（東海大）・川村有二・松山優治（海洋大）

4．Adeke Land沖における密度逆転の分布と内部波の関係　……○平野大輔　北出裕二郎（海洋大）

5．カリフォルニア沿岸湧昇域における沖合い方向への炭素輸送に渦とフィラメントが果たす役割に関する数値実験……○長井健容（海洋大）

6．流出油モニタリングのためのヘリコプター搭載型蛍光ライダーの開発
……○篠野雅彦・樋富和夫・山之内博（海技研・運航シス）

午後（14：00−15：00）

7．CO_2海洋隔離におけるpH値による生物影響評価の基礎研究
……○中村倫明・和田明・長谷川一幸（日大・院・環境科学）

8．紅藻ピリヒバ（*Corallina pilulifera*）の光合成特性
……○高原涼・佐藤博雄・田中次郎（海洋大）

9．無機懸濁粒子がアサリの受精卵および浮遊幼生に与える影響
……○赤塚利之・荒川久幸・森永勤（海洋大）・瀬戸雅文（福井県大）・小林豊（千葉県・水総セ）

2. 2007年 6 月 4 日（土）日仏会館において評議員会後第48回（平成19年度）総会が開かれた
議題は次の通り。

1．平成18年度事業報告

1）庶務

会員異動状況

	H18年4月	入会	退会	逝去	資格変更	19年3月
名誉会員	2	−	−	−	−	2
正会員	261	14	13	1	−	261
学生会員	4	6	−	−	−	10
賛助会員	7	−	−	−	−	7

2）活動状況

評議員会　1 回（18/6/4　日仏会館）
幹 事 会　2 回（18/12/7，19/4/10　日仏会館）
総　　会　1 回（18/6/4　日仏会館）
学術研究発表会　1 回（18/6/4　日仏会館）
学会誌発行　43巻 3 号〜44巻 3，4 号

3）編集関係

学会誌「La mer」43(3)・43(4)44(1)合併・44(2)・44（3，4）発刊

2．平成18度収支決算報告

収入の部（備考）		
前年度繰越金	763,338	
正会員会費	1,000,000	125名
65歳以上会員	132,000	22名
学生会員会費	24,000	6 名（4000× 6 名）
賛助会員会費	120,000	（7 社，12日）
学会誌売上金	58,210	
広告料	50,000	
別刷り印刷費	442,400	
掲載料，超過頁印刷費	550,000	
雑収入	103,146	（研究発表会，学術著作権使用料他）
寄付金	0	
合　計	3,243,094	

支出の部

学会誌印刷費	1,597,250	43(3), 43(4)・44(1)合併号,44(2)各350部
送料・通信費	159,615	
事務費	663,592	人件費，事務用品，封筒他
交通費	14,700	
会議費	4,248	
学会賞経費	0	メダル，賞状他
雑費	14,751	郵便・銀行振込手数料他
次年度繰越（銀行残高）	788,938	
合　計	3,243,094	

原案通り承認された

3．平成19年度事業

1）総会　学術研究発表会　幹事会　評議員会　開催
2）学会会則の見直し
3）La mer発刊
4）学会賞のメダルの変更
5）バックナンバーのDVD化
6）仏日シンポジウムの準備
7）その他（平成20．21年度　評議員．会長選出）

4．平成19年度予算

収入の部

正会員会費	800,000	100名×8000円
65歳以上会員	132,000	30名×6000円
学生会員会費	24,000	6名×4000円
賛助会員会費	120,000	（7社，12口）
学会誌売上金	60,000	
広告料	50,000	
別刷り印刷費	480,000	
掲載料，超過頁印刷費	800,000	16編×50000円
雑収入	100,000	（要旨集売上，学術著作権使用料他）
17年度繰越（銀行残高）	788,938	
合　計	3,354,938	

支出の部

学会誌印刷費	2,120,000	4冊×530000円
送料・通信費	100,000	
事務費	700,000	人件費，事務用品，封筒他
交通費	20,000	
会議費	5,000	
学会賞経費	50,000	メダル，賞状他
雑費	25,000	郵便・銀行振込手数料他
予備費	334,938	学会誌バックナンバー電子化
合　計	3,354,938	

原案通り承認された

5．平成19年度　学会賞・論文賞受賞候補者推薦委員会委員

荒川久幸　石丸　隆　今脇資郎　磯田　豊　奥田邦明
神田穣太　北出裕二郎　河野　博　小林雅人　小松輝久
櫻本和美　千手智晴　田中祐志　前田昌詞　吉田次郎

6．その他

その後，アトレ恵比寿店ライオンにおいて懇親会がひらかれた。

●日仏海洋学会会則の改正

平成19年6月9日総会において下記の様に改正され承認されました。

日仏海洋学会会則　新会則（改正条文　下線部分が改正部分）

第3条　上記の目的を達成するために本会は次の事業を行う。
（1）海洋および水産に関する研究会および講演会の開催
（2）定期刊行物，学術上の刊行物の発行
（3）学会賞の授与
（4）日仏両国を主とする海洋および水産に関する共同研究成果の発表，ならびに，技術開発成果の導入および普及
（5）両国の海洋・水産関係者の交流促進および親睦をはかること
（6）その他本会の目的を達成するために必要な事業

第9条　本会は評議員会によって運営される。
評議員の定数は28名以内とし，24名は正会員および学生会員の投票によって選出される。
会長は評議員会の同意を得て4名以内の正会員および学生会員を評議員に委嘱することができる。
評議員の任期は2年とする。ただし，重任を妨げない。

第10条　評議員はその内より次の役員を選ぶ。ただし，監事は評議員以外からも選ぶことができる。
会長1名，副会長2名，幹事10名以上12名以内，監事2名
役員の任期は2年とする。ただし，重任を妨げない。

第13条　通常総会は毎年1回会長が招集する。
会長は必要に応じて評議員会の決議を経て臨時総会を招集することができる。
総会では評議員会の報告に基づいて，会の重要

問題を審議する。
総会は正会員および学生会員の 6 分の 1 以上の出席がなければ成立しない。ただし，出席できない正会員および学生会員は委任状により他の出席会員または議長に決議を委任し，出席会員とみなすことができる。

日仏海洋学会評議員・役員選出規定　改正が検討される項目の改正案

2．評議員の選出は直会員および学生会員の24名連記無記名投票による。

（以下略）

日仏海洋学会賞規定　改正が検討される項目の改正案

3．委員会の委員は 9 名とする。委員は毎年春の評論員会で選出し，委員長は委員の互選により定める。委員の任期は 2 年とし，隔年に 4 名および 5 名を交代する。会長は委員会が必要と認めた場合，評議員の同意を得て 2 名まで委員を追加委嘱することができる。ただし，追加委嘱された委員の任期はその年度限りとする。

賛 助 会 員

アレック電子株式会社	神戸市西区井吹台東町７－２－３
株式会社 イーエムエス	神戸市中央区東川崎町１－３－３ 神戸ハーバランドセンタービル　13F
有限会社 英和出版印刷	文京区千駄木４－20－６
株式会社 内田老鶴圃 内田　悟	文京区大塚３－34－３
財団法人 海洋生物環境研究所	千代田区神田神保町３－29　帝国書院ビル５Ｆ
株式会社 川合海苔店	大田区大森本町２－31－８
ケー・エンジニアリング株式会社	台東区浅草橋５－14－10
いであ株式会社	世田谷区駒沢３－15－１
三洋測器株式会社	渋谷区恵比須南１－２－８
株式会社高岡屋	台東区上野６－７－22
テラ株式会社	文京区湯島４－１－13－402
渡邊機開工業株式会社	愛知県渥美郡田原町神戸大坪230

日仏海洋学会入会申込書

（正会員・学生会員）

	年度より入会	年　月　日申込
氏　名 ローマ字		年　月　日　生
住　所　〒 勤務先　機関名 電　話　E-mail:		
自　宅　住　所　〒 電　話　E-mail:		
紹介会員氏名		
送付金額　円	送金方法	
会誌の送り先（希望する方に○をつける）	勤務先　自　宅	

（以下は学会事務局用）

受付	名簿 原簿	会費 原簿	あて名 カード	学会 記事

入会申込書送付先：〒150-0013 東京都渋谷区恵比寿 3-9-25

（財）日仏会館内

日 仏 海 洋 学 会

郵便振替番号：00150−7−96503